International Ocean Discovery Program Expedition 363 Scientific Prospectus

Western Pacific Warm Pool

Neogene and Quaternary records of Western Pacific Warm Pool paleoceanography

Yair Rosenthal
Co-Chief Scientist
Department of Marine Sciences and Earth and Planetary Sciences
Rutgers, the State University of New Jersey
71 Dudley Road
New Brunswick NJ 08901
USA

Ann Holbourn
Co-Chief Scientist
Institute of Geosciences
Christian-Albrechts Universität zu Kiel
Ludewig-Meyn-Strasse 10-14
D-24118 Kiel
Germany

Denise Kulhanek
Expedition Project Manager/Staff Scientist
International Ocean Discovery Program
Texas A&M University
1000 Discovery Drive
College Station TX 77845
USA

IODP
INTERNATIONAL OCEAN DISCOVERY PROGRAM

Publisher's notes

This publication was prepared by the International Ocean Discovery Program *JOIDES Resolution* Science Operator (IODP JRSO) as an account of work performed under the International Ocean Discovery Program. Funding for the program is provided by the following implementing organizations and international partners:

National Science Foundation (NSF), United States
Ministry of Education, Culture, Sports, Science and Technology (MEXT), Japan
European Consortium for Ocean Research Drilling (ECORD)
Ministry of Science and Technology (MOST), People's Republic of China
Korea Institute of Geoscience and Mineral Resources (KIGAM)
Australian-New Zealand IODP Consortium (ANZIC)
Ministry of Earth Sciences (MoES), India
Coordination for Improvement of Higher Education Personnel, Brazil (CAPES)

Portions of this work may have been published in whole or in part in other International Ocean Discovery Program documents or publications.

This IODP *Scientific Prospectus* is based on precruise *JOIDES Resolution* Facility advisory panel discussions and scientific input from the designated Co-Chief Scientists on behalf of the drilling proponents. During the course of the cruise, actual site operations may indicate to the Co-Chief Scientists, the Staff Scientist/Expedition Project Manager, and the Operations Superintendent that it would be scientifically or operationally advantageous to amend the plan detailed in this prospectus. It should be understood that any proposed changes to the science deliverables outlined in the plan presented here are contingent upon the approval of the IODP JRSO Director.

Disclaimer

Copyright

Citation

Rosenthal, Y., Holbourn, A., and Kulhanek, D.K., 2016. *Expedition 363 Scientific Prospectus: Western Pacific Warm Pool*. International Ocean Discovery Program. http://dx.doi.org/10.14379/iodp.sp.363.2016

ISSN
World Wide Web: 2332-1385

February 2016

Abstract

Expedition 363 seeks to document the regional expression of climate variability (e.g., temperature, precipitation, and productivity) in the Western Pacific Warm Pool (WPWP) as it relates to global and regional climate change from the middle Miocene to Late Pleistocene on millennial, orbital, and secular timescales. The WPWP is the largest reservoir of warm surface water on Earth and thus is a major source of heat and moisture to the atmosphere. Variations in sea-surface temperature and the extent of the WPWP influence the location and strength of convection and thus impact oceanic and atmospheric circulation, heat transport, and tropical hydrology. Given its documented importance for modern climatology, changes in the WPWP are assumed to have also played a key role in the past. The proposed drill sites are strategically located at the heart of the WPWP (northern Papua New Guinea and south of Guam) and around its western edge (western margin of Australia to the south and southern Philippine Islands to the north) to capture the most salient features of the WPWP. Combining marginal and open ocean sites will allow us to study these time intervals at different temporal resolutions. The coring program prioritizes seven primary sites and nine alternate sites in 880–3427 m water depth. This depth range will allow the reconstruction of intermediate and deepwater properties through time.

Schedule for Expedition 363

International Ocean Discovery Program (IODP) Expedition 363 is based on IODP drilling Proposals 799-Full2 and 799-Add (available at **http://iodp.tamu.edu/scienceops/expeditions/pacific_warm_pool.html**). Following ranking by the IODP Scientific Advisory Structure, the expedition was scheduled for the research vessel R/V *JOIDES Resolution*, operating under contract with Texas A&M University. At the time of publication of this *Scientific Prospectus*, the expedition is scheduled to start in Singapore on 6 October 2016 and to end in Guam on 8 December (Figure **F1**). A total of 63 days will be available for the transit, drilling, coring, and downhole measurements described in this report (for the current detailed schedule, see **http://iodp.tamu.edu/scienceops/**). Further details about the facilities aboard the *JOIDES Resolution* can be found at **http://iodp.tamu.edu**.

Introduction

The Indo-Pacific Warm Pool (IPWP) is the largest source of heat for the global atmosphere and a location of deep atmospheric convection and heavy rainfall. Small variations in the sea-surface temperature (SST) of the Western Pacific Warm Pool (WPWP), within the IPWP, influence the location and strength of convection in the rising limbs of the Hadley and Walker circulations, perturbing planetary-scale atmospheric circulation, atmospheric heating globally, and tropical hydrology (Neale and Slingo, 2003; Wang and Mehta, 2008). Seasonal to interannual climate variations in the WPWP are dominated by fluctuations in precipitation associated with the seasonal march of the monsoons, migration of the Intertropical Convergence Zone (ITCZ), and interannual changes associated with variability of El Niño Southern Oscillation (ENSO) (e.g., Ropelewski and Halpert, 1987; Halpert and Ropelewski, 1992; Rasmusson and Arkin, 1993). At present, departures from expected weather patterns associated with ENSO impact the lives of many people not only in the tropics but also in many regions around the world; El Niño events are associated with a nearly global fingerprint of temperature and precipitation anomalies (Ropelewski and Halpert, 1987; Rasmusson and Arkin, 1993; Cane and Clement, 1999).

Considerable uncertainty exists regarding the response of the tropical Pacific climate, primarily precipitation, to rising greenhouse gases because of our limited understanding of past variability of the WPWP and conflicting data-model results. For example, models simulating the response of the equatorial Pacific to greenhouse gas forcing disagree about whether the zonal temperature gradient will increase or decrease and what the implications will be for the Walker circulation and the hydrologic cycle in the tropics. These simulations typically use an ENSO analogy to predict future climate, with the idea that changes in ENSO variation are intimately linked to long-term changes in the equatorial Pacific mean climate state as expressed in the east–west SST gradient. However, recent simulations of global warming effects suggest that the tropical Pacific does not become more El Niño- or La Niña-like in response to increased greenhouse gases (DiNezio et al., 2009). Instead, the new simulations suggest a different equilibrium state, whereby shoaling and increased tilt of the equatorial Pacific thermocline is associated with weakening of the trade winds without a concomitant change in the zonal SST pattern, which is a departure from the ENSO analogy (DiNezio et al., 2010). In turn, changes in the structure of the thermocline can have a major effect on the ocean heat content and thus global climate, which has been documented for the Last Glacial Maximum (LGM) (Ford et al., 2015) and is also suggested to explain today's climate trends (e.g., England et al., 2014). A primary goal of this expedition is to assess the regional expression of climate variability (precipitation and temperature) within the WPWP in the context of changing global background state from the middle Miocene to Late Pleistocene. Drill sites have been chosen to provide broad spatial coverage to capture the most salient features of the WPWP (Figures **F1**, **F2**) at different temporal resolutions from the late Neogene to the present (Figure **F3**). At depth, these sites are bathed by Antarctic Intermediate Water (AAIW) and Upper Circumpolar Deepwater (UCDW) (Figure **F4**) and thus will allow the reconstruction of intermediate and deepwater end-member properties through time and at relatively high resolution.

The causes and extent of past precipitation changes in the WPWP are not well constrained in terms of the relative importance of extra-tropical controls, such as the position of the ITCZ versus equatorial Pacific dynamics, which affect the SST pattern and location of maximum convection (Figure **F5**). Paleo-precipitation records suggest a southward shift in the ITCZ position apparently synchronous with North Atlantic cold events including the Younger Dryas, Heinrich Event 1, and marine isotope stage (MIS) 3 stadials (Stott et al., 2002, 2004; Oppo et al., 2003; Dannenmann et al., 2003, Gibbons et al., 2014). These results are consistent with models that suggest climate conditions at high latitudes influence the position of the ITCZ (Broccoli et al., 2006; Chiang and Bitz, 2005). However, lithologic records of chemical weathering (e.g., Ti/Ca) from Mindanao and northern Papua New Guinea (PNG), which are used as a precipitation proxy (Kissel et al., 2010; Tachikawa et al., 2011), as well as a speleothem record from Borneo (Carolin et al., 2013), show a dominant precession signal but no significant correlation with glacial–interglacial variability, suggesting a strong control of local insolation on regional precipitation. The relatively wide distribution of drill sites within the IPWP and their proximity to riverine inputs will allow us to examine the relationships between tropical Pacific

hydroclimate variability and low/high latitude forcing under different background states.

On secular timescales, the relationships between different equilibrium states of the tropical Pacific, changes in ocean circulation, and their implications for global climate evolution from the middle Miocene through the Late Pleistocene have become a topic of intensive scientific research. Specifically, the long-term Cenozoic cooling was interrupted by periods of relative global warmth during the Middle Miocene Climate Optimum (MMCO; ~17–15 Ma) and the early Pliocene warm period (4.5–3 Ma) (Zachos et al., 2001). This latter interval is of special interest due to a perceived decoupling between global SSTs and variations in atmospheric pCO_2 (e.g., LaRiviere et al., 2012). The early Pliocene warm period is of particular interest as global surface temperatures were ~2–3°C higher than at present (Dowsett et al., 2009), which is comparable with projections for the twenty-first century, whereas atmospheric pCO_2 was arguably similar with today's levels (~400 ppm) (Kürschner et al., 1996; Pagani et al., 2010). Studies suggest that this period was characterized by reduced Pacific zonal temperature gradient due to substantial warming of the eastern equatorial Pacific SST (e.g., Wara et al., 2005). The spatial extent and magnitude of the SST change in the WPWP and their implications for tropical precipitation are currently debated (Brierley et al., 2009; Fedorov et al., 2010; Zhang et al., 2014; Ravelo et al., 2014), and new records from this expedition should contribute to this discussion.

The MMCO was also characterized by a warm and humid climate (Mosbrugger et al., 2005; Bruch et al., 2007), with some evidence for even weaker meridional temperature gradients (Flower and Kennett, 1994; Bruch et al., 2007; Holbourn et al., 2010) than in the Pliocene, although there are very few data particularly from the WPWP to help constrain global temperature gradients. After the MMCO, climate cooled gradually through the late Miocene in many regions but was still warmer than today. It is currently debated whether the WPWP temperature was, on average, similar to today through the late Miocene (Nathan and Leckie, 2009) or significantly warmer (Zhang et al., 2014; Ravelo et al., 2014).

The climate mechanisms that explain past warmth during the MMCO, the late Miocene, and the early Pliocene are not yet fully understood, but greenhouse gas forcing and ocean circulation are considered to be important factors. Recent data suggest that pCO_2 was higher than today during the MMCO (Kürschner et al., 2008; Retallack, 2009; Zhang et al., 2013; Greenop et al., 2014) and in the early Pliocene warm period (Pagani et al., 2010; Seki et al., 2010). However, reconstructions suggest pCO_2 was relatively low in the late Miocene and similar to levels during the Pleistocene, even though climate was relatively warm and Northern Hemisphere ice sheets were only starting to develop. At face value, this indicates that for a given pCO_2 forcing, more than one climate state (i.e., late Miocene warmth and Late Pleistocene glaciation) is possible. Thus, factors other than pCO_2, such as ocean circulation possibly related to tectonic opening or closure of oceanic gateways (Cane and Molnar, 2001; Steph et al., 2010) or different modes of deepwater production and circulation (Woodard et al., 2014), might have played a critical role in determining global climate. In particular, tectonic changes affecting the transport of water from the western Pacific to the Indian Ocean is one of the mechanisms proposed to explain changes in global climate (Cane and Molnar, 2001).

Tectonic and climatic changes in the equatorial Pacific play an important role in determining the low-latitude interocean exchange through their effect on the Indonesian Throughflow (ITF) (Kuhnt et al., 2004). At present, the ITF transports annually 10–15 Sv from the western Pacific to the Indian Ocean and controls interocean heat and salt exchange, likely with major implications for climate variability (Gordon, 2005; Oppo and Rosenthal, 2010). Modern observations indicate that ITF transport is affected by the Pacific–Indian Ocean sea level pressure gradient, which varies interannually with ENSO and seasonally with the East Asian Monsoon (EAM). On longer timescales, sea level changes leading to the exposure and flooding of the Sunda Shelf (Xu et al., 2008; Linsley et al., 2010) and tectonic closure of the Indonesian seaways (Cane and Molnar, 2001; Kuhnt et al., 2004) likely exerted the strongest controls on the properties and strength of the ITF. By comparing records from sites located in the heart of the WPWP and off northwest Australia, near the exit of the ITF into the Indian Ocean, we intend to study the evolution of the Indo-Pacific equatorial thermocline in relation to changes in background climate state and the ITF transport from the late Neogene to present. Using new high sedimentation rate cores will allow us not only to study secular changes in ITF (e.g., Karas et al., 2009, 2011) but also to assess long-term variability at orbital and suborbital timescales.

Background

Studies of climate variability in the WPWP have relied primarily on the low sedimentation rate Ocean Drilling Program (ODP) Hole 806B from the Ontong Java Plateau (OJP), which serves as a warm end-member to monitor broad-scale zonal and meridional gradients throughout the Neogene. Higher resolution sites are available from marginal seas in the western equatorial Pacific, but they are strongly impacted by local processes. Thus, there is a gap in the spatial and temporal coverage of the WPWP that prevents assessment of climate change in this region on various timescales. Over the past decade new coring efforts have demonstrated the possibility of obtaining records from key locations in the WPWP with comparable resolution to records from high-latitude oceans, cave deposits, and ice cores. Although substantial progress in understanding WPWP climate variability has been made by studying long piston cores, there are fundamental questions that cannot be addressed without drilling new sites with a broader spatial distribution and extended temporal resolution.

Our scientific objectives require a wide spatial distribution of IPWP climate records in a variety of geologic settings. Proposed Sites WP-02A, WP-21A, WP-03A, and WP-04A are located on Eocene-age ocean crust of the Caroline plate. Proposed Sites WP-05A, WP-06A, and WP-14A are on Pliocene age ocean crust of the adjacent Manus Basin. Proposed Sites WP-71A and WP-72A are in a fore-arc region south of the New Guinea Trench. Proposed Site WP-09A is located in a complex arc terrain of the southern Philippine Islands, whereas WP-13A is on a basalt edifice in the West Philippine Basin. Proposed Sites WP-11B, WP-12D, WP-12A, and WP-12C are adjacent to some of the world's oldest in situ ocean crust still preserved, just seaward of the continental slope of northwest Australia. Alternate proposed Site WP-15A is a redrill of Site 806, located on the OJP.

Geological setting

Caroline Basin and northern Papua New Guinea

Proposed Sites WP-02A, WP-03A, WP-05A, and WP-71A and alternate proposed Sites WP-04A, WP-06A, WP-14A, WP-21A,

and WP-72A are located within or adjacent to the Caroline Basin north of PNG (Figure F6). The Caroline plate is surrounded on all sides by either subduction zones or weakly organized spreading ridges. Consequently, the region is well suited as an archive of climate signals preserved in open-marine biogenic sediment, free of the complications of submarine fan sedimentation. The wide, aseismic Eauripik Rise, which trends approximately north–south and stands 1000 m above the surrounding seafloor, separates the West and East Caroline Basins. It was formed by a series of northward-trending spreading centers and represents the youngest spreading of the Caroline plate (Hamilton, 1979). This extinct spreading center is characterized by a broad crest at ~2500 m water depth with gently sloping sides. Ocean crust of Eocene to recent age makes up basement in the region of interest. Marine magnetic Anomalies C13–C9 trend roughly east–west, indicating seafloor spreading from 36 to 27 Ma. These anomalies are asymmetrically arranged about relict spreading centers now called the Kiilsgaard and West Caroline Basin Troughs. The asymmetric arrangement of crustal ages was the result of poorly organized back-arc spreading north of a northward-dipping subduction zone in the Oligocene. That ancient volcanic arc is now part of the PNG highlands. The northern edge of the Australian landmass collided with the trench and brought a halt to spreading at ~27 Ma (magnetic Anomaly 9) (Hegarty and Weissel, 1988), and by the early Miocene the subduction orientation had switched, with the Caroline plate subducting beneath the Australian plate north of its former location (i.e., on the north side of what is now PNG) (figure 13 in Hegarty and Weissel, 1988). Plate reorganization during this tectonic rearrangement led to off-axis volcanism in the central Caroline Basin, where the Eauripik Rise is now (e.g., at Deep Sea Drilling Project [DSDP] Site 62), providing a ready explanation for the lack of traceable magnetic lineations across this structural feature.

Complex plate interactions then moved to the northern boundary of the Caroline Plate as two processes developed. First, crust older than 15 Ma encountered younger crust of the Philippine Sea plate and began subducting north and west, forming the Palau, Yap, and Mariana Trenches. Second, based on their alkalic chemistry and progressively younger radiometric ages from west to east (Fischer et al., 1971; Ridley et al., 1974), basalts along the Caroline Islands Ridge erupted on the seafloor from a deep-seated mantle hot spot. Hegarty and Weissel (1988) speculated that the deep root and current topographic relief of the Eauripik Rise are due in part to the passage of this hot spot. Extension with little magmatism produced the Sorol Trough to the north, and extension with volcanism and preserved magnetic isochrons indicate opening of the Ayu Trough to the west during the last 5 Ma.

The last tectonic event following the Neogene reorganization was the generation of ocean crust within the Bismarck Sea plate to form the Manus Basin immediately southeast of the New Guinea Trench (figure 13 in Hegarty and Weissel, 1988). Magnetic isochrons indicate spreading in the north-northwest–south-southeast direction beginning in the late Pliocene (3.5 Ma; Taylor, 1979) in the Manus Basin and elsewhere on the Bismarck Sea plate. This young age explains the shallow depths of most of the Bismarck Sea plate and its ability to override the Caroline plate to form the southward-dipping Manus Trench. Plate kinematic studies, however, indicate that present motion along this new plate boundary is almost entirely left lateral, with little or no convergence.

Proposed Sites WP-02A and WP-21A are located at the northern end of the Eauripik Rise (Figure F6), where it terminates in a tectonically complex region that includes Sorol Fault, Sorol Trough, and Caroline Ridge (Hegarty and Weissel, 1988). Magnetic anomalies are progressively younger northward along the rise (Hamilton, 1979), suggesting that basement underlying proposed Site WP-02A and alternate proposed Site WP-21A is younger than that beneath proposed Site WP-03A and alternate proposed Site WP-04A to the south (Hamilton, 1979). This explains the lower sediment thickness above basement at these sites (~400 m) than at proposed Site WP-03A and alternate proposed Site WP-04A (~700 m).

Proposed Site WP-05A and alternate proposed Sites WP-06A and WP-14A are located south of Manus Island on the North Bismarck microplate on Pliocene-age ocean crust formed by a poorly understood ocean ridge or back-arc spreading system within the Bismarck Sea plate. The lack of modern seismicity along the Manus Trench suggests that left-lateral plate motion is today occurring almost entirely along the very well defined Bismarck Sea seismic lineation trending east–west at roughly 3.5°S latitude, ~100 km south of proposed Site WP-05A and alternate proposed Sites WP-06A and WP-14A. Within this complex tectonic regime, the southwestern side of Manus Basin is considered one of the more stable regions. The seafloor age is unknown but must be relatively young, as the basin formed due to rapid asymmetric spreading along the active Bismarck seismic lineation since 3.5 Ma (Taylor, 1979). Surface currents here are controlled by local winds associated with the southeast trades and the Australian–Asian monsoon system (Kuroda, 2000). Manus Island lies in the path of the South Equatorial Current (SEC) as it is deflected around New Ireland to the east. The proposed drill sites are west of Manus Island where high chlorophyll-a concentrations, indicative of upwelling, are observed when the southeast trade winds are strong (Steinberg et al., 2006).

Proposed Site WP-71A and alternate proposed Site WP-72A are located <50 km offshore of the north coast of PNG in a tectonically complex region east of the Cyclops Mountains and west of the Sepik River estuary (figure 2 in Baldwin et al., 2012). The region is bounded to the south by the Bewani-Torricelli fault zone on land, which links to offshore transform faults that eventually connect with seafloor spreading along the Bismarck Sea seismic lineation to the east (Baldwin et al., 2012). Northwest of the proposed drill sites, the southward subduction of the Caroline plate forms the New Guinea Trench. The continental shelf in this region is exceedingly narrow (<2 km), allowing large amounts of terrigenous sediment discharged from coastal rivers to accumulate in deeper water (Milliman et al., 1999). The proposed drill sites are located in ~1000 m water depth and experience high sedimentation rates due to sediment bypassing of the continental shelf. Monsoon winds control the surface hydrography of the region, such that the New Guinea Coastal Current flows westward over the proposed drill sites during the southeasterly monsoon (Kuroda, 2000), likely delivering sediment from the Sepik estuary and multitudes of other tributaries along the coast. The surface current reverses during the boreal winter northwesterly monsoon (Kuroda, 2000). During the northwesterly monsoon wind regime, the surface sediment plume from the Sepik River is observed to meander out across the Bismarck Sea (Steinberg et al., 2006). The New Guinea Coastal Undercurrent persists in a westward direction year round at a primary water depth of ~220 m, widening and strengthening during the boreal summer (Kuroda, 2000). This undercurrent supplies terrigenous sediment from the near-bottom river plumes to the drill sites. With very high sedimentation rates (~500 m/million years) expected, drilling this pair of sites will provide a record of millennial-scale variability in

the WPWP during the Late Pleistocene with comparable resolution to that of proposed Site WP-09A in Davao Bay to the northwest.

Philippine Islands region

Cenozoic plate interactions affecting the Philippine Islands and adjacent regions have been especially complex. Today the tectonic settings of proposed Site WP-09A and alternate proposed Site WP-13A show few similarities; however, their tectonic histories are related. During the Eocene, at ~40 Ma, both Sites WP-09A and WP-13A were located in the Southern Hemisphere. The Philippine Islands were a volcanic arc along the north side of the Indo-Australian/Philippine Sea plate boundary. A spreading center oriented roughly along the paleoequator was the locus of seafloor spreading that had been generating ocean crust since before 57 Ma (Chron 24), which formed what would eventually become the West Philippine Basin. Hall (1996) suggested that the Benham Rise (alternate proposed Site WP-13A) formed between 45 and 40 Ma along this spreading center due to excess volcanism at or near the ridge axis. Spreading continued to widen the paleo-West Philippine Basin in the north–south direction. Northward motion of the Indo-Australian plate brought PNG into collision with the northward-dipping trench associated with the paleo-southern Philippine Islands and the future location of proposed Site WP-09A.

Spreading within the Philippine Sea plate jumped eastward and changed to east–west opening along a roughly north–south back-arc spreading center at ~25 Ma (Hall, 1996). This formed what is now the Parece Vela Basin due to trench roll-back along the Philippine Sea/Pacific plate boundary. From 25 to 5 Ma, the distance between Sites WP-09A and WP-13A remained relatively constant, although both were carried northward on the western edge of the West Philippine Basin. During this northward journey, the western edge of the Philippine Sea plate shared a convergent to transcurrent plate boundary with the Eurasian plate, adding arc volcanics to the already complex arc and ophiolitic terranes of the Philippine Islands.

The current arrangement of the Philippine Islands was achieved by plate adjustment in the late Neogene when left-lateral transcurrent faulting brought Luzon into close overlap with Mindanao (figure 2 in Hall, 1996). The Philippine Fault runs the length of the Philippine Islands, passing east of proposed Site WP-09A along the land peninsula forming the eastern bank of Davao Bay (Figure **F6**). Without identifiable marine magnetic anomalies in the present Molucca Sea or extreme southwest part of the West Philippine Basin (Figure **F6**) it is difficult to trace the precise motion of the arc fragments that comprise Mindanao. However, the Philippine Trench appeared within the last 5 Ma, consistent with opening of the Ayu Trough, Manus Basin, and other features immediately adjacent to the Caroline plate described previously (Figure **F6**). Since this development, the locations of proposed Site WP-09A and alternate proposed Site WP-13A reside on different plates.

Davao Bay in southern Mindanao Island, where proposed Site WP-09A is located, is directly to the west of the Pacific Trench, where the denser oceanic Philippine plate to the east is being subducted beneath the more buoyant Sunda plate to the west. Sangihe Basin, spaning from the Molucca Sea through the Celebes Sea into Davao Bay, represents the fore-arc basin of the Sangihe arc and has existed since the late Pliocene (Hall and Wilson, 2000). Davao Bay is deeper in the north and is comprised of two basins filled with ~2000 m of hemipelagic carbonates and discrete wind-transported volcanic ash layers (Krause, 1966). Within the basins, there are several irregular and solitary mounds with differences in height of 25–100 m that are supposed to represent deformed swells of the basement (Krause, 1966). Other characteristics of Davao Bay are the left-lateral Cotabato Fault that extends from northwest to southeast Mindanao and the "southern section" of the 1200 km long, sinistral strike-slip Philippine Fault that spans from central Masbate to Davao Bay (Bischke et al., 1990; Pubellier et al., 1999).

Davao Bay provides one of the best areas to retrieve expanded sedimentary sequences for western Pacific paleoceanographic and paleoclimatic studies because sediment in the bay is largely protected from bottom currents and fed by terrigenous material from the Davao River. Assuming an average accumulation rate of 60 cm/ky, the sediment age at 500 m below seafloor (mbsf) corresponds to ~800 ka and at 200 mbsf to 300 ka. These high sedimentation rates offer the potential to resolve Late Pleistocene centennial- to millennial-scale climate variability. Thus, it is possible that this site will become the marine "type section" for centennial- to millennial-scale climate variability in the WPWP for the late Quaternary (~0–500 ka), with comparable resolution to the Greenland ice core and Chinese speleothem records. Furthermore, comparing the record from Davao Bay with those from PNG (Sites WP-71A/72A) will allow us to resolve meridional from zonal controls (e.g., ITCZ movement versus El Niño-like effects, respectively) on the hydroclimate of the WPWP.

Alternate proposed Site WP-13A is located on the northwestern-most edge of the WPWP and is thus suited to assess long-term changes in its extent. The site targets the thickened sedimentary package accumulating on Benham Rise, ~250 km offshore eastern Luzon, in the northern corner of the West Philippine Basin (Shipboard Scientific Party, 1975). Benham Rise is a seismically active extinct volcanic plateau emplaced on the Philippine Sea plate during the early Cenozoic (Hall et al., 1995). The region is bordered to the west–southwest by the Philippine Trench, the southern part of which is active due to underthrusting of the Philippine Sea plate beneath the Philippine Islands (Hall et al., 1995). The Philippine Trench is presently inactive in the north near Benham Rise, possibly due to regional faulting and the underthrusting Eurasian plate, which forms the Manila Trench west of Luzon (Xianglong et al., 2008; Acharya and Aggarwal, 1980).

Northwest Australia

Proposed Sites WP-11B (Timor Sea) and WP-12D and alternate proposed Sites WP-12A and WP-12C (Scott Plateau) are located on the northwest Australian margin adjacent to some of the oldest ocean crust still in the world's ocean (figure 1 in Blevin et al., 1997). This region has remained a stable passive margin since the breakup of Gondwanaland and the separation of northwest Australia from a long-disappeared Tethyan landmass. The northward movement of the Indo-Australian plate relative to the Eurasian and other microplates of southeast Asia subducted much of this old ocean floor beneath Eurasia. At present, the continent/ocean boundary, as defined by identifiable magnetic anomalies, lies ~200 km seaward of the drill sites. Proposed Site WP-11B is situated at the northwestern margin of northeast-trending Browse Basin, which underlies the Australian northwest margin between the onshore Kimberley Basin and the Scott Plateau (Symonds et al., 1994). Alternate proposed Sites WP-12A and WP-12C and proposed Site WP-12D are located on the Scott Plateau, which corresponds to a subsided platform area that forms the northwestern flank of Browse Basin. The Mesozoic section beneath the plateau is strongly influenced by breakup-re-

lated volcanism, which forms the acoustic basement through much of the Scott Plateau area (Stagg and Exon, 1981). The postbreakup sedimentary succession forms an ~2000 m thick, relatively uniform blanket over Scott Plateau and the northeastern margin of Browse Basin. During the Pleistocene to late Miocene, a continuous succession of deepwater, clay-rich nannoplankton ooze was deposited in this area with average sedimentation rates of ~5–9 cm/ky (proposed Site WP-11B) and ~3–3.5 cm/ky (alternate proposed Sites WP-12A and WP-12C and proposed Site WP-12D). This well-preserved and complete sediment succession provides an ideal archive to reconstruct the climate and circulation history at the southwestern edge of the IPWP.

The location of these sites is within the prominent hydrographic front that separates tropical and subtropical water masses, which makes them suitable to monitor changes in the southward extent of tropical warm water related either to circulation or global climate trends. Sites WP-11B, WP-12A, WP-12C, and WP-12D are located close to the oceanographic front between relatively cool, nutrient-rich water carried northward in the Eastern Indian Ocean by the West Australian Current and warm, oligotrophic Leeuwin Current waters, which results in a steep north–south SST gradient (Figure **F2**). This strategic location will allow reconstruction of the southwestern extent of the IPWP and monitoring of the ITF outflow into the Indian Ocean. We target two closely located sites with different Pleistocene sedimentation rates that will enable reconstruction of Pleistocene–Pliocene climate variability on suborbital timescales at proposed Site WP-11B, whereas the Lower Pleistocene sedimentation rates at alternate proposed Sites WP-12A and WP-12C and proposed Site WP-12D will allow penetration down to the middle Miocene reflector. This prominent reflector marks the major eustatic sea level fall at ~13.8 Ma that is associated with the main expansion of the East Antarctic Ice Sheet during the Neogene. Recovery of a middle to upper Miocene continuous succession in the eastern Indian Ocean will provide an exceptional, continuous paleoceanographic archive that will complement records from the Pacific, Atlantic, and Southern Oceans and will be crucial in constraining regional and global circulation modes and Miocene ice volume variations. The older record from Sites WP-12A, WP-12C, and WP-12D is also ideally suited to test the hypothesis of a major restriction of warm water throughflow originating from the South Pacific between 3 and 5 Ma (Cane and Molnar, 2001).

Ontong Java Plateau

Alternate proposed Site WP-15A (redrill of Site 806; 0°19.11′N, 159°21.69′E; 2520 m water depth) is located on the northeastern margin of the OJP close to the equator (Kroenke, Berger, Janecek, et al., 1991). The OJP forms a broad oceanic plateau in the western equatorial Pacific, north of the Solomon Islands. With an area of ~2 million km^2, the OJP represents the world's largest oceanic plateau of volcanic origin. It was emplaced during two major pulses of volcanism at ~122 and ~90 Ma, and over much of its more recent Cenozoic history it appears to have maintained its present depth (Kroenke, Berger, Janecek, et al., 1991). Its surface rises to ~1700 m in the central part but generally lies between 2 and 3 km water depth. The OJP is characterized by a thick pelagic sediment cover, which makes it ideally suited for paleoceanographic studies. The thickness of the sediment at Site 806 is ~1200 m, and a near continuous section was recovered from three holes. The drilled succession exhibits an average sedimentation rate of 30 m/million years and extends to the base of the Miocene (Kroenke, Berger, Janecek, et al., 1991). The deepest hole, 806B, was cored with the advanced piston corer (APC) to refusal (320 mbsf), reaching the lower upper Miocene. This hole was deepened with the extended core barrel (XCB) downhole to 743.1 mbsf and was terminated in the lowermost Miocene because of poor recovery. Over the years, Site 806 has become a reference site to monitor large-scale zonal and meridional gradients in the WPWP through the Miocene to Pleistocene (e.g., Lea et al., 2000; de Garidel-Thoron et al., 2005; Zhang et al., 2014; Ford et al., 2015). This sedimentary archive is now becoming depleted and redrilling Site 806 would offer the opportunity to extend previous investigations and to apply new state-of-the-art climate proxies at this strategic WPWP location.

Seismic studies and previous drilling

Caroline Basin and northern Papua New Guinea

At proposed Site WP-02A, horizontally bedded strata continue downward to ~70 mbsf, where reflector geometry shows a dramatic change in depositional process. From ~3.26 to ~3.60 s two-way traveltime (TWT), there is an apparently uninterrupted accumulation of current-controlled mud waves, with the exception of a possible break at 3.27 s. Other multichannel seismic (MCS) lines in the survey grid surrounding proposed Site WP-02A show these mudwaves as well. They are ~1 km in wavelength and oriented southwest–northeast (perpendicular to Line wp21) with 15–18 m maximum amplitudes that gradually decrease upsection. The presence of these features had not been anticipated before surveying this site and presents an opportunity to recover a several million–year record of current-controlled bedforms together with the information that such an archive reveals. When extrapolating the Pleistocene sedimentation rate of 1.5 cm/ky, this 270 m interval corresponds to ~18 million years of mudwave deposition. However, based on previous mudwave studies, sedimentation rates are likely to be several times this estimate. This pattern began sometime in the middle to late Miocene and was remarkably continuous until the Pleistocene. This allows us the opportunity to link the vigor of intermediate water circulation at proposed Site WP-02A to a global record of high-latitude forcing. The proposed penetration at Site WP-02A is 250 mbsf (estimated age of ~17 Ma), but we are approved to drill to 430 mbsf. Proposed penetration at alternate proposed Site WP-21A is 100 mbsf, with an estimated age at this depth of ~5 Ma (Table **T1**).

Proposed Site WP-03A on the southern edge of the Eauripik Ridge is ~15 nm northwest of DSDP Site 62 and close to the location of Core MD97-2140, previously used to reconstruct the Pleistocene SST history of the WPWP (de Garidel-Thoron et al., 2005). The site is characterized by pelagic carbonate-rich sediment with good preservation and a sedimentation rate of ~2.1 cm/ky throughout the Pleistocene (de Garidel-Thoron et al., 2005). Site 62 recovered a nearly continuous sequence of upper Oligocene–Quaternary chalk and carbonate-rich ooze (Winterer et al., 1971). The age model for this site suggests higher sedimentation rates (up to 4 cm/ky) during the middle–late Miocene and then decreasing in the Pliocene and Pleistocene. Target penetration at proposed Site WP-03A is 300 mbsf (estimated age of ~15 Ma) with maximum allowable depth of 500 mbsf. Alternate proposed Site WP-04A (~82 km to the west of proposed Site WP-03A) is intended mainly for recovering pore water $\delta^{18}O$ and salinity records for the LGM, with planned penetration to 150 mbsf (Table **T1**).

The MCS profiles at proposed Site WP-05A and alternate proposed Sites WP-06A and WP-14A south of Manus Island show a relatively uniform hemipelagic sediment cover, with basement at

~225 mbsf. Proposed Site WP-05A and alternate proposed Site WP-06A are located upslope from Core MD05-2920, which has an isotope record indicating a sedimentation rate of ~10–14 cm/ky, substantially higher than in other open-ocean Pacific sites and without discernible disturbance for the past ~400 ky (Tachikawa et al., 2011, 2013). The high accumulation rate reflects the large input of terrigenous sediment eroded from PNG due to high precipitation rates and then its transfer by ocean currents to this area. The $CaCO_3$ content ranges from 25% to 45% over the past ~400 ky, and the foraminifers are well preserved. Assuming the sedimentation rate does not change much with depth, recovery of a complete Pleistocene record is expected. DSDP Site 63 (Winterer et al., 1971) is the closest drilled site, located 450 km northeast of Sites WP-05A and WP-06A in a water depth of 4472 m on 35 Ma old crust in the East Caroline Basin. This water depth indicates that the site was below the calcite compensation depth and located largely north of the reach of sedimentation from the Sepik and other PNG rivers during the 0–3.5 Ma time interval of interest. Quaternary–Pliocene sediments were continuously cored at Site 63 from 0–25 mbsf and are comprised of calcareous pelagic clay. We plan to core to 200 mbsf (estimated age of ~2.2 Ma) at proposed Site WP-05A. Similar records would be recovered at alternate proposed Sites WP-06A and WP-14A, with proposed penetrations of 200 mbsf (~2.2 Ma) and 175 mbsf (~1.9 Ma), respectively (Table **T1**).

The MCS survey of Sites WP-71A and WP-72A shows >650 m sediment thickness in both locations. The RR1313 MCS data suggest that the sedimentation rate in the upper part of the sediment column is higher at alternate proposed Site WP-71A, whereas the sedimentation rate in the deep portion is higher at alternate proposed Site WP-72A. Therefore, we propose to drill to 225 mbsf at proposed Site WP-71A (~0.5 Ma) or to 315 mbsf at alternate proposed Site WP-72A (~0.6 Ma) (Table **T1**). The goal is to reach beyond MIS 13 (>0.5 Ma) so that the combined record spans the mid-Brunhes event. As defining the chronology of these marginal sites may be challenging, we will drill either past the nannofossil Zone NN19/NN20 boundary (~440 ka, near the end of MIS 12) or to the approved target depth if we do not reach that boundary. An isotope record from a 7 m long piston core (RR1313 23PC) located close to proposed Sites WP-71A and WP-72A indicates that the Holocene extends over ~6 m, implying sedimentation rates of ~50–60 cm/ky. The sediment consists of a mixture of clay and volcanic sand containing planktonic and benthic foraminifers with pristine (glassy) preservation.

Philippine Islands

Swath bathymetry surrounding proposed Site WP-09A together with the MCS lines that intersect at the drill site provide first-order estimates of the type of sediment that will be found in the subsurface. Local bathymetry suggests that bedload sediment flows out of Davao Bay from the north and travels south to the area surrounding the proposed drill site. Fine-grained suspended load during episodes of especially voluminous bedload events can be expected to spread laterally and blanket the flanks of the north–south ridges located on either side. Site WP-09A is located on the flank of one such topographic high that runs approximately north–south along 125°54′E. Such suspension "overflows" and the large amount of suspended sediment that settles on this site at less energetic times have built a thick mantle of silty clay on the flank of this ridge. High-productivity surface water provides a steady rain of biogenic material as well, and the result is an excellent archive of climate variability in a key location.

The seismic facies around proposed Site WP-09A are relatively uniform and suggest continuous sedimentation. Sediment thicknesses available from the National Geophysical Data Center indicate ~3800 m of sediment resting on the basement at proposed Site WP-09A (Divins, 2003); however, the maximum depth of undisturbed sediment at the site location is ~318 mbsf. Five piston cores (MD98-2181, MD06-2069, MD06-2071, MD06-2073, and MD06-2075) were collected in Davao Gulf, close to proposed Site WP-09A. The sediment in these cores consists of nannofossil ooze with a variable terrigenous component and irregularly dispersed ash layers (Laj et al., 2006). These cores provide insights on the hydrology of the WPWP and millennial-scale variability of the EAM over the past ~150 ka (Stott et al., 2002; 2004; Saikku et al., 2009; Bolliet et al., 2011; Fraser et al., 2014). No deeper drilling is available in the vicinity of proposed Site WP-09A. We propose coring to 350 mbsf (~0.6 Ma) at proposed Site WP-09A, with a maximum allowable penetration of 500 mbsf (Table **T1**).

Alternate proposed Site WP-13A is located 28 km north-northeast of DSDP Site 292 (Karig, Ingle, et al., 1975). Although Site 292 is located on the northwestern flank of a significant bathymetric mound (Benham Rise), alternate proposed Site WP-13A is on relatively flat seafloor on a topographic plateau characterized by evenly laminated acoustic reflectors to ~350 mbsf. Drilling at Site 292 to ~450 mbsf recovered a Cenozoic sediment record consisting of hemipelagic to pelagic calcareous ooze interbedded with volcaniclastics with a sedimentation rate of 8 m/million years (Horng et al., 2003; Shipboard Scientific Party, 1975). Recovery in the uppermost 175 mbsf was variable (40%–100%) and generally low deeper than that. A major unconformity at ~115 mbsf is associated with the middle Miocene sea level fall at ~13.8 Ma. The sedimentation rate appears to have been slightly higher (~12 m/million years) prior to the hiatus. Although we do not anticipate occupying this alternate site, we are approved to core to 280 mbsf (~35 Ma) (Table **T1**).

Northwest Australia

Proposed Site WP-11B is situated at the cross-point of seismic Lines BR98-117 and BR98-168, ~0.8 nm southeast of the ~40 m long piston Core MD01-2378, which provides excellent insights into Late Pleistocene sedimentation and stratigraphy at this location. The interpretation of Miocene seismic reflectors is based on comparison to the AGSO regional seismic survey Line 119-04 (well control by Buffon 1 and Brewster 1A) and the BBHR Line 175/10 (well control of distal part by Argus 1). A major unconformity marks the top of the prograding sequence at 0.72 s TWT below seafloor and is interpreted as the middle Miocene sequence boundary corresponding to a major sea level drop associated with rapid expansion of the Antarctic Ice Sheet (Mi-3; 13.8 Ma). We propose coring to 350 mbsf (~3.9 Ma) at proposed Site WP-11B but are approved to core as deeply as 700 mbsf (Table **T1**).

Alternate proposed Site WP-12C is located at the cross-point of seismic Lines HBR2000A-3032 and BR98-84, whereas proposed Site WP-12D is located ~600 m northwest of this cross-point on Line HBR2000A-3032. Alternate Site WP-12A is located near the cross-points of seismic Lines AGSO 119-2 and HB2000A-3003 and seismic Lines AGSO 119-2 and BR98-017. The top of the first prominent reflector corresponding to the middle Miocene sequence boundary (Mi-3; 13.8 Ma) is 0.55 s TWT below seafloor. Assuming the same depth-velocity relationship as for proposed Site WP-11B, the drilling depth to reach this reflector is ~500 mbsf, resulting in an average Neogene sedimentation rate of 3.5 cm/ky, which is slightly lower than the Late Pleistocene sedimentation rate

(4.4 cm/ky for MIS 1–6) in nearby gravity Core SO185-18499 (14°54.49′S, 120°34.0′E; 1383 m water depth). Coring to 490 mbsf at this site will extend the high-resolution paleoceanographic record of proposed Site WP-11B in intermediate resolution back to ~14 Ma (Table **T1**).

Proposed Site WP-11B is situated close to Core MD01-2378 at the northwestern margin of the Scott Plateau, where the Timor Sea merges with the western Indian Ocean. Ship track, echosoundings of coring locations, core descriptions, and multisensor track measurements were published in the WEPAMA cruise report (Bassinot and Blatzer, 2002). Isotope stratigraphy (MIS 1–12) and a reconstruction of paleoproductivity fluctuations are available in Holbourn et al. (2005). Alternate proposed Sites WP-12A and WP-12C and proposed Site WP-12D are situated near gravity Core SO185-18499 on the Scott Plateau. Ship track, echosoundings of coring locations, initial core descriptions, and multisensor track measurements were provided in the SO185 VITAL cruise report (Kuhnt et al., 2005). DSDP Site 261 (~5670 m water depth) and ODP Site 765 (~5710 m water depth) were drilled in the Argo Abyssal Plain, northwest of proposed Sites WP-11B and WP-12D and alternate proposed Sites WP-12A and WP-12C. Drilling at Site 262 (~2300 m water depth), located northeast of proposed Sites WP-11B and WP-12D and alternate proposed Sites WP-12A and WP-12C, recovered a thick (>400 m) sequence of partially redeposited Pliocene–Pleistocene clay-rich nannofossil ooze that accumulated in the rapidly subsiding Timor Trough. Drilling at ODP Sites 759–764 on the Exmouth and Wombat Plateaus, to the southwest of proposed Sites WP-11B and WP-12D and alternate proposed Sites WP-12A and WP-12C, recovered thick successions of shallow-water carbonates and deltaic deposits of Triassic to Cretaceous age that are overlain by thinner, hemipelagic Cenozoic sequences.

Ontong Java Plateau

The original seismic profiles across the OJP were taken during the ROUNDABOUT survey cruise on board the *Thomas Washington* in December 1988. The detailed survey conducted in the area of ODP Site 806 (Dasher; 2600–2800 m water depth) shows gently dipping parallel reflectors with little disturbance except at depths below 800 mbsf (Mayer et al., 1991). Seafloor topography is generally flat, and individual reflectors can be correlated over large distances in this part of the OJP (figures 3 and 9 in Mayer et al., 1991). The parallel reflectors indicate that pelagic sedimentation processes dominate in the vicinity of Site 806. The location of Site 806 was selected as a primary target for Leg 130 because it showed a slightly expanded section that was not subjected to apparent erosion (Mayer et al., 1991). Should we occupy alternate proposed Site WP-15A, we propose to core to 500 mbsf (~16.7 Ma) (Table **T1**).

The supporting site survey data for Expedition 363 are archived at the IODP Site Survey Data Bank. Data can be accessed at **http://ssdb.iodp.org/SSDBquery/SSDBquery.php** by selecting the appropriate proposal number.

Scientific objectives

The proposed sites have wide spatial coverage (Figure **F1**; Table **T1**) at variable temporal resolution that will allow us to address the following areas.

Role and response of the WPWP to millennial-scale climate variability

The origin of sub-Milankovitch climate variability and its spatial and temporal extent are significantly less understood than mechanisms related to orbital climate forcing. Most hypotheses attribute millennial-scale changes during the last glacial interval to either instabilities in the Northern Hemisphere ice sheets (e.g., MacAyeal, 1993) or a response to variations in Atlantic thermohaline circulation (e.g., Rahmstorf, 2002) driven by meltwater inputs to the North Atlantic (e.g., Clark et al., 2001, 2004). Much of the evidence for suborbital climate variability and its glacial amplification comes from the North Atlantic and regions that are directly affected by temperature or thermohaline variations in the North Atlantic. In low-latitude and tropical regions, millennial-scale variability is mainly expressed as changes in precipitation, which are synchronous with the North Atlantic climatic oscillations. The global extent and apparent synchroneity of millennial-scale variability have been attributed to fast transmission of climate signals through the atmosphere in response to North Atlantic climate change (Schmittner et al., 2003; Gibbons et al., 2014). However, other studies suggest an important role of the tropical ocean due to orbital modulation of tropical dynamics possibly related to the monsoon and ENSO variability in response to changes in the mean climate state of the equatorial Pacific (Clement et al., 2001; Koutavas et al., 2002, 2006; Stott et al., 2002). Accordingly, changes in the distribution of tropical Pacific SST may have large impacts on global temperatures (Clement et al., 2001; Brown et al., 2015) and low- to mid-latitude heat and moisture transport, which can amplify small radiative perturbations (Tachikawa et al., 2013).

As a major source of heat and moisture, the WPWP may have played an important role in millennial-scale variability through changes in its extent and hydrography. Obtaining extended records from the WPWP with comparable resolution to the Greenland ice cores, Chinese speleothems, and high-resolution sediment cores from other regions will provide better insights into the mechanisms causing centennial- to millennial-scale climate variability in the context of varying background climate states. Specifically, we plan to

- Document the spatial and temporal extent of climate variability in the WPWP and assess whether it is expressed primarily in the hydrologic cycle and/or in SST variability.
- Assess the relationships between global ice volume and the magnitude of millennial-scale climate variability in the WPWP. We seek to determine whether there is an ice volume threshold to the appearance of millennial-scale variability in the tropical Pacific.
- Document the response of the thermocline and intermediate water masses to millennial-scale variability in the WPWP in relation to tropical and extra-tropical forcings.

Modern sedimentation rates at proposed Sites WP-09A and WP-71A and alternate proposed Site WP-72A exceed 50 cm/ky, thus providing the potential to resolve Late Pleistocene centennial- to millennial-scale climate variability in different regions of the IPWP. Comparing these high-resolution records with comparable ones from the North Atlantic and eastern equatorial Pacific will al-

low us to better constrain the mechanisms influencing millennial-scale variability and its effects around the globe.

Orbital-scale climate variability and secular trends since the middle Miocene

Significant glacial–interglacial variability characterizes SST and $\delta^{18}O_{seawater}$ reconstructions from the WPWP with the amplitude increasing from ~2°C in the Pliocene to 3°C in the Pleistocene (de Garidel-Thoron et al., 2005; Medina-Elizalde and Lea, 2005, 2010). Because the tropical Pacific is located far from the polar ice sheets, studies have suggested that the glacial–interglacial variability of tropical Pacific SST is mostly driven by changes in atmospheric pCO_2 (e.g., Lea, 2004; Hansen et al., 2008) and to a lesser extent by changes in local insolation (e.g., Tachikawa et al., 2013). Lithologic proxy records of precipitation from the western equatorial Pacific suggest that precession-driven interhemispheric changes in local insolation exert the strongest control on the equatorial Pacific hydroclimate, primarily associated with the migration of the ITCZ (Kissel et al., 2010; Tachikawa et al., 2011) and possibly modulated by ENSO-type processes (Dang et al., 2015). In contrast with millennial-scale events, during the last few glacial cycles there appears to have been no clear linkage between tropical precipitation and glacial–interglacial changes in the North Atlantic (e.g., Kissel et al., 2010; Tachikawa et al., 2011; Carolin et al., 2013). However, recent studies suggest that the southward position of the ITCZ associated with a weak EAM might have played an important role in the inception of glacial terminations through its influence on the position of the southwesterly winds and, thus, the upwelling of CO_2-rich deep water around Antarctica (Denton et al., 2010; Anderson et al., 2009). Modeling studies supported with new records confirm the idea of "interhemispheric teleconnection," whereby warming (cooling) the Northern Hemisphere causes both the ITCZ and the Southern Hemispheric mid-latitude jet to shift northward (southward) (Lee et al., 2011; Ayliffe et al., 2013; Ceppi et al., 2013). Investigating these interconnections and their evolution under different background climate states throughout the Neogene to Late Pleistocene is one of the overarching goals of this expedition. Currently, interpretations with profound implications for predicting warm climate dynamics rest heavily on data from a few sites, mainly the legacy ODP Site 806 on the OJP, which serves as the warm end-member used to monitor broad-scale zonal and meridional gradients. Thus, there is a gap in the spatial coverage needed to allow assessment of meridional changes in the extent of the WPWP. Indeed, based on available records, the magnitude of the contraction of the WPWP is unclear (Jia et al., 2008; Russon et al., 2010). The proposed north–south transect of new drill sites will fill this gap and allow us to

- Determine the spatial extent of SST variability in the WPWP under different climate background states in relation to changes in radiative forcings (CO_2 and insolation) and equatorial hydrography (ITCZ shifts and thermocline structure) to better constrain climate sensitivity throughout the Neogene to Late Pleistocene;
- Reconstruct the evolution of the Australian-Asian Monsoon system and WPWP precipitation using multiple sites in the IPWP;
- Assess the contribution of changes in the monsoon system and WPWP hydroclimate to the inception of glacial terminations;
- Reconstruct intermediate and deep water temperatures, heat content, and carbonate chemistry to assess their relation to surface processes over orbital and secular time scales; and
- Assess whether the trends observed during the Holocene are typical of other interglacials with similar orbital forcings to test the hypothesis that anthropogenic CO_2 has significantly affected the late Holocene climate (Ruddiman, 2005).

Proposed Sites WP-05A and WP-11B, in addition to proposed Sites WP-71A and WP-09A and alternate proposed Site WP-72A, will provide insights on orbital-scale variability during the Pliocene and Pleistocene at high resolution (40–100 m/million years). Sites WP-05A, WP-71A, and WP-72A are ideally located to monitor the contribution from the New Guinea Coastal Current and Undercurrent and AAIW, which are the southern branches of the westward, cross-equatorial flowing SEC, and constitute the main southern Pacific contributions to the ITF (Figure **F2**). Proposed Sites WP-02A, WP-21A, WP-03A, and WP-12D and alternate proposed Sites WP-12A and WP-12C (and Site WP-13A if drilled) will document secular trends throughout the Neogene to Late Pleistocene.

Changes in the ITF

There are several outstanding questions about the long-term evolution of the ITF in response to

1. Tectonic and bathymetric changes in the Indonesian Archipelago,
2. Changes in the mean climate state of the WPWP, and
3. Orbital- and millennial-scale variability.

For example, tectonic changes in the Indonesian region between ~5 and 3 Ma, associated with the northward movement of PNG, are thought to have been important in reducing the contribution of warm southern Pacific water to the ITF, whereas the northwestern Pacific contribution increased (Cane and Molnar, 2001). This led to cooling of the Indian Ocean thermocline and surface water (Karas et al., 2009, 2011), which may have been a key factor in the aridification of East Africa and hominid evolution (Cane and Molnar, 2001). With the new high sedimentation rate cores we will be able to

- Reconstruct ITF variability on millennial to orbital timescales in relation to climatic and tectonic changes since the middle Miocene.

Proposed Sites WP-11B and WP-12D and alternate proposed Sites WP-12A and WP-12C are suited to address these questions and will be compared with the records recovered at proposed Sites WP-03, WP-05A, and WP-09A.

Interstitial water studies

The LGM left the ocean ~3.5% enriched in salt and ~1.0‰ enriched in $\delta^{18}O$ from the growth of land-based ice sheets. We propose to reconstruct the local enrichment in these two quantities at two sites by measuring the interstitial fluid profiles downhole to ~100 mbsf and applying a 1-D advection/diffusion equation to estimate the amplitude of the LGM boundary condition. This approach reconstructs the salinity, and when combined with foraminiferal $\delta^{18}O_{calcite}$, the temperature of the LGM ocean. Whereas most of the LGM deep ocean was at or near freezing, there was a larger range in salinity than there is in the modern ocean (Adkins et al., 2002). The saltiest water formed around Antarctica in the past as opposed to around Greenland today. Overall the picture is of a salinity-stratified ocean with different water mass geometries. However, to date there is only one record from the southern Pacific Ocean (ODP Site 1123). The most important next step is to drill a geographically focused bathymetric transect that will provide LGM profiles of tem-

perature, salinity, and $\delta^{18}O$ of the water column. This proposal targets Pacific sites that fall between ~1 and ~3 km water depth, which represents a nearly ideal set. We plan to measure the $[Cl^-]$ and $\delta^{18}O$ of interstitial water at two sites (sampling the upper ~100 mbsf of the core at ~1.5 m resolution) to create a past ocean profile of the deepwater structure. This will allow us to address two major objectives:

1. To generate interstitial water profiles of salinity and $\delta^{18}O$ to reconstruct the LGM salinity and temperature of intermediate and deep Pacific water masses and
2. To generate interstitial water profiles that will be used to reconstruct secular changes in seawater chemistry (elemental and isotopic variations in B, Li, Mg, Ca, S and Sr, for example).

LGM insterstitial water $\delta^{18}O$ will be measured at proposed Sites WP-03A and WP-05A (or alternate proposed Sites WP-04A and WP-06A).

Drilling and coring strategy

Expedition 363 aims to achieve an ambitious coring program that prioritizes seven primary sites and nine alternate sites in 880–3427 m water depth (Tables **T1**, **T2**, **T3**). Two of the sites are in Philippine waters (proposed Site WP-09A and alternate proposed Site WP-13A), three sites are in Australian waters (proposed Site WP-12D and alternate proposed Sites WP-12A and WP-12C), one primary site is within the Australian seabed treaty area with Indonesia (proposed Site WP-11B), five are in PNG waters (proposed Sites WP-71A and WP-05A and alternate proposed Sites WP-72A, WP-06A, and WP-14A), four sites are in the Federated States of Micronesia waters (proposed Sites WP-02A and WP-03A and alternate proposed Sites WP-04A and WP-21A), and one site is in international waters (alternate proposed Site WP-15A) (Table **T1**). In addition to the primary operations plan (Table **T2**), we have an alternate operations plan (Table **T4**) should we be unable to occupy primary Site WP-09A (located in Davao Bay) due to separatist/terrorist activity. The final operations plan and number of sites to be cored is contingent upon the *JOIDES Resolution* operations schedule, operational risks (see **Risks and contingency**), and the outcome of requests for territorial permission to occupy these sites. This expedition includes significant transit (~19 days in the primary operations plan), and should ship speed be less than the estimated average of 10.5 kt, the drilling schedule could be significantly impacted.

The planned sequence of drill sites, coring/downhole measurements, and time estimates are provided in Tables **T2**, **T3**, and **T4**. The sites will be occupied to minimize transit and maximize operational efficiency. The coring strategy will consist of double- or triple-APC coring using nonmagnetic core barrels at each site to ~250 mbsf or refusal and then deepening two of the holes to the target depth (if necessary) using the XCB. Triple-APC holes will allow us to construct a complete stratigraphic section at each site for the upper ~250 mbsf, and double XCB should allow us to extend the composite section deeper at proposed Sites WP-12D, WP-11B, and WP-03A. At this time, all APC cores will be oriented using the Icefield MI-5 tool. Temperature measurements will be taken in Hole A at each site using the advanced piston corer temperature tool (APCT-3). Downhole wireline logging is planned only at proposed Site WP-12D.

For planning purposes, the APC refusal depth is estimated at 250 mbsf, although we anticipate this may be exceeded at some of the more mud rich sites with target depths greater than 250 mbsf. APC refusal is conventionally defined as a complete stroke (determined from the standpipe pressure after the shot) not being achieved because the formation is too hard and/or excess force (>100,000 lb) is required to pull the core barrel out of the formation because the sediment is too cohesive or "sticky." In cases where a significant stroke can be achieved but excessive force cannot retrieve the barrel, the core barrel can be "drilled over" (i.e., after the core barrel is successfully shot into the formation, the bit is advanced to some depth to free the core barrel). When APC refusal occurs in a hole before the target depth is reached, the half-length APC (HLAPC) system may be used to deepen the hole before switching to the XCB system.

According to the current primary operations plan, Expedition 363 will core ~6015 m of sediment and potentially recover ~5669 m of core. The estimated amount of core recovered is based on 100% recovery with the APC system and 65% recovery with the XCB system.

Downhole measurements strategy

Formation temperature measurements

We plan to use the APCT-3 to measure formation temperature in the first hole of each site to reconstruct the thermal gradient. This tool can only be deployed with the APC system. The operations plan includes four temperature measurements per site, typically beginning with the fourth core. Should the first three measurements be successful, we may opt not to take a fourth measurement to save time.

Core orientation

We plan to orient all APC cores with the Icefield MI-5 tool. This tool will be used in conjunction with nonmagnetic coring hardware to the maximum extent possible.

Downhole wireline logging

The downhole wireline logging plan aims to provide a broad set of physical property measurements that can be used for characterization of in situ formation properties (e.g., lithology, structure, and petrophysics) and orbital- and millennial-scale cyclicities. The plan includes deploying two standard IODP tool strings in the final hole at proposed Site WP-12D (Table **T2**). Coring is the top priority at this site, and the scheduled logging program may be modified or abandoned if the coring objectives are not met in the allotted time.

The first logging run will be the triple combination (triple combo) tool string, which logs formation resistivity (High-Resolution Laterolog Array/Phasor Dual Induction-Spherically Focused Resistivity Tool), density (Hostile Environment Litho-Density Sonde), porosity (Accelerator Porosity Sonde), natural gamma radiation (NGR; Hostile Environment NGR Sonde/Enhanced Digital Telemetry Cartridge), and borehole diameter. The Magnetic Susceptibility Sonde (MSS) may be added to the triple combo tool string in place of the porosity tool to provide magnetic field and magnetic susceptibility information. The borehole diameter log provided by the caliper on the density tool will allow assessment of hole conditions (e.g., washouts of sandy beds), log quality, and the potential for success of the following run(s).

The second logging run will be the Formation MicroScanner (FMS)-sonic tool string, which provides an oriented resistivity image of the borehole wall and logs of formation acoustic velocity, NGR, magnetometry from the fluxgate magnetometer on the General Purpose Inclinometry Tool, and borehole diameter. To provide a link between borehole stratigraphy and the seismic section, sonic velocity and density data can be combined to generate synthetic seismograms for detailed well-seismic correlations. The NGR tool is run with the FMS-sonic tool string to provide a means to depth-match the different logging runs.

Risks and contingency

The potential risks identified are as follows:

- Obtaining approval from the Philippines, Australia, PNG, and the Federated States of Micronesia to conduct drilling and coring operations in their territorial waters.
- Unstable hole conditions that can impact coring and downhole logging operations. If the risk is considered to be significant, the radioactive source will be left out of the density tool during logging.
- The presence of sand beds or unconsolidated volcaniclastics that can be detrimental to core recovery.
- The expedition is scheduled to begin near the end of the peak cyclone season (October) in the Pacific, so weather could have some impact on operations.
- An extremely ambitious operations plan for the time available. Good time management will be extremely important to mitigate this risk.
- Potential separatist/terrorist activity in Mindanao, Philippines, which could preclude us from conducting operations at proposed Site WP-09A.

All of these factors may affect drilling, coring, and downhole logging operations.

Sampling and data sharing strategy

Shipboard and shore-based researchers should refer to the IODP Sample, Data, and Obligations Policy and Implementation Guidelines (**http://www.iodp.org/program-policies/**). This document outlines the policy for distributing IODP samples and data to research scientists, curators, and educators. The document also defines the obligations that sample and data recipients incur. The Sample Allocation Committee (SAC) will work with the entire scientific party to formulate a formal expedition-specific sampling plan for shipboard and postexpedition sampling. The SAC is composed of the Co-Chief Scientists, Expedition Project Manager/Staff Scientist, and IODP Curator on shore or curatorial representative on board the ship.

Every member of the science party is obligated to carry out scientific research for the expedition and publish the results. Shipboard and potential shore-based scientists are expected to submit sample and data requests using the Sample and Data Request Database (**http://iodp.tamu.edu/sdrm/**) at least 4–5 months before the beginning of the expedition. Based on shipboard and shore-based research plans submitted by this deadline, the SAC will prepare a tentative sampling plan, which will be revised on the ship as dictated by recovery and cruise objectives. The sampling plan will be subject to modification depending upon the actual material recovered and collaborations that may evolve between scientists during the expedition. The SAC must approve modifications of the strategy during the expedition. Given the specific objectives of Expedition 363, great care will be taken to maximize shared sampling to promote integration of data sets and enhance scientific collaboration among members of the scientific party so that our scientific objectives are met and each scientist has the opportunity to contribute. All sample frequencies and sizes must be justified on a scientific basis and will depend on core recovery, the full spectrum of other requests, and the expedition objectives. Some redundancy of measurement is unavoidable, but minimizing the duplication of measurements among the shipboard party and identified shore-based collaborators will be a major factor in evaluating sample requests. Substantial collaboration and cooperation will be required.

Shipboard sampling will be restricted to acquiring ephemeral data types and shipboard measurements. Limited low-resolution sampling for personal research to help target postexpedition sampling will be at the discretion of the SAC. The data collected during the expedition will be used to produce stratigraphic spliced sections and age models for each site, which are critical to the overall objectives of the expedition and for planning for higher resolution sampling postexpedition. Whole-round samples may be taken for interstitial water measurements and physical property measurements as dictated by the shipboard sampling plan that will be finalized during the first few days of the expedition. Most sampling for postexpedition research will be postponed until a shore-based sampling party that will be implemented approximately 4–5 months after the end of the expedition at the Gulf Coast Repository in College Station, Texas, USA.

If some critical intervals are recovered, there may be considerable demand for samples from a limited amount of cored material. These intervals may require special handling, a higher sampling density, reduced sample size, or continuous core sampling for the highest priority research objectives. The SAC may require an additional formal sampling plan before critical intervals are sampled and a special sampling plan will be developed to maximize scientific participation and to preserve some material for future studies. The SAC can decide at any stage during the expedition or during the moratorium period which recovered intervals should be considered critical. During the expedition, all archive halves will be permanent archives. Following the expedition, the curator will finalize the archive halves designated as permanent over intervals cored in multiple holes.

Following Expedition 363, cores will be delivered to the IODP Gulf Coast Repository in College Station. All collected data and samples will be protected by a 1 y moratorium period following the completion of the postexpedition sampling meeting, during which time data and samples will be available only to the Expedition 363 science party and approved shore-based participants.

Expedition scientists and scientific participants

The current list of participants for Expedition 363 can be found at **http://iodp.tamu.edu/scienceops/expeditions/pacific_warm_pool.html**.

References

Acharya, H.K., and Aggarwal, Y.P., 1980. Seismicity and tectonics of the Philippine Islands. *Journal of Geophysical Research: Solid Earth,* 85(B6):3239–3250. **http://dx.doi.org/10.1029/JB085iB06p03239**

Adkins, J.F., McIntyre, K., and Schrag, D.P., 2002. The salinity, temperature, and $\delta^{18}O$ of the glacial deep ocean. *Science,* 298(5599):1769–1773. **http://dx.doi.org/10.1126/science.1076252**

Anderson, R.F., Ali, S., Bradtmiller, L.I., Nielsen, S.H.H., Fleisher, M.Q., Anderson, B.E., and Burckle, L.H., 2009. Wind-driven upwelling in the Southern Ocean and the deglacial rise in atmospheric CO_2. *Science,* 323(5920):1443–1448. **http://dx.doi.org/10.1126/science.1167441**

Ayliffe, L.K., Gagan, M.K., Zhao, J., Drysdale, R.N., Hellstrom, J.C., Hantoro, W.S., Griffiths, M.L., Scott-Gagan, H., St Pierre, E., Cowley, J.A., Suwargadi, B.W., 2013. Rapid interhemispheric climate links via the Australasian monsoon during the last deglaciation. *Nature Communications,* 4:2908. **http://dx.doi.org/10.1038/ncomms3908**

Baldwin, S.L., Fitzgerald, P.G., and Webb, L.E., 2012. Tectonics of the New Guinea region. *Annual Review of Earth and Planetary Sciences,* 40(1):495–520. **http://dx.doi.org/10.1146/annurev-earth-040809-152540**

Bassinot, F., and Blatzer, A., 2002. *Les rapports de campagne à la mer* (Vol. 2002-01): *WEPAMA Cruise MD 122-IMAGES VII Leg 1, Port Hedland (Australia), 01-05-2001 to Keelung (Taiwan), 26-05-2001; Leg 2, Keelung (Taiwan), 27-05-2001 to Kochi (Japan), 18-06-2001: on board RV* "Marion Dufresne": Plouzané, France (Institut Polaire Français Paul Émile Victor [IPEV]).

Bischke, R.E., Suppe, J., and del Pilar, R., 1990. A new branch of the Philippine fault system as observed from aeromagnetic and seismic data. *Tectonophysics,* 183(1–4):243–264. **http://dx.doi.org/10.1016/0040-1951(90)90419-9**

Blevin, J.E., Struckmeyer, H.I.M., Boreham, C.J., Cathro, D.L., Sayers, J., and Totterdell, J.M., 1997. Browse Basin high resolution seismic study—North West Shelf, Australia—interpretation report. *Australian Geological Survey Organisation,* Record 1997/38. **http://www.ga.gov.au/metadata-gateway/metadata/record/23689/**

Bolliet, T., Holbourn, A., Kuhnt, W., Laj, C., Kissel, C., Beaufort, L., Kienast, M., Andersen, N., and Garbe-Schönberg, D., 2011. Mindanao Dome variability over the last 160 kyr: episodic glacial cooling of the West Pacific Warm Pool. *Paleoceanography,* 26(1):PA1208. **http://dx.doi.org/10.1029/2010PA001966**

Brierley, C.M., Fedorov, A.V., Liu, Z., Herbert, T.D., Lawrence, K.T., and LaRiviere, J.P., 2009. Greatly expanded tropical warm pool and weakened Hadley circulationin the early Pliocene. *Science,* 323(5922):1714–1718. **http://dx.doi.org/10.1126/science.1167625**

Broccoli, A.J., Dahl, K.A., and Stouffer, R.J., 2006. Response of the ITCZ to Northern Hemisphere cooling. *Geophysical Research Letters,* 33(1):L01702. **http://dx.doi.org/10.1029/2005GL024546**

Brown, J.N., Langlais, C., and Sen Gupta, A., 2015. Projected sea surface temperature changes in the equatorial Pacific relative to the Warm Pool edge. *Deep Sea Research, Part II: Topical Studies in Oceanography,* 113:47–58. **http://dx.doi.org/10.1016/j.dsr2.2014.10.022**

Bruch, A.A., Uhl, D., and Mosbrugger, V., 2007. Miocene climate in Europe—patterns and evolution: a first synthesis of NECLIME. *Palaeogeography, Palaeoclimatology, Palaeoecology,* 253(1–2):1–7. **http://dx.doi.org/10.1016/j.palaeo.2007.03.030**

Carolin, S.A., Cobb, K.M., Adkins, J.F., Clark, B., Conroy, J.L., Lejau, S., Malang, J., and Tuen, A.A., 2013. Varied response of Western Pacific hydrology to climate forcings over the last glacial period. *Science,* 340(6140):1564–1566. **http://dx.doi.org/10.1126/science.1233797**

Cane, M., and Clement, A.C., 1999. A role for the tropical Pacific coupled ocean-atmosphere system on Milankovitch and millennial timescales, Part II: global impacts. *In* Clark, P.U., Webb, R.S., and Keigwin, L.D. (Eds.), *Mechanisms of Global Climate Change at Millennial Time Scales.* Geophysical Monograph, 112:373–383.

Cane, M.A., and Molnar, P., 2001. Closing of the Indonesian Seaway as a precursor to East African aridification around 3–4 million years ago. *Nature,* 411(6834):157–162. **http://dx.doi.org/10.1038/35075500**

Ceppi, P., Hwang, Y.-T., Liu, X., Frierson, D.M.W., and Hartmann, D.L., 2013. The relationship between the ITCZ and the Southern Hemispheric eddy-driven jet. *Journal of Geophysical Research: Atmospheres,* 118(11):5136–5146. **http://dx.doi.org/10.1002/jgrd.50461**

Chiang, J.C.H., and Bitz, C.M., 2005. Influence of high latitude ice cover on the marine Intertropical Convergence Zone. *Climate Dynamics,* 25(5):477–496. **http://dx.doi.org/10.1007/s00382-005-0040-5**

Clark, P.U., Marshall, S.J., Clarke, G.K.C., Hostetler, S.W., Licciardi, J.M., and Teller, J.T., 2001. Freshwater forcing of abrupt climate change during the last glaciation. *Science,* 293(5528):283–287. **http://dx.doi.org/10.1126/science.1062517**

Clark, P.U., McCabe, A.M., Mix, A.C., and Weaver, A.J., 2004. Rapid rise of sea level 19,000 years ago and its global implications. *Science,* 304(5674):1141–1144. **http://dx.doi.org/10.1126/science.1094449**

Clement, A.C., Cane, M.A., and Seager, R., 2001. An orbitally driven tropical source for abrupt climate change. *J. Clim.,* 14(11):2369–2375. **http://dx.doi.org/10.1175/1520-0442(2001)014<2369:AODTSF>2.0.CO;2**

Dang, H., Jian, Z., Kissel, C., and Bassinot, F., 2015. Precessional changes in the western equatorial Pacific hydroclimate: a 240 kyr marine record from the Halmahera Sea, East Indonesia. *Geochemistry, Geophysics, Geosystems,* 16(1):148–164. **http://dx.doi.org/10.1002/2014GC005550**

Dannenmann, S., Linsley, B.K., Oppo, D.W., Rosenthal, Y., and Beaufort, L., 2003. East Asian monsoon forcing of suborbital variability in the Sulu Sea during marine isotope Stage 3: link to Northern Hemisphere climate. *Geochemistry, Geophysics, Geosystems,* 4(1):1–13. **http://dx.doi.org/10.1029/2002GC000390**

de Garidel-Thoron, T., Rosenthal, Y., Bassinot, F., and Beaufort, L., 2005. Stable sea surface temperatures in the western Pacific warm pool over the past 1.75 million years. *Nature,* 433(7023):294–298. **http://dx.doi.org/10.1038/nature03189**

Denton, G.H., Anderson, R.F., Toggweiler, J.R., Edwards, R.L., Shaefer, J.M., and Putnam, A.E., 2010. The last glacial termination. *Science,* 328(5986):1652–1656. **http://dx.doi.org/10.1126/science.1184119**

DiNezio, P., Clement, A., and Vecchi, G., 2010. Reconciling differing views of tropical Pacific climate change. *Eos, Transactions of the American Geophysical Union,* 91(16):141–142. **http://dx.doi.org/10.1029/2010EO160001**

DiNezio, P.N., Clement, A.C., Vecchi, G.A., Soden, B.J., Kirtman, B.P., and Lee, S.-K., 2009. Climate response of the equatorial Pacific to global warming. *Journal of Climate,* 22(18):4873–4892. **http://dx.doi.org/10.1175/2009JCLI2982.1**

Divins, D.L., 2003. *Total Sediment Thickness of the World's Oceans & Marginal Seas:* Boulder, CO (NOAA National Geophysical Data Center). **http://www.ngdc.noaa.gov/mgg/sedthick/sedthick.html**

Dowsett, H.J., Robinson, M.M., and Foley, K.M., 2009. Pliocene three-dimensional global ocean temperature reconstruction. *Climate of the Past,* 5(4):769–783. **http://dx.doi.org/10.5194/cp-5-769-2009**

England, M.H., McGregor, S., Spence, P., Meehl, G.A., Timmermann, A., Cai, W., Sen Gupta, A., McPhaden, M.J., Purich, A., and Santoso, A., 2014. Recent intensification of wind-driven circulation in the Pacific and the ongoing warming hiatus. *Nature Climate Change,* 4(3):222–227. **http://dx.doi.org/10.1038/nclimate2106**

Fedorov, A.V., Brierley, C.M., and Emanuel, K., 2010. Tropical cyclones and permanent El Niño in the early Pliocene epoch. *Nature,* 463(7284):1066–1070. **http://dx.doi.org/10.1038/nature08831**

Fischer, A.G., et al., 1971. *Initial Reports of the Deep Sea Drilling Program,* 6. Washington, DC (U.S. Government Printing Office). **http://dx.doi.org/10.2973/dsdp.proc.6.1971**

Flower, B.P., and Kennett, J.P., 1994. The middle Miocene climatic transition: East Antarctic ice sheet development, deep ocean circulation and global carbon cycling. *Palaeogeography, Palaeoclimatology, Palaeoecology,* 108(3–4):537–555. **http://dx.doi.org/10.1016/0031-0182(94)90251-8**

Ford, H.L., Ravelo, A.C., and Polissar, P.J., 2015. Reduced El Niño–Southern Oscillation during the Last Glacial Maximum. *Science,* 347(6219):255–258. **http://dx.doi.org/10.1126/science.1258437**

Fraser, N., Kuhnt, W., Holbourn, A., Bolliet, T., Andersen, N., Blanz, T., and Beaufort, L., 2014. Precipitation variability within the West Pacific Warm Pool over the past 120 ka: evidence from the Davao Gulf, southern Philippines. *Paleoceanography,* 29(11):1094–1110. **http://dx.doi.org/10.1002/2013PA002599**

Gibbons, F.T., Oppo, D.W., Mohtadi, M., Rosenthal Y., Cheng, J., Liu, Z., and Linsley, B.K., 2014. Deglacial $\delta^{18}O$ and hydrologic variability in the tropical Pacific and Indian Oceans. *Earth and Planetary Science Letters,* 387:240–251. **http://dx.doi.org/10.1016/j.epsl.2013.11.032**

Gordon, A.L., 2005. Oceanography of the Indonesian seas and their throughflow. *Oceanography,* 18(4):14–27. **http://dx.doi.org/10.5670/oceanog.2005.01**

Greenop, R., Foster, G.L., Wilson, P.A., and Lear, C.H., 2014. Middle Miocene climate instability associated with high-amplitude CO_2 variability. *Paleoceanography,* 29(9):845–853. **http://dx.doi.org/10.1002/2014PA002653**

Hall, R., 1996. Reconstructing Cenozoic SE Asia. *In* Hall, R., and Blundell, D.J. (Eds.), *Tectonic Evolution of Southeast Asia.* Geological Society Special Publication, 106(1):153–184.**http://dx.doi.org/10.1144/GSL.SP.1996.106.01.11**

Hall, R., Ali, J.R., Anderson, C.D., and Baker, S.J., 1995. Origin and motion history of the Philippine Sea plate. *Tectonophysics,* 251(1–4):229–250. **http://dx.doi.org/10.1016/0040-1951(95)00038-0**

Hall, R., and Wilson, M.E.J., 2000. Neogene sutures in eastern Indonesia. *Journal of Asian Earth Sciences,* 18(6):781–808. **http://dx.doi.org/10.1016/S1367-9120(00)00040-7**

Halpert, M.S., and Ropelewski, C.F., 1992. Surface temperature patterns associated with the Southern Oscillation. *Journal of Climate,* 5(6):577–593. **http://dx.doi.org/10.1175/1520-0442(1992)005<0577:STPAWT>2.0.CO;2**

Hamilton, W.B., 1979. Tectonics of the Indonesian Region. *U.S. Geological Survey Professional Paper,* 1078.

Hansen, J., Sato, M., Kharecha, P., Beerling, D., Berner, R., Masson-Delmotte, V., Pagani, M., Raymo, M., Royer, D.L., and Zachos, J.C., 2008. Target atmospheric CO_2: where should humanity aim? *The Open Atmospheric Science Journal,* 2(1):217–231. **http://dx.doi.org/10.2174/1874282300802010217**

Hegarty, K.A., and Weissel, J.K., 1988. Complexities in the developments of the Caroline plate region, western Equatorial Pacific. *In* Nairn, A.E.M., Stehli, F.G., and Uyeda, S. (Eds.), *The Pacific Ocean:* New York (Plenum), 277–301.

Holbourn, A., Kuhnt, W., Kawamura, H., Jian, Z., Grootes, P., Erlenkeuser, H., and Xu, J., 2005. Orbitally paced paleoproductivity variations in the Timor Sea and Indonesian Throughflow variability during the last 460 kyr. *Paleoceanography,* 20(3):PA3002. **http://dx.doi.org/10.1029/2004PA001094**

Holbourn, A., Kuhnt, W., Regenberg, M., Schulz, M., Mix, A., and Andersen, N., 2010. Does Antarctic glaciation force migration of the tropical rain belt? *Geology,* 38(9):783–786. **http://dx.doi.org/10.1130/G31043.1**

Horng, C.-S. Roberts, A.P., and Liang, W.-T., 2003. A 2.14-Myr astronomically tuned record of relative geomagnetic paleointensity from the western Philippine Sea. *Journal of Geophysical Research: Solid Earth,* 108(B1):2059. **http://dx.doi.org/10.1029/2001JB001698**

Jia, G., Chen, F., and Peng, P., 2008. Sea surface temperature differences between the western equatorial Pacific and northern South China Sea since the Pliocene and their paleoclimatic implications. *Geophysical Research Letters,* 35(18):L18609. **http://dx.doi.org/10.1029/2008GL034792**

Karas, C., Nürnberg, D., Gupta, A.K., Tiedemann, R., Mohan, K., and Bickert, T., 2009. Mid-Pliocene climate change amplified by a switch in Indonesian subsurface throughflow. *Nature Geoscience,* 2(6):434–438. **http://dx.doi.org/10.1038/ngeo520**

Karas, C., Nürnberg, D., Tiedemann, R., and Garbe-Schönberg, D., 2011. Pliocene Indonesian Throughflow and Leeuwin Current dynamics: implications for Indian Ocean polar heat flux. *Paleoceanography,* 26(2):PA2217. **http://dx.doi.org/10.1029/2010PA001949**

Karig, D.E., Ingle, J.C., Jr., et al., 1975. *Initial Reports of the Deep Sea Drilling Project,* 31: Washington, DC (U.S. Government Printing Office). **http://dx.doi.org/10.2973/dsdp.proc.31.1975**

Kissel, C., Laj, C., Kienast, M., Bolliet, T., Holbourn, A., Hill, P., Kuhnt, W., and Braconnot, P., 2010. Monsoon variability and deep oceanic circulation in the western equatorial Pacific over the last climatic cycle: insights from sedimentary magnetic properties and sortable silt. *Paleoceanography,* 25(3):PA3215. **http://dx.doi.org/10.1029/2010PA001980**

Koutavas, A., Lynch-Steiglitz, J., Marchitto, T.M., Jr., and Sachs, J.P., 2002. El Niño-like pattern in Ice Age tropical Pacific sea surface temperature. *Science,* 297(5579):226–230. **http://dx.doi.org/10.1126/science.1072376**

Koutavas, A., deMendocal, P.B., Olive, G.C., and Lynch-Stieglitz, J., 2006. Mid-Holocene El Niño–Southern Oscillation (ENSO) attenuation revealed by individual foraminifera in eastern tropical Pacific sediments. *Geology,* 34(12):993–996. **http://dx.doi.org/10.1130/G22810A.1**

Krause, D.C., 1966. Tectonics, marine geology, and bathymetry of the Celebes Sea-Sulu Sea region. *Geological Society of America Bulletin,* 77(8):813–832. **http://dx.doi.org/10.1130/0016-7606(1966)77[813:TMGABO]2.0.CO;2**

Kroenke, L.W., Berger, W.H., Janecek, T.R., et al., 1991. *Proceedings of the Ocean Drilling Program, Initial Reports,* 130: College Station, TX (Ocean Drilling Program). **http://dx.doi.org/10.2973/odp.proc.ir.130.1991**

Kuhnt, W., Holbourn, A.E., Hall, R., Zuvela, M., and Käse, R., 2004. Neogene History of the Indonesian Throughflow. In: Clift, P., Hayes, D., Kuhnt, W., and Wang P. (eds.), Continent-Ocean Interactions in the East Asian Marginal Seas. American Geophysical Union Monograph, 149, 299-320.

Kuhnt, W., Blümel, M., Boch, R., Dewi, K.T., da Costa Monteiro, F., Dürkop, A., Hanebuth, T., Heidemann, U., Holbourn, A., Jian, Z., van der Kaars, S., Kawamura, H., Kawohl, H., Nürnberg, D., Opdyke, B., Petersen, A., Regenberg, M., Rosenthal, Y., Rühlemann, C., Sadekov, A., Salomon, B., Tian, J., Xu, J., and Zuraida, R., 2005. Cruise Report SO185, VITAL–Variability of the Indonesian throughflow and Australasian climate history of the last 150000 years, Darwin–Jakarta, September 15 2005–October 06 2005. *IFM-GEOMAR Reports.* **http://dx.doi.org/10.2312/cr_so185**

Kuroda, Y., 2000. Variability of currents off the northern coast of New Guinea. *Journal of Oceanography,* 56(1):103–116. **http://dx.doi.org/10.1023/A:1011122810354**

Kürschner, W.M., Kvacek, Z., and Dilcher, D.L., 2008. The impact of Miocene atmospheric carbon dioxide fluctuations on climate and the evolution of terrestrial ecosystems. *Proceedings of the National Academy of Sciences of the United States of America* , 105(2):449–453. **http://dx.doi.org/10.1073/pnas.0708588105**

LaRiviere, J.P., Ravelo, A.C., Crimmins, A., Dekens, P.S., Ford, H.L., Lyle, M., and Wara, M.W., 2012. Late Miocene decoupling of oceanic warmth and atmospheric carbon dioxide forcing. *Nature,* 486(7401):97–100. **http://dx.doi.org/10.1038/nature11200**

Laj, C., Wang, P., and Balut, Y., 2005. *Les rapports de campagne à la mer: MD147/MARCO POLO- IMAGES XII à bord du* "Marion Dufresne": Plouzané, France (Institut Polaire Français Paul Émile Victor [IPEV]).

Lea, D.W., 2004. The 100,000-yr cycle in tropical SST, greenhouse forcing, and climate sensitivity. *J. Climatol.,* 17(11):2170–2179. **http://dx.doi.org/10.1175/1520-0442(2004)017<2170:TYCITS>2.0.CO;2**

Lea, D.W., Pak, D.K., and Spero, H.J., 2000. Climate impact of late Quaternary equatorial Pacific sea surface temperature variations. *Science,* 289(5485):1719–1724. **http://dx.doi.org/10.1126/science.289.5485.1719**

Lee, S.-Y., Chiang, J.C.H., Matsumoto, K., and Tokos, K.S., 2011. Southern Ocean wind response to North Atlantic cooling and the rise in atmospheric CO_2: modeling perspective and paleoceanographic implications. *Paleoceanography,* 26(1):PA1214. **http://dx.doi.org/10.1029/2010PA002004**

Linsley, B.K., Rosenthal, Y., and Oppo, D.W., 2010. Holocene evolution of the Indonesian Throughflow and Western Pacific Warm Pool. *Nature Geoscience,* 3(8):578–583. **http://dx.doi.org/10.1038/ngeo920**

MacAyeal, D., 1993. Binge/purge oscillations of the Laurentide ice sheet as a cause of the North Atlantic's Heinrich events. *Paleoceanography,* 8(6):775–784. **http://dx.doi.org/10.1029/93PA02200**

Mayer, L.A., Shipley, T.H., Winterer, E.L., Mosher, D., and Hagen, R.A., 1991. SeaBeam and seismic reflection surveys on the Ontong Java plateau. *In* Kroenke, L.W., Berger, W.H., Janecek, T.R., et al., *Proceedings of the Ocean*

Drilling Program, Initial Reports, 130: College Station, TX (Ocean Drilling Program), 45–75. **http://dx.doi.org/10.2973/odp.proc.ir.130.103.1991**

Medina-Elizalde, M., and Lea, D.W., 2005. The mid-Pleistocene transition in the tropical Pacific. *Science,* 310(5750):1009–1012. **http://dx.doi.org/10.1126/science.1115933**

Medina-Elizalde, M., and Lea, D.W., 2010. Late Pliocene equatorial Pacific. *Paleoceanography,* 25(2):PA2208–PA2217. **http://dx.doi.org/10.1029/2009PA001780**

Milliman, J.D., Farnsworth, K.L., and Albertin, C.S., 1999. Flux and fate of fluvial sediments leaving large islands in the East Indies. *Journal of Sea Research,* 41(1–2):97–107. **http://dx.doi.org/10.1016/S1385-1101(98)00040-9**

Mosbrugger, V., Utescher, T., and Dilcher, D.L., 2005. Cenozoic continental climatic evolution of central Europe. *Proceedings of the National Academy of Sciences of the United States of America,* 102(42):14964–14969. **http://dx.doi.org/10.1073/pnas.0505267102**

Nathan, S.A., and Leckie, R.M., 2009. Early history of the Western Pacific Warm Pool during the middle to late Miocene (~13.2–5.8 Ma): role of sea-level change and implications for equatorial circulation. *Palaeogeography, Palaeoclimatology, Palaeoecology,* 274(3–4):140–159. **http://dx.doi.org/10.1016/j.palaeo.2009.01.007**

Neale, R., and Slingo, J., 2003. The maritime continent and its role in the global climate: a GCM study. *Journal of Climate,* 16(5):834–848. **http://dx.doi.org/10.1175/1520-0442(2003)016<0834:TMCAIR>2.0.CO;2**

Oppo, D.W., Linsley, B.K., Rosenthal, Y., Dannenmann, S., and Beaufort, L., 2003. Orbital and suborbital climate variability in the Sulu Sea, western tropical Pacific. *Geochemistry, Geophysics, Geosystems,* 4(1):1–20. **http://dx.doi.org/10.1029/2001GC000260**

Oppo, D.W., and Rosenthal, Y., 2010. The great Indo-Pacific communicator. *Science,* 328(5985):1492–1494. **http://dx.doi.org/10.1126/science.1187273**

Pagani, M., Liu, Z., LaRiviere, J., and Ravelo, A.C., 2010. High Earth-system climate sensitivity determined from Pliocene carbon dioxide concentrations. *Nature Geoscience,* 3:27–30. **http://dx.doi.org/10.1038/ngeo724**

Pubellier, M., Bader, A.G., Rangin, C., Deffontaines, B., and Quebral, R., 1999. Upper plate deformation induced by subduction of a volcanic arc: the Snellius Plateau (Molucca Sea, Indonesia and Mindanao, Philippines). *Tectonophysics,* 304(4):345–368. **http://dx.doi.org/10.1016/S0040-1951(98)00300-X**

Rahmstorf, S., 2002. Ocean circulation and climate during the past 120,000 years. *Nature,* 419(6903):207–214. **http://dx.doi.org/10.1038/nature01090**

Rasmusson, E.M., and Arkin, P.A., 1993. A global view of large-scale precipitation variability. *Journal of Climate,* 6(8):1495–1522. **http://dx.doi.org/10.1175/1520-0442(1993)006<1495:AGVOLS>2.0.CO;2**

Ravelo, A.C., Lawrence, K.T., Fedorov, A., and Ford, H.L., 2014. Comment on "A 12-million-year temperature history of the tropical Pacific Ocean". *Science,* 346(6216):1467. **http://dx.doi.org/10.1126/science.1257618**

Retallack, G.J., 2009. Refining a pedogenic-carbonate CO_2 paleobarometer to quantify a middle Miocene greenhouse spike. *Palaeogeography, Palaeoclimatology, Palaeoecology,* 281(1–2):57–65. **http://dx.doi.org/10.1016/j.palaeo.2009.07.011**

Ridley, W.I., Rhodes, J.M., Reid, A.M., Jakes, P., Shih, C., and Bass, M.N., 1974. Basalts from Leg 6 of the Deep-Sea Drilling Project. *Journal of Petrology,* 15(1):140–159. **http://dx.doi.org/10.1093/petrology/15.1.140**

Ropelewski, C.F., and Halpert, M.S., 1987. Global and regional scale precipitation patterns associated with the El Niño/Southern Oscillation. *Monthly Weather Review,* 115(8):1606–1626. **http://dx.doi.org/10.1175/1520-0493(1987)115<1606:GARSPP>2.0.CO;2**

Ruddiman, W.F., 2005. The early anthropogenic hypothesis a year later: an editorial reply. *Climatic Change,* 69(2):427–434. **http://dx.doi.org/10.1007/s10584-005-7272-6**

Russon, T., Elliot, M., Sadekov, A., Cabioch, G., Corrège, T., and De Deckker, P., 2010. Inter-hemispheric asymmetry in the early Pleistocene Pacific Warm Pool. *Geophysical Research Letters,* 37(11):L11601. **http://dx.doi.org/10.1029/2010GL043191**

Saikku, R., Stott, L., and Thunell, R., 2009. A bi-polar signal recorded in the western tropical Pacific: Northern and Southern Hemisphere climate records from the Pacific Warm Pool during the last Ice Age. *Quaternary Science Reviews,* 28(23–24):2374–2385. **http://dx.doi.org/10.1016/j.quascirev.2009.05.007**

Schmittner, A., Saenko, O.A., and Weaver, A.J., 2003. Coupling of the hemispheres in observations and simulations of glacial climate change. *Quaternary Science Reviews,* 22(5–7):659–671. **http://dx.doi.org/10.1016/S0277-3791(02)00184-1**

Seki, O., Foster, G.L., Schmidt., D.N., Mackensen, A., Kawamura, K., and Pancost, R.D., 2010. Alkenone and boron-based Pliocene pCO_2 records. *Earth and Planetary Science Letters,* 292(1–2):201–211. **http://dx.doi.org/10.1016/j.epsl.2010.01.037**

Shipboard Scientific Party, 1975. Site 292. *In* Karig, D.E., Ingle, J.C., Jr., et al., *Initial Reports of the Deep Sea Drilling Project,* 31: Washington, DC (U.S. Government Printing Office), 67–129. **http://dx.doi.org/10.2973/dsdp.proc.31.104.1975**

Stagg, H.M.J., and Exon, N.F., 1981. Geology of the Scott Plateau and Rowley Terrace, off northwestern Australia. *Bureau of Mineral Resources, Geology and Geophysics Bulletin,* 213. **http://www.ga.gov.au/corporate_data/62/Bull_213.pdf**

Steinberg, C.R., Choukroun, S.M., Slivkoff, M.M., Mahoney, M.V., and Brinkman, R.M., 2006. Currents in the Bismarck Sea and Kimbe Bay, Papua New Guinea. *TNC Pacific Island Countries Report,* 6/06. **http://www.conservationgateway.org/Files/Pages/currents-bismarck-sea-and.aspx**

Steph, S., Tiedemann, R., Prange, M., Groeneveld, J., Schulz, M., Timmermann, A., Nürnberg, D., Rühlemann, C., Saukel, C., and Haug, G.H., 2010. Early Pliocene increase in thermohaline overturning: a precondition for the development of the modern equatorial Pacific cold tongue. *Paleoceanography,* 25(2). **http://dx.doi.org/10.1029/2008PA001645**

Stott, L., Cannariato, K., Thunell, R., Haug, G.H., Koutavas, A., and Lund, S., 2004. Decline of surface temperature and salinity in the western tropical Pacific Ocean in the Holocene epoch. *Nature,* 431(7004):56–59. **http://dx.doi.org/10.1038/nature02903**

Stott, L., Poulsen, C., Lund, S., and Thunell, R., 2002. Super ENSO and global climate oscillations at millennial time scales. *Science,* 297(5579):222–226. **http://dx.doi.org/10.1126/science.1071627**

Symonds, P.A., Collins, C.D.N., and Bradshaw, J., 1994. Deep structure of the Browse Basin: implications for basin development and petroleum exploration. *In* Purcell, P.G., and Purcell, R.R. (Eds.), *The Sedimentary Basins of Western Australia: Proceedings of the West Australian Basins Symposium:* Perth, Australia (Petroleum Exploration Society of Australia), 315–331.

Tachikawa, K., Cartapanis, O., Vidal, L., Beaufort, L., Barlyaeva, T., and Bard, E., 2011. The precession phase of hydrological variability in the Western Pacific Warm Pool during the past 400 ka. *Quaternary Science Reviews,* 30(25–26):3716–3727. **http://dx.doi.org/10.1016/j.quascirev.2011.09.016**

Tachikawa, K., Timmermann, A., Vidal, L., Sonzogni, C., and Timm, O.E., 2013. Southern Hemisphere orbital forcing and its effects on CO_2 and tropical Pacific climate. *Climate of the Past Discussions,* 9(2):1869–1900. **http://dx.doi.org/10.5194/cpd-9-1869-2013**

Taylor, B., 1979. Bismarck Sea: evolution of a back-arc basin. *Geology,* 7(4):171–174. **http://dx.doi.org/10.1130/0091-7613(1979)7<171:BSEOAB>2.0.CO;2**

Wang, H., and Mehta, V.M., 2008. Decadal variability of the Indo-Pacific Warm Pool and its association with atmospheric and oceanic variability in the NCEP–NCAR and SODA reanalyses. *Journal of Climate,* 21(21):5545–5565. **http://dx.doi.org/10.1175/2008JCLI2049.1**

Wara, M.W., Ravelo, A.C., and Delaney, M.L., 2005. Permanent El Niño-like conditions during the Pliocene warm period. *Science,* 309(5735):758–761. **http://dx.doi.org/10.1126/science.1112596**

Winterer, E.L., et al., 1971. *Initial Reports of the Deep Sea Drilling Project,* 7. Washington, DC (U.S. Government Printing Office). **http://dx.doi.org/10.2973/dsdp.proc.7.1971**

Woodard, S.C., Rosenthal, Y., Miller, K.G., Wright, J.D., Chiu, B.K., and Lawrence, K.T., 2014. Antarctic role in Northern Hemisphere glaciation. *Science,* 346(6211):847–851. **http://dx.doi.org/10.1126/science.1255586**

Xianglong, N., Shiguo, W., and Ryuichi, S., 2008. Tectonics in the northwestern West Philippine Basin. *Journal of China University of Geosciences,* 19(3):191–199. **http://dx.doi.org/10.1016/S1002-0705(08)60038-2**

Xu, J., Holbourn, A., Kuhnt, W., Jian, Z., and Kawamura, H., 2008. Changes in the thermocline structure of the Indonesian outflow during Terminations I and II. *Earth and Planetary Science Letters,* 273(1–2):152–162. **http://dx.doi.org/10.1016/j.epsl.2008.06.029**

Zachos, J., Pagani, M., Sloan, L., Thomas, E., and Billups, K., 2001. Trends, rhythms, and aberrations in global climate 65 Ma to present. *Science,* 292(5517):686–693. **http://dx.doi.org/10.1126/science.1059412**

Zhang, Y.G., Pagani, M., and Liu, Z., 2014. A 12-million-year temperature history of the tropical Pacific Ocean. *Science,* 344(6179):84–87. **http://dx.doi.org/10.1126/science.1246172**

Zhang, Y.G., Pagani, M., Liu, Z., Bohaty, S.M., and DeConto, R., 2013. A 40-million-year history of atmospheric CO_2. *Philosophical Transactions of the Royal Society, A: Mathematical, Physical & Engineering Sciences,* 371(2001):1–20. **http://dx.doi.org/10.1098/rsta.2013.0096**

Table T1. Primary and alternate drill sites, Expedition 363. EPSP = Environmental Protection and Safety Panel.

Proposed site	Priority	Latitude	Longitude	Water depth	Jurisdiction	Proposed Penetration (mbsf)	EPSP approved penetration (mbsf)	Anticipated age at proposed penetration depth (Ma)	Sedimentation rate (m/Myr)
WP-12D	Primary	15°03.3240′S	120°26.1000′E	1470	Australia	490	490	14.0	35
WP-11B	Primary	13°05.2380′S	121°48.2430′E	1790	Australia (sea-bed treaty)	350	700	3.9	90
WP-09A	Primary	6°20.8140′N	125°50.8902′E	2080	Philippines	350	500	0.6	600
WP-71A	Primary	3°07.92216′S	142°46.96998′E	1030	Papua New Guinea	225	225	0.5	500
WP-05A	Primary	2°22.3374′S	144°36.0690′E	1337	Papua New Guinea	200	225	2.2	90
WP-03A	Primary	2°2.5905′N	141°45.286698′E	2600	Federated States of Micronesia Extended Continental Shelf	300	500	15.0	20
WP-02A	Primary	5°48.9492′N	142°39.25932′E	2355	Federated States of Micronesia	250	430	16.7	15
WP-72A	Primary for alternate operations plan	03°06.15882′S	142°47.5746′E	1147	Papua New Guinea	315	325	0.6	500
WP-21A	Primary for alternate operations plan	5°49.58770′N	142°37.333998′E	2355	Federated States of Micronesia	100	150	5.0	20
WP-12A	Alternate	15°05.6460′S	120°25.7400′E	1480	Australia	500	800	14.3	35
WP-12C	Alternate	15°03.5640′S	120°26.3100′E	1470	Australia	490	490	14.0	35
WP-13A	Alternate	16°03.97752′N	124°42.0294′E	3077	Philippines	280	280	35.0	8
WP-06A	Alternate	2°18.77658′S	144°50.4738′E	880	Papua New Guinea	200	215	2.2	90
WP-14A	Alternate	2°19.9980′S	144°49.16334′E	880	Papua New Guinea	175	177	1.9	90
WP-04A	Alternate	2°07.19886′N	141°01.66398′E	3427	Federated States of Micronesia Extended Continental Shelf	150	200	10.0	15
WP-15A	Alternate	0°19.1100′N	159°21.6900′E	2520	International	500	750	16.7	30

Table T2. Primary operations plan, Expedition 363. EPSP = Environmental Protection and Safety Panel. APC = advanced piston corer, XCB = extended core barrel, APCT-3 = advanced piston corer temperature tool. FMS = Formation MicroScanner, VSI = Versatile Seismic Imager.

Site No.	Location (Latitude Longitude)	Seafloor Depth (mbrf)	Operations Description	Transit (days)	Drilling Coring (days)	Log (days)
Singapore			Begin Expedition 5.0	port call days		
			Transit ~1474 nmi to WP-12D @ 10.5	5.9		
WP-12D	15° 3.3240' S	1481	Hole A - APC to 250 mbsf with orientation, APCT-3, and non-mag barrels	0	1.5	0.0
EPSP	120° 26.1000' E		Hole B - APC/XCB to 490 mbsf with orientation and non-mag barrels	0	2.2	0.0
to 490 mbsf			Hole C - APC/XCB to 490 mbsf with orientation and non-mag barrels. Log with triple combo and FMS-sonic.	0	2.5	1.0
			Sub-Total Days On-Site: 7.2			
			Transit ~144 nmi to WP-11B @ 10.5	0.6		
WP-11B	13° 5.2380' S	1801	Hole A - APC to 250 mbsf with orientation, APCT-3, and non-mag barrels	0	1.5	0.0
EPSP	121° 48.2430' E		Hole B - APC/XCB to 350 mbsf with orientation and non-mag barrels	0	1.7	0.0
to 700 mbsf			Hole C - APC/XCB to 350 mbsf with orientation and non-mag barrels	0	1.9	0.0
			Sub-Total Days On-Site: 5.1			
			Transit ~1359 nmi to WP-09A @ 10.5	5.5		
WP-09A	6° 20.8140' N	2091	Hole A - APC to 250 mbsf with orientation, APCT-3, and non-mag barrels	0	1.5	0.0
EPSP	125° 50.8902' E		Hole B - APC/XCB to 350 mbsf with orientation and non-mag barrels	0	1.7	0.0
to 500 mbsf			Hole C - APC/XCB to 350 mbsf with orientation and non-mag barrels	0	2.0	0.0
			Sub-Total Days On-Site: 5.2			
			Transit ~1163 nmi to WP-71A @ 10.5	4.6		
WP-71A	3° 7.92216' S	1041	Hole A - APC to 225 mbsf with orientation, APCT-3, and non-mag barrels	0	1.0	0.0
EPSP	142° 46.96998' E		Hole B - APC to 225 mbsf with orientation and non-mag barrels	0	0.9	0.0
to 225 mbsf			Hole C - APC to 225 mbsf with orientation and non-mag barrels	0	1.1	0.0
			Sub-Total Days On-Site: 2.9			
			Transit ~118 nmi to WP-05A @ 10.5	0.5		
WP-05A	2° 22.3374' S	1348	Hole A - APC to 200 mbsf with orientation, APCT-3, and non-mag barrels	0	1.1	0.0
EPSP	144° 36.0690' E		Hole B - APC to 200 mbsf with orientation and non-mag barrels	0	0.8	0.0
to 225 mbsf			Hole C - APC to 200 MBSF with orientation and non-mag barrels	0	1.0	0.0
			Sub-Total Days On-Site: 2.8			
			Transit ~315 nmi to WP-03A @ 10.5	1.3		
WP-03A	2° 2.5905' N	2611	Hole A - APC to 250 mbsf with orientation, APCT-3, and non-mag barrels	0	1.6	0.0
EPSP	141° 45.286698' E		Hole B - APC/XCB to 300 mbsf with orientation and non-mag barrels	0	1.6	0.0
to 500 mbsf			Hole C - APC/XCB to 300 mbsf with orientation and non-mag barrels	0	1.9	0.0
			Sub-Total Days On-Site: 5.1			
			Transit ~233 nmi to WP-02A @ 10.5	0.9		
WP-02A	5° 48.9492' N	2366	Hole A - APC to 250 mbsf with orientation, APCT-3, and non-mag barrels	0	1.6	0.0
EPSP	142° 39.25932' E		Hole B - APC to 250 mbsf with orientation and non-mag barrels	0	1.3	0.0
to 430 mbsf			Hole C - APC to 250 mbsf with orientation and non-mag barrels	0	1.3	0.0
			Sub-Total Days On-Site: 4.2			
			Transit ~474 nmi to Guam @ 10.5	1.9		
Guam			End Expedition	20.9	31.5	1.0

Port Call:	5.0	Total Operating Days:	53.5
Sub-Total On-Site:	32.5	Total Expedition:	58.5

Table T3. Alternate site operations plan, Expedition 363.EPSP = Environmental Protection and Safety Panel. APC = advanced piston corer, XCB = extended core barrel, APCT-3 = advanced piston corer temperature tool. FMS = Formation MicroScanner.

Site No.	Location (Latitude Longitude)	Seafloor Depth (mbrf)	Operations Description	Drilling Coring (days)	LWD/MWD Log (days)
WP-04A	2° 7.19886' S	3438	Hole A - APC to 150 mbsf with orientation, APCT-3, and non-mag barrels	1.7	0.0
EPSP	141° 1.66398' E				
to 200 mbsf					
			Sub-Total Days On-Site: 1.7		
WP-06A	2° 18.77658' S	891	Hole A - APC to 200 mbsf with orientation, APCT-3, and non-mag barrels	0.9	0.0
EPSP	144° 50.4738' E		Hole B - APC to 200 mbsf with orientation and non-mag barrels	0.7	0.0
to 215 mbsf			Hole C - APC to 200 mbsf with orientation and non-mag barrels	0.8	0.0
			Sub-Total Days On-Site: 2.4		
WP-12A	15° 5.6460' S	1457	Hole A - APC to 250 mbsf with orientation, APCT-3, and non-mag barrels	1.5	0.0
EPSP	120° 25.7400' E		Hole B - APC/XCB to 500 mbsf with orientation and non-mag barrels	2.3	0.0
to 800 mbsf			Hole C - APC/XCB to 500 mbsf with orientation and non-mag barrels. Log with triple combo and FMS sonic	2.5	1.0
			Sub-Total Days On-Site: 7.2		
WP-12C	15° 3.5640' S	1481	Hole A - APC to 250 mbsf with orientation, APCT-3, and non-mag barrels	1.5	0.0
EPSP	120° 26.3100' E		Hole B - APC/XCB to 490 mbsf with orientation and non-mag barrels	2.3	0.0
to 490 mbsf			Hole C - APC/XCB to 490 mbsf with orientation and non-mag barrels. Log with triple combo and FMS sonic	2.5	1.0
			Sub-Total Days On-Site: 7.2		
WP-13A	16° 3.97752' N	3088	Hole A - APC to 250 mbsf with orientation, APCT-3, and non-mag barrels	1.8	0.0
EPSP	124° 42.0294' E		Hole B - APC/XCB to 280 MBSF with orientation and non-mag barrels	1.6	0.0
to 280 mbsf			Hole C - APC/XCB to 280 MBSF with orientation and non-mag barrels	1.7	0.0
			Sub-Total Days On-Site: 5.1		
WP-14A	2° 19.9980' S	891	Hole A - APC to 175 mbsf with orientation, APCT-3, and non-mag barrels	0.8	0.0
EPSP	144° 49.16334' E		Hole B - APC to 175 mbsf with orientation and non-mag barrels	0.6	0.0
to 177 mbsf			Hole C - APC to 175 mbsf with orientation and non-mag barrels	0.8	0.0
			Sub-Total Days On-Site: 2.2		
WP-15A	0° 19.1100' N	2531	Hole A - APC to 250 mbsf with orientation, APCT-3, and non-mag barrels	1.6	0.0
EPSP	159° 21.6900' E		Hole B - APC/XCB to 500 MBSF with orientation and non-mag barrels	2.9	0.0
to 750 mbsf			Hole C - APC/XCB to 500 MBSF with orientation and non-mag barrels	2.9	0.0
			Sub-Total Days On-Site: 7.4		
WP-21A	5° 49.58770' N	2366	Hole A - APC to 100 mbsf with orientation, APCT-3, and non-mag barrels	0.7	0.0
EPSP	142° 37.333998' E		Hole B - APC to 100 mbsf with orientation and non-mag barrels	0.8	0.0
to 150 mbsf					
			Sub-Total Days On-Site: 1.5		
WP-72A	3° 6.15882' S	1158	Hole A - APC/XCB to 315 mbsf with orientation, APCT-3, and non-mag barrels	1.5	0.0
EPSP	142° 47.5746' E		Hole B - APC/XCB to 315 mbsf with orientation and non-mag barrels	1.3	0.0
to 325 mbsf					
			Sub-Total Days On-Site: 2.8		

Table T4. Alternate operations plan, Expedition 363. EPSP = Environmental Protection and Safety Panel. APC = advanced piston corer, XCB = extended core barrel, APCT-3 = advanced piston corer temperature tool. FMS = Formation MicroScanner.

Site No.	Location (Latitude Longitude)	Seafloor Depth (mbrf)	Operations Description	Transit (days)	Drilling Coring (days)	LWD/MWD Log (days)
Singapore			Begin Expedition 5.0	port call days		
			Transit ~1474 nmi to WP-12D @ 10.5	5.9		
WP-12D	15° 3.3240' S	1481	Hole A - APC to 250 mbsf with orientation, APCT-3, and non-mag barrels	0	1.5	0.0
EPSP	120° 26.1000' E		Hole B - APC/XCB to 490 mbsf with orientation and non-mag barrels	0	2.2	0.0
to 490 mbsf			Hole C - APC/XCB to 490 mbsf with orientation and non-mag barrels. Log with triple combo and FMS sonic	0	2.4	1.0
			Sub-Total Days On-Site: 7.1			
			Transit ~143 nmi to WP-11B @ 10.5	0.6		
WP-11B	13° 5.2380' S	1801	Hole A - APC to 250 mbsf with orientation, APCT-3, and non-mag barrels	0	1.5	0.0
EPSP	121° 48.2430' E		Hole B - APC/XCB to 350 mbsf with orientation and non-mag barrels	0	1.7	0.0
to 700 mbsf			Hole C - APC/XCB to 350 mbsf with orientation and non-mag barrels	0	1.9	0.0
			Sub-Total Days On-Site: 5.1			
			Transit ~1949 nmi to WP-72A @ 10.5	7.8		
WP-72A	3° 6.15882' S	1158	Hole A - APC/XCB to 315 mbsf with orientation, APCT-3, and non-mag barrels	0	1.5	0.0
EPSP	142° 47.5746' E		Hole B - APC/XCB to 315 mbsf with orientation and non-mag barrels	0	1.3	0.0
to 325 mbsf						
			Sub-Total Days On-Site: 2.8			
			Transit ~2 nmi to WP-71A @ 1.5	0.1		
WP-71A	3° 7.92216' S	1041	Hole A - APC to 225 mbsf with orientation, APCT-3, and non-mag barrels	0	1.0	0.0
EPSP	142° 46.96998' E		Hole B - APC to 225 mbsf with orientation and non-mag barrels	0	0.9	0.0
to 225 mbsf			Hole C - APC to 225 mbsf with orientation and non-mag barrels	0	1.1	0.0
			Sub-Total Days On-Site: 2.9			
			Transit ~118 nmi to WP-05A @ 10.5	0.5		
WP-05A	2° 22.3374' S	1348	Hole A - APC to 200 mbsf with orientation, APCT-3, and non-mag barrels	0	1.1	0.0
EPSP	144° 36.0690' E		Hole B - APC to 200 mbsf with orientation and non-mag barrels	0	0.8	0.0
to 225 mbsf			Hole C - APC to 200 MBSF with orientation and non-mag barrels	0	1.0	0.0
			Sub-Total Days On-Site: 2.8			
			Transit ~315 nmi to WP-03A @ 10.5	1.3		
WP-03A	2° 2.5905' N	2611	Hole A - APC to 250 mbsf with orientation, APCT-3, and non-mag barrels	0	1.6	0.0
EPSP	141° 45.286698' E		Hole B - APC/XCB to 300 mbsf with orientation and non-mag barrels	0	1.6	0.0
to 500 mbsf			Hole C - APC/XCB to 300 mbsf with orientation and non-mag barrels	0	1.9	0.0
			Sub-Total Days On-Site: 5.1			
			Transit ~233 nmi to WP-02A @ 10.5	0.9		
WP-02A	5° 48.9492' N	2366	Hole A - APC to 250 mbsf with orientation, APCT-3, and non-mag barrels	0	1.6	0.0
EPSP	142° 39.25932' E		Hole B - APC to 250 mbsf with orientation and non-mag barrels	0	1.3	0.0
to 430 mbsf			Hole C - APC to 250 mbsf with orientation and non-mag barrels	0	1.3	0.0
			Sub-Total Days On-Site: 4.2			
			Transit ~2 nmi to WP-21A @ 1.5	0.1		
WP-21A	5° 49.58770' N	2366	Hole A - APC to 100 mbsf with orientation, APCT-3, and non-mag barrels	0	0.7	0.0
EPSP	142° 37.333998' E		Hole B - APC to 100 mbsf with orientation and non-mag barrels	0	0.8	0.0
to 150 mbsf						
			Sub-Total Days On-Site: 1.5			
			Transit ~474 nmi to Guam @ 10.5	1.9		
Guam			End Expedition	18.8	30.6	1.0

Port Call:	5.0	Total Operating Days:	50.4
Sub-Total On-Site:	31.6	Total Expedition:	55.4

Figure F1. Primary (yellow circles with white text) and alternate (red squares with red text) drill sites, Expedition 363. Orange text indicates primary sites for the backup operations plan. See Table **T1** for details. Arrows mark the path of Indonesian Throughflow.

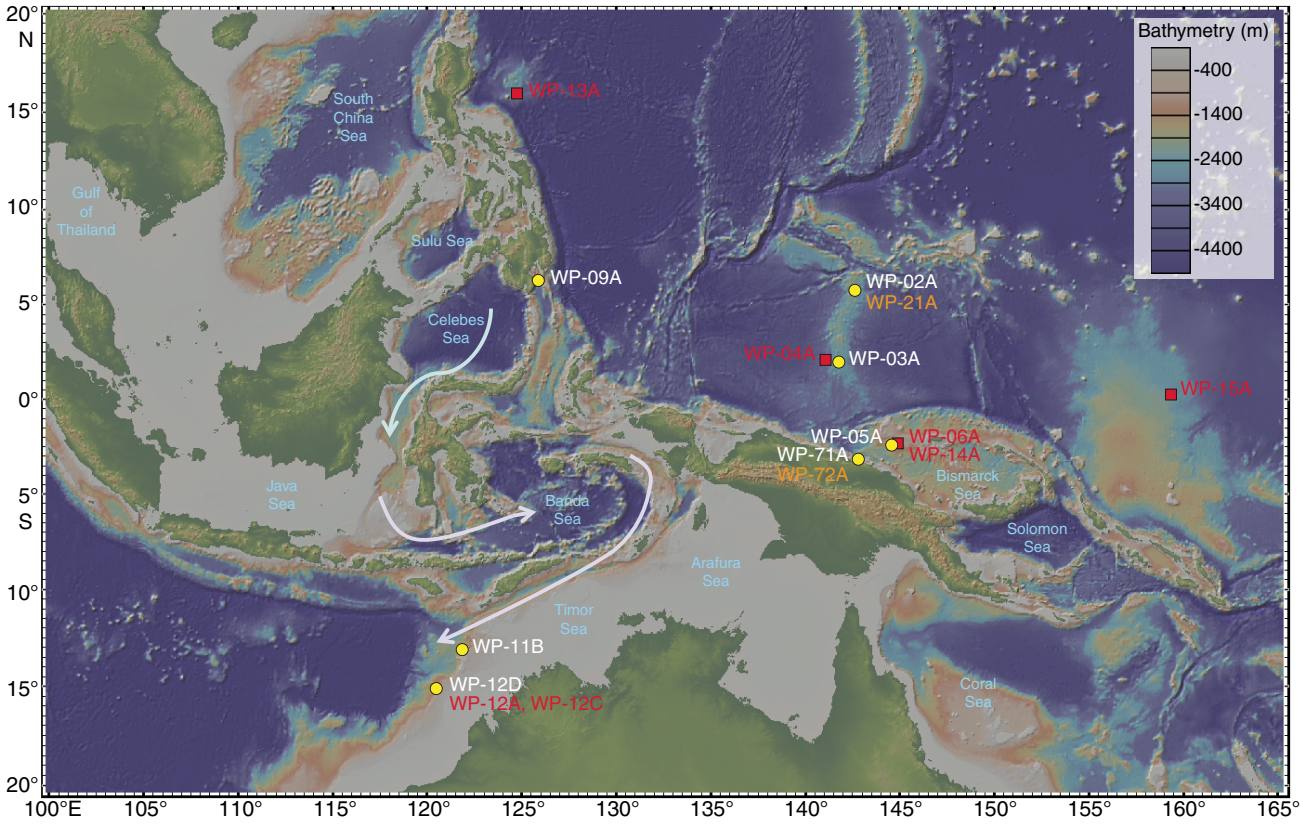

Figure F2. Primary (white text) and alternate (black text) Expedition 363 drill sites on a map of mean annual sea-surface temperature (SST). Black arrows mark the path of Indonesian Throughflow.

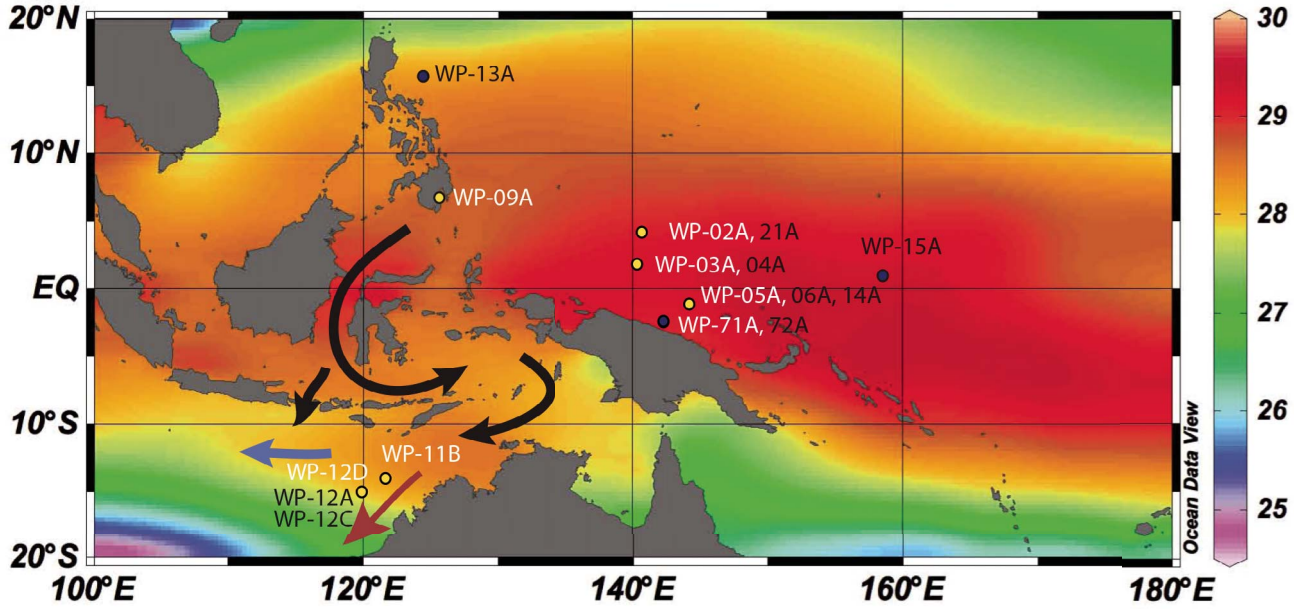

Figure F3. Operational plans for primary Expedition 363 coring sites shown with estimated sedimentation rates and expected bottom depths/ages.

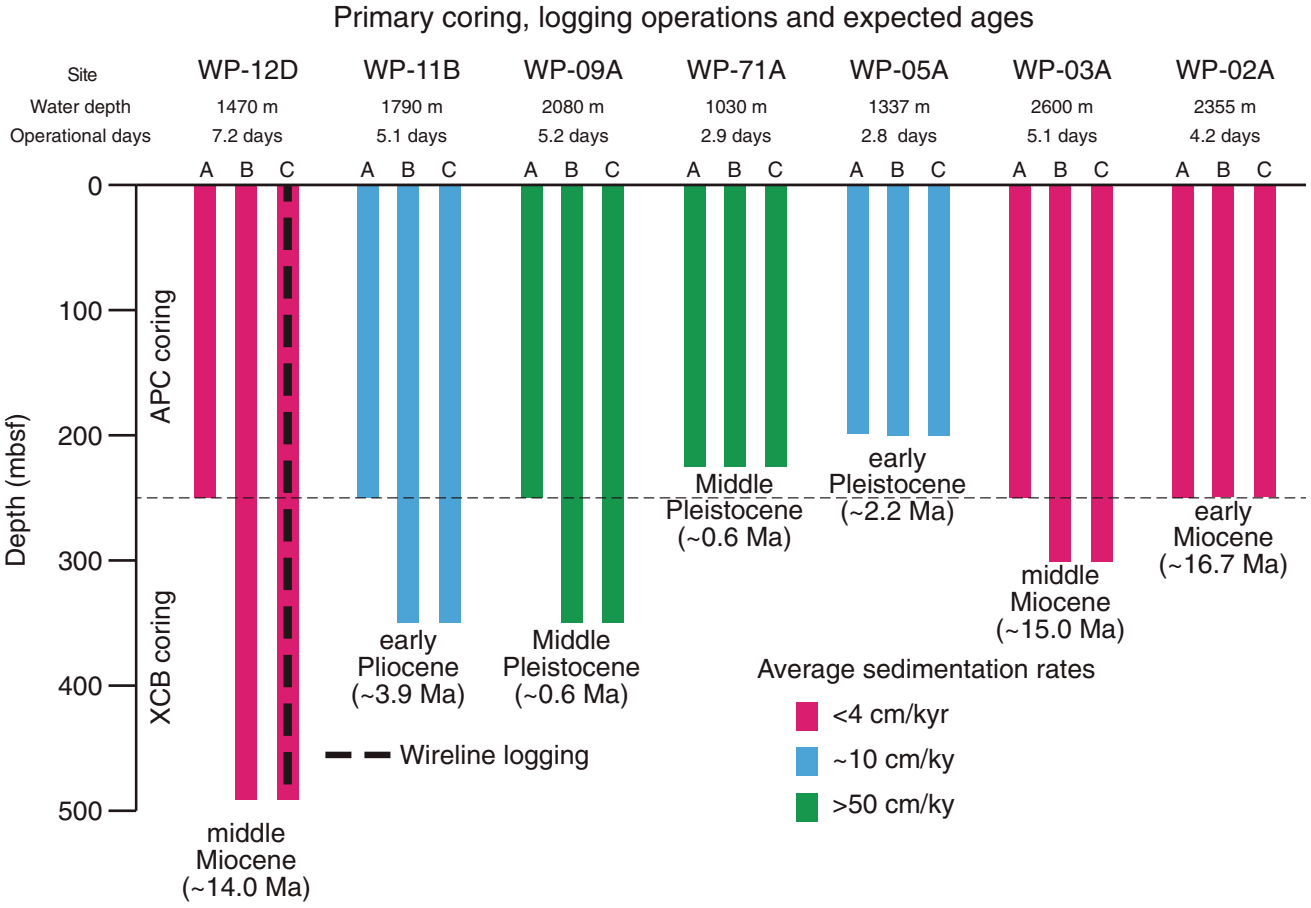

Figure F4. Temperature, salinity, dissolved oxygen, and $\delta^{18}O_{seawater}$ profiles in stations in eastern Philippine Islands and northern Papua New Guinea. Main water masses at each site are shown. NPIW = North Pacific Intermediate Water (low salinity/low oxygen), AAIW = Antarctic Intermediate Water (low salinity/high oxygen), UCDW = Upper Circumpolar Deepwater. SMOW = standard marine ocean water.

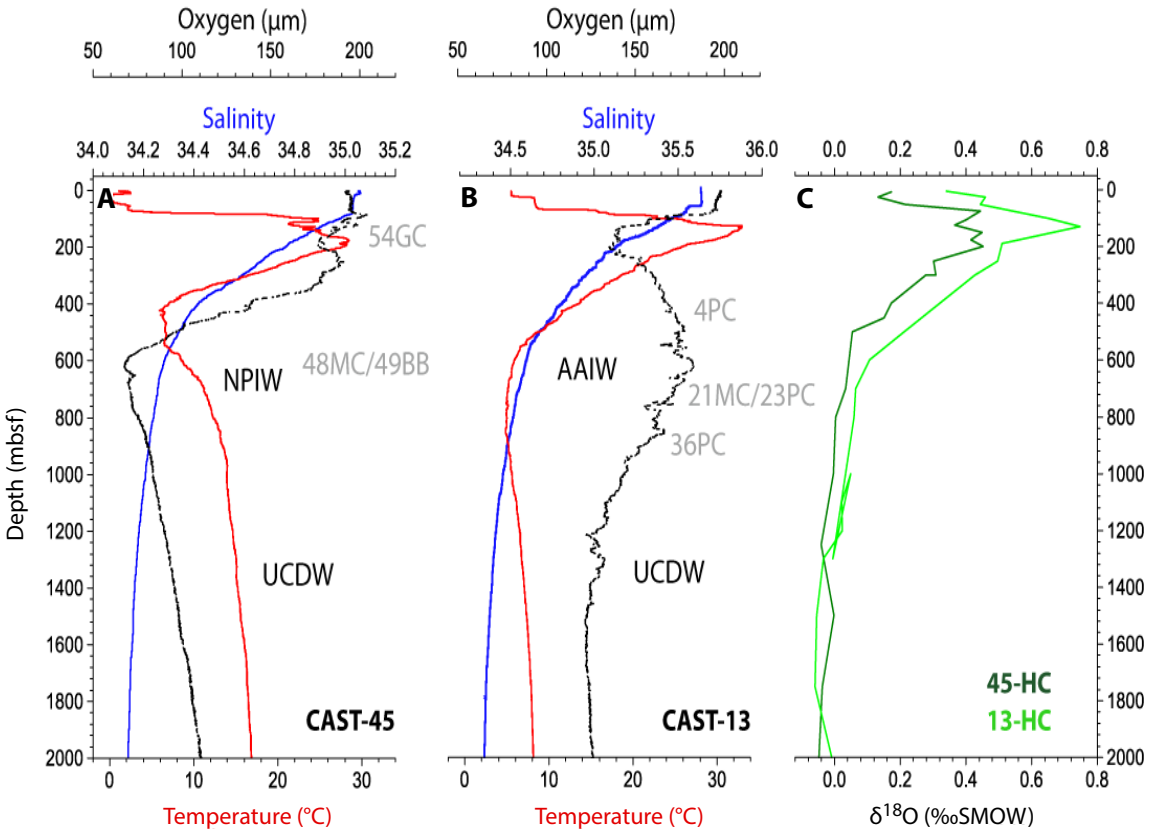

Figure F5. Climatological (A) winter and (B) summer precipitation for 1979–2009 and (C) winter and (D) summer precipitation anomalies during the 1997–1978 El Niño event.

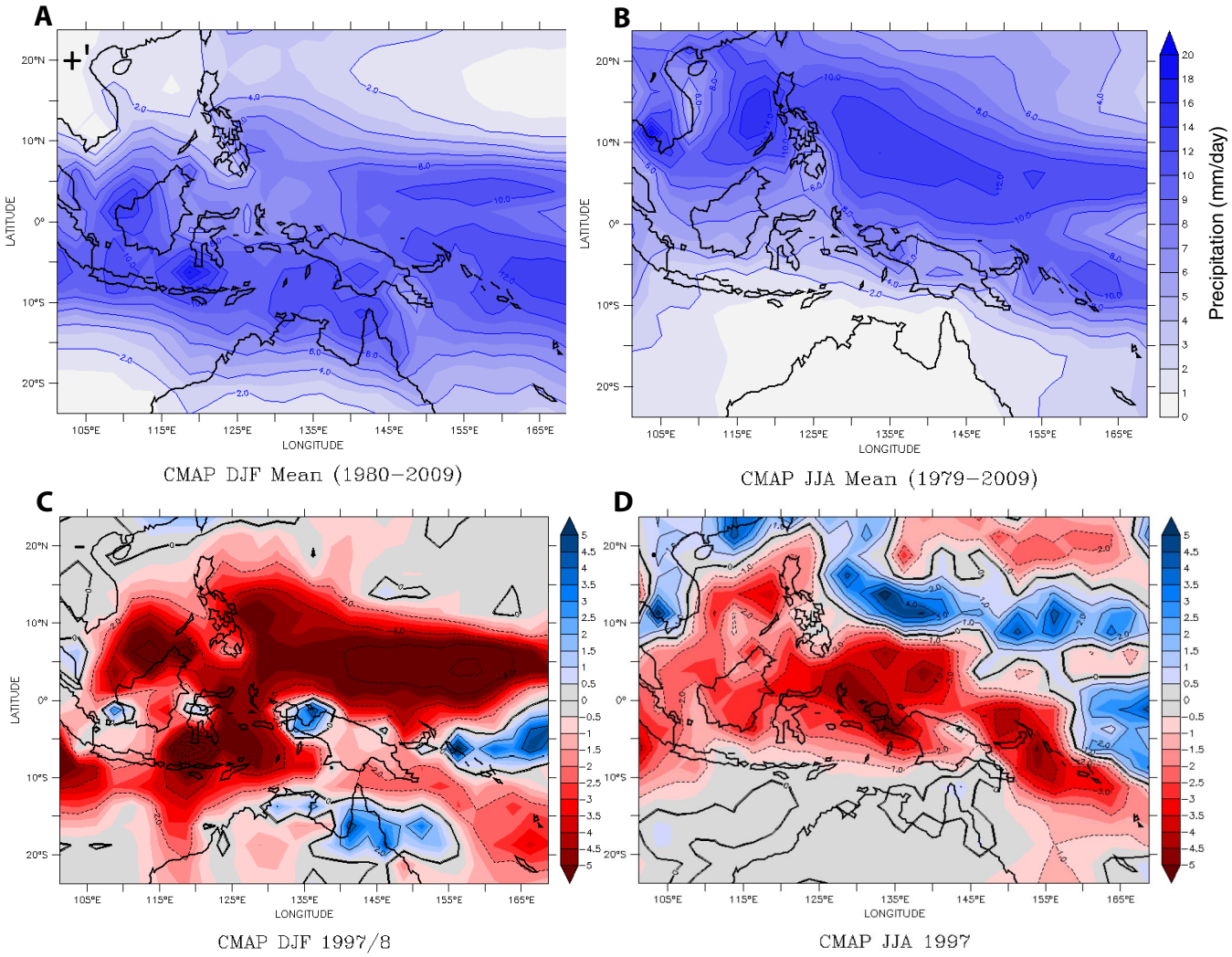

Figure F6. Tectonic configuration of southeast Asia with proposed drill sites (red). Shaded areas on landmasses represent ophiolitic, arc, and other accreted material emplaced during the Tertiary. Principal marine magnetic anomalies are shown schematically and double lines represent active spreading centers. Narrow lines outline principal bathymetric features. Complexities in the Bismarck-Solomon Sea regions are not shown (from Hall, 1996).

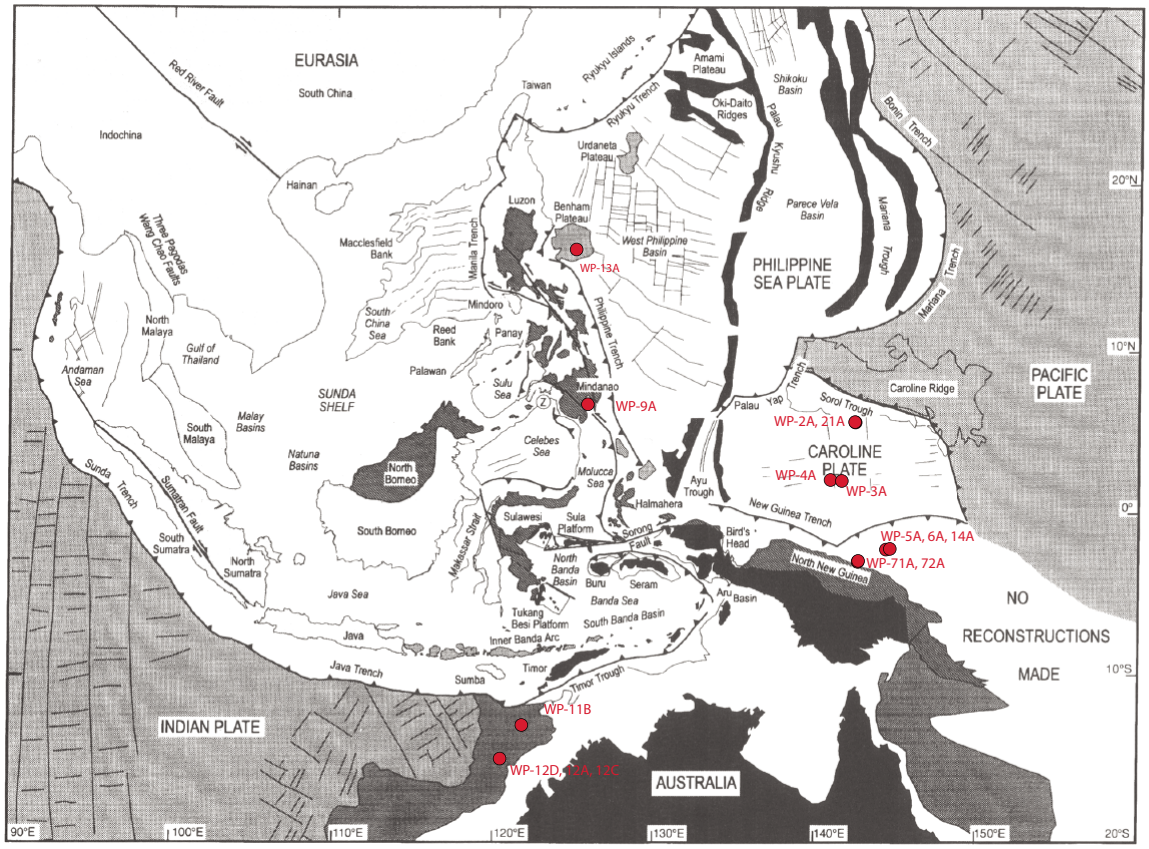

Site summaries

Site WP-12D

Priority:	Primary
Position:	15°3.3240′S, 120°26.1000′E
Water depth (m):	1470
Target drilling depth (mbsf):	490
Approved maximum penetration (mbsf):	490
Survey coverage (track map; seismic profile):	Bathymetric sketch and site track map (Figure **AF1**) Deep-penetration seismic reflection: • Primary line: HBR2000A-3032 (SP 440) (Figure **AF2**) • Crossing line: BR98-84-3003 (projected at SP 7183.01) (Figure **AF3**)
Objective(s):	• Reconstruct orbital-scale evolution of the Western Pacific Warm Pool back to the middle Miocene • Reconstruct Indonesian Throughflow and Australian Monsoon climate history
Drilling program:	Hole A: • APC to 250 mbsf with nonmagnetic core barrels, orientation (IceField tool), and APCT-3 Hole B: • APC to refusal with nonmagnetic core barrels and orientation (IceField tool) • XCB to 490 mbsf Hole C: • APC to refusal with nonmagnetic core barrels and orientation (IceField tool) • XCB to 490 mbsf
Logging program:	Hole C: • Triple combo • FMS-sonic
Nature of rock anticipated:	Clay-rich nannofossil ooze, calcareous mudstone

Site WP-12A

Priority:	Alternate
Position:	15°5.6460′S, 120°25.7400′E
Water depth (m):	1480
Target drilling depth (mbsf):	500
Approved maximum penetration (mbsf):	800
Survey coverage (track map; seismic profile):	Bathymetric sketch and site track map (Figure **AF1**) Deep-penetration seismic reflection: • Primary line: BR98-17 (SP 9564) (Figure **AF4**) • Crossing line: HBR2000A-3034 (Figure **AF5**)
Objective(s):	• Reconstruct orbital-scale evolution of the Western Pacific Warm Pool back to the middle Miocene • Reconstruct Indonesian Throughflow and Australian Monsoon climate history
Drilling program:	Hole A: • APC to 250 mbsf with nonmagnetic core barrels, orientation (IceField tool), and APCT-3 Hole B: • APC to refusal with nonmagnetic core barrels and orientation (IceField tool) • XCB to 500 mbsf Hole C: • APC to refusal with nonmagnetic core barrels and orientation (IceField tool) • XCB to 500 mbsf
Logging program:	Hole C: • Triple combo • FMS-sonic
Nature of rock anticipated:	Clay-rich nannofossil ooze, calcareous mudstone

Site WP-12C

Priority:	Alternate
Position:	15°3.5640′S, 120°26.3100′E
Water depth (m):	1470
Target drilling depth (mbsf):	490
Approved maximum penetration (mbsf):	490
Survey coverage (track map; seismic profile):	Bathymetric sketch and site track map (Figure **AF1**) Deep-penetration seismic reflection: • Primary line: HBR2000A-3032 (SP 409.08) (Figure **AF2**) • Crossing line: BR98-84 (SP 7183.01) (Figure **AF3**)
Objective(s):	• Reconstruct orbital-scale evolution of the Western Pacific Warm Pool back to the middle Miocene • Reconstruct Indonesian Throughflow history and Australian Monsoon climate history
Drilling program:	Hole A: • APC to 250 mbsf with nonmagnetic core barrels, orientation (IceField tool), and APCT-3 Hole B: • APC to refusal with nonmagnetic core barrels and orientation (IceField tool) • XCB to 490 mbsf Hole C: • APC to refusal with nonmagnetic core barrels and orientation (IceField tool) • XCB to 490 mbsf
Logging program:	Hole C: • Triple combo • FMS-sonic
Nature of rock anticipated:	Clay-rich nannofossil ooze, calcareous mudstone

Site WP-11B

Priority:	Primary
Position:	13°5.2380′S, 121°48.2430′E
Water depth (m):	1790
Target drilling depth (mbsf):	350
Approved maximum penetration (mbsf):	700
Survey coverage (track map; seismic profile):	Bathymetric sketch and site track map (Figure **AF6**) Deep-penetration seismic reflection: • Primary line: BR98-168 (SP 14431) (Figure **AF7**) • Crossing line: BR98-117 (projected at SP 2723) (Figure **AF8**)
Objective(s):	• Reconstruct Pliocene–Pleistocene evolution of the Western Pacific Warm Pool at suborbital timescales • Reconstruct Indonesian Throughflow and Australian Monsoon climate history
Drilling program:	Hole A: • APC to 250 mbsf with nonmagnetic core barrels, orientation (IceField tool), and APCT-3 Hole B: • APC to refusal with nonmagnetic core barrels and orientation (IceField tool) • XCB to 350 mbsf Hole C: • APC to refusal with nonmagnetic core barrels and orientation (IceField tool) • XCB to 350 mbsf
Logging program:	None
Nature of rock anticipated:	Hemipelagic calcareous mud

Site WP-09A

Priority:	Primary
Position:	6°20.8140′N, 125°50.8902′E
Water depth (m):	2080
Target drilling depth (mbsf):	350
Approved maximum penetration (mbsf):	500
Survey coverage (track map; seismic profile):	Bathymetric sketch and site track map (Figure **AF9**) Deep-penetration seismic reflection: • Primary line: GeoB13-075 (SP 1360) (Figure **AF10**) • Crossing line: GeoB13-068 (SP 398) (Figure **AF11**)
Objective(s):	• Examine late Pleistocene centennial to millennial scale climate variability related to the East Asian Monsoon and the Western Pacific Warm Pool • Examine meridional versus zonal controls on the hydroclimate of the Western Pacific Warm Pool through comparison to records from proposed Sites WP-71A/WP-72A (off Papua New Guinea)
Drilling program:	Hole A: • APC to 250 mbsf with nonmagnetic core barrels, orientation (IceField tool), and APCT-3 Hole B: • APC to refusal with nonmagnetic core barrels and orientation (IceField tool) • XCB to 350 mbsf Hole C: • APC to refusal with nonmagnetic core barrels and orientation (IceField tool) • XCB to 350 mbsf
Logging program:	None
Nature of rock anticipated:	Hemipelagic sediment

Site WP-13A

Priority:	Alternate for WP-09A
Position:	16°3.97752′N, 124°42.0294′E
Water depth (m):	3077
Target drilling depth (mbsf):	280
Approved maximum penetration (mbsf):	280
Survey coverage (track map; seismic profile):	Bathymetric sketch and site track map (Figure **AF12**) Deep-penetration seismic reflection: • Primary line: RR1313-1 (CDP 540) (Figure **AF13**) • Crossing line: GeoB13-068 (projected at CDP 480) (Figure **AF14**)
Objective(s):	• Assess long term changes in the extent of the Western Pacific Warm Pool over the Neogene
Drilling program:	Hole A: • APC to 250 mbsf with nonmagnetic core barrels, orientation (IceField tool), and APCT-3 Hole B: • APC to refusal with nonmagnetic core barrels and orientation (IceField tool) • XCB to 350 mbsf Hole C: • APC to refusal with nonmagnetic core barrels and orientation (IceField tool) • XCB to 350 mbsf
Logging program:	None
Nature of rock anticipated:	Calcareous ooze with interbedded volcaniclastics

Site WP-71A

Priority:	Primary
Position:	3°7.92216′S, 142°46.96998′E
Water depth (m):	1030
Target drilling depth (mbsf):	225
Approved maximum penetration (mbsf):	225
Survey coverage (track map; seismic profile):	Bathymetric sketch and site track map (Figure **AF15**) Deep-penetration seismic reflection: • Primary line: RR1313 WP7-2 (CDP 400) (Figure **AF16**) • Crossing line: RR1313 WP7-5 (projected at CDP 782) (Figure **AF17**)
Objective(s):	• Reconstruct Late Pleistocene centennial to millennial-scale variability of the Western Pacific Warm Pool • Monitor riverine discharge off Papua New Guinea
Drilling program:	Hole A: • APC to 225 mbsf with nonmagnetic core barrels, orientation (IceField tool), and APCT-3 Hole B: • APC to 225 mbsf with nonmagnetic core barrels and orientation (IceField tool) Hole C: • APC to 225 mbsf with nonmagnetic core barrels and orientation (IceField tool)
Logging program:	None
Nature of rock anticipated:	Hemipelagic mud

Site WP-72A

Priority:	Primary for backup operations plan
Position:	3°6.158826′S, 142°47.5746′E
Water depth (m):	1147
Target drilling depth (mbsf):	315
Approved maximum penetration (mbsf):	325
Survey coverage (track map; seismic profile):	Bathymetric sketch and site track map (Figure **AF15**) Deep-penetration seismic reflection: • Primary line: RR1313 WP7-2 (CDP 950) (Figure **AF16**) • Crossing line: RR1313 WP7-5 (projected at CDP 782) (Figure **AF17**)
Objective(s):	• Reconstruct Late Pleistocene centennial to millennial-scale variability of the Western Pacific Warm Pool • Monitor riverine discharge off Papua New Guinea
Drilling program:	Hole A: • APC to refusal (or 315 mbsf) with nonmagnetic core barrels, orientation (IceField tool), and APCT-3 • XCB to 315 mbsf Hole B: • APC to refusal (or 315 mbsf) with nonmagnetic core barrels and orientation (IceField tool) • XCB to 315 mbsf
Logging program:	None
Nature of rock anticipated:	Hemipelagic mud

Site WP-05A

Priority:	Primary
Position:	2°22.3374′S, 144°36.0690′E
Water depth (m):	1337
Target drilling depth (mbsf):	200
Approved maximum penetration (mbsf):	225
Survey coverage (track map; seismic profile):	Bathymetric sketch and site track map (Figure **AF18**) Deep-penetration seismic reflection: • Primary line: GeoB13-084 (SP 570) (Figure **AF19)** • Crossing line: GeoB13-088 (SP 1159) (Figure **AF20**)
Objective(s):	• Reconstruct Pleistocene evolution of the Western Pacific Warm Pool at suborbital timescales • Monitor riverine discharge off Papua New Guinea
Drilling program:	Hole A: • APC to 200 mbsf with nonmagnetic core barrels, orientation (IceField tool), and APCT-3 Hole B: • APC to 200 mbsf with nonmagnetic core barrels and orientation (IceField tool) Hole C: • APC to 200 mbsf with nonmagnetic core barrels and orientation (IceField tool)
Logging program:	None
Nature of rock anticipated:	Hemipelagic sediments

Site WP-06A

Priority:	Alternate for WP-05A
Position:	2°18.77658′S, 144°50.4738′E
Water depth (m):	880
Target drilling depth (mbsf):	200
Approved maximum penetration (mbsf):	215
Survey coverage (track map; seismic profile):	Bathymetric sketch and site track map (Figure **AF21**) Deep-penetration seismic reflection: • Primary line: RR1313 WP6-5 (CDP 2630) (Figure **AF22**) • Crossing line: RR1313 WP6-3a (projected at CDP 1013) (Figure **AF23**)
Objective(s):	• Reconstruct Pleistocene evolution of the Western Pacific Warm Pool at suborbital timescales • Monitor riverine discharge off Papua New Guinea
Drilling program:	Hole A: • APC to 200 mbsf with nonmagnetic core barrels, orientation (IceField tool), and APCT-3 Hole B: • APC to 200 mbsf with nonmagnetic core barrels and orientation (IceField tool) Hole C: • APC to 200 mbsf with nonmagnetic core barrels and orientation (IceField tool)
Logging program:	None
Nature of rock anticipated:	Hemipelagic sediment

Site WP-14A

Priority:	Alternate for WP-05A
Position:	2°19.9980′S, 144°49.16334′E
Water depth (m):	880
Target drilling depth (mbsf):	175
Approved maximum penetration (mbsf):	177
Survey coverage (track map; seismic profile):	Bathymetric sketch and site track map (Figure **AF21**) Deep-penetration seismic reflection: • Primary line: RR1313 WP6-5 (CDP 2100) (Figure **AF22**) • Crossing line: RR1313 WP6-3a (projected at CDP 1013) (Figure **AF23**)
Objective(s):	• Reconstruct Pleistocene evolution of the Western Pacific Warm Pool at suborbital timescales • Monitor riverine discharge off Papua New Guinea
Drilling program:	Hole A: • APC to 175 mbsf with nonmagnetic core barrels, orientation (IceField tool), and APCT-3 Hole B: • APC to 175 mbsf with nonmagnetic core barrels and orientation (IceField tool) Hole C: • APC to 175 mbsf with nonmagnetic core barrels and orientation (IceField tool)
Logging program:	None
Nature of rock anticipated:	Hemipelagic sediment

Site WP-03A

Priority:	Primary
Position:	2°2.5905′N, 141°45.2866998′E
Water depth (m):	2600
Target drilling depth (mbsf):	300
Approved maximum penetration (mbsf):	500
Survey coverage (track map; seismic profile):	Bathymetric sketch and site track map (Figure **AF24**) Primary line RR1313 WP3-1 (CDP 580) (Figure **AF25**) Crossing line: RR1313 WP3-3 (projected at CDP1346) (Figure **AF26**)
Objective(s):	Reconstruct orbital-scale evolution of the Western Pacific Warm Pool back to the middle Miocene Examine zonal controls on Western Pacific Warm Pool hydroclimate through comparison to records from proposed Sites WP-11A/WP-12B (off NW Australia)
Drilling program:	Hole A: APC to 250 mbsf with nonmagnetic core barrels, orientation (Icefield tool), and APCT-3 Hole B: APC to refusal with nonmagnetic core barrels and orientation (Icefield tool) XCB to 450 mbsf Hole C: APC to refusal with nonmagnetic core barrels and orientation (Icefield tool) XCB to 450 mbsf
Logging program:	None
Nature of rock anticipated:	Pelagic calcareous mud

Site WP-04A

Priority:	Alternate for WP-03A
Position:	2°7.19886′N, 141°01.66398′E
Water depth (m):	3427
Target drilling depth (mbsf):	150
Approved maximum penetration (mbsf):	200
Survey coverage (track map; seismic profile):	Bathymetric sketch and site track map (Figure **AF27**) Deep-penetration seismic reflection: • Primary line: RR1313 WP4-2 (CDP 1163) (Figure **AF28**) • Crossing line: RR1313 WP4-3 (CDP 253) (Figure **AF29**)
Objective(s):	Reconstruct secular changes in seawater chemistry
Drilling program:	Hole A: • APC to 150 mbsf with nonmagnetic core barrels, orientation (IceField tool), and APCT-3
Logging program:	None
Nature of rock anticipated:	Calcareous ooze

Site WP-02A

Priority:	Primary
Position:	5°48.9492′N, 142°39.25932′E
Water depth (m):	2355
Target drilling depth (mbsf):	250
Approved maximum penetration (mbsf):	430
Survey coverage (track map; seismic profile):	Bathymetric sketch and site track map (Figure **AF30**) Deep-penetration seismic reflection: • Primary line: RR1313 WP2-1 (CDP 650) (Figure **AF31**) • Crossing line: RR1313 WP2-6 (projected at CDP 844) (Figure **AF32**)
Objective(s):	• Reconstruct intermediate and deepwater heat content and carbonate chemistry • Monitor changes in circulation in relation to high-latitude forcing since the middle Miocene
Drilling program:	Hole A: • APC to 250 mbsf with nonmagnetic core barrels, orientation (IceField tool), and APCT-3 Hole B: • APC to refusal with nonmagnetic core barrels and orientation (IceField tool) • XCB to 350 mbsf Hole C: • APC to refusal with nonmagnetic core barrels and orientation (IceField tool) • XCB to 350 mbsf
Logging program:	None
Nature of rock anticipated:	Foraminiferal sand

Site WP-21A

Priority:	Primary for backup operations plan
Position:	5°49.58770′N, 142°37.333998′E
Water depth (m):	2355
Target drilling depth (mbsf):	100
Approved maximum penetration (mbsf):	150
Survey coverage (track map; seismic profile):	Bathymetric sketch and site track map (Figure **AF30**) Deep-penetration seismic reflection: • Primary line: RR1313 WP2-1 (CDP 1249) (Figure **AF31**) • Crossing line: RR1313 WP2-6 (CDP 844) (Figure **AF32**)
Objective(s):	• Reconstruct intermediate and deepwater heat content and carbonate chemistry • Monitor changes in circulation in relation to high-latitude forcing since the Pliocene
Drilling program:	Hole A: • APC to 125 mbsf with nonmagnetic core barrels, orientation (IceField tool), and APCT-3 Hole B: • APC to 125 mbsf with nonmagnetic core barrels and orientation (IceField tool)
Logging program:	None
Nature of rock anticipated:	Calcareous ooze

Site WP-15A

Priority:	Alternate
Position:	0°19.1100′N, 159°21.6900′E
Water depth (m):	2520
Target drilling depth (mbsf):	500
Approved maximum penetration (mbsf):	Requested to 750 mbsf
Survey coverage (track map; seismic profile):	Bathymetric sketch (Figure **AF33**) Site track map (Figure **AF34**) • Deep-penetration seismic reflection: • Primary line: Ar33.0387 (SP 3250) (Figure **AF35**)
Objective(s):	• Redrill of Site 806, which is a reference site used to monitor broad scale zonal and meridional gradients throughout the Neogene
Drilling program:	Hole A: • APC to 250 mbsf with nonmagnetic core barrels, orientation (Icefield tool), and APCT-3 Hole B: • APC/XCB to 500 mbsf with nonmagnetic core barrels and orientation (Icefield tool) Hole C: • APC/XCB to 500 mbsf with nonmagnetic core barrels and orientation (Icefield tool)
Logging program:	None
Nature of rock anticipated:	Nannofossil ooze/chalk

Figure AF1. Contoured bathymetric map showing the location of primary proposed Site WP-12B (red circle) on seismic reflection Profiles HBR2000A-3032 (dip line; see Figure **AF2**) and HBR2000A-3003 (strike line; see Figure **AF3**), as well as alternate proposed Site WP-12A (yellow circle) on seismic reflection Profiles BR98-17 (dip line; see Figure **AF4**) and HBR2000A-3034 (strike line; see Figure **AF5**). Bathymetry is based on an EM122 multibeam survey completed on *Sonne* Cruise SO-185. Contour interval = 100 m.

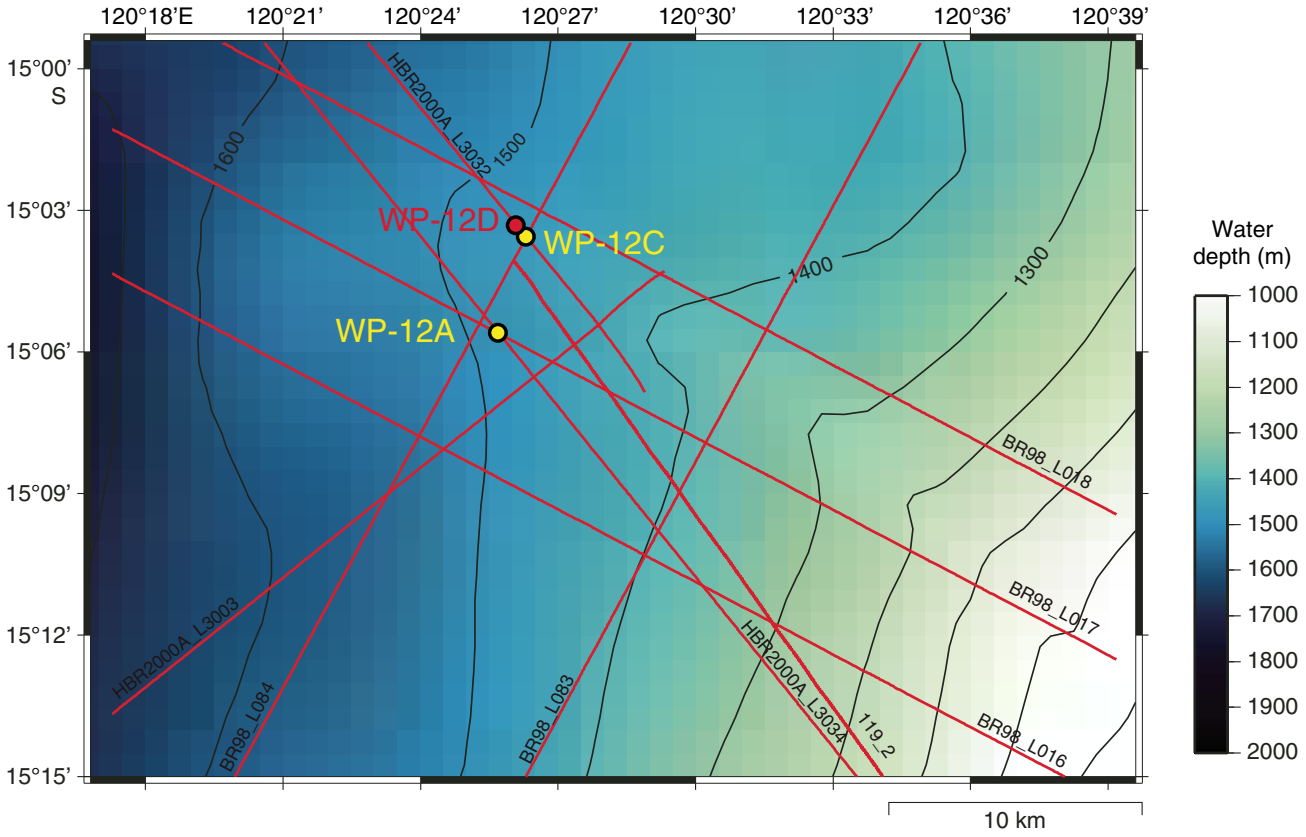

Figure AF2. Seismic reflection profile Line HBR2000A-3032 with location of proposed Site WP-12B (15°5.43′S, 120°27.88′E; shotpoint [SP] 178.57; water depth = 1430 m; target depth = 500 mbsf; requesting permission to drill as deep as 800 mbsf). Locations of crossing seismic profile lines shown with dashed lines at top.

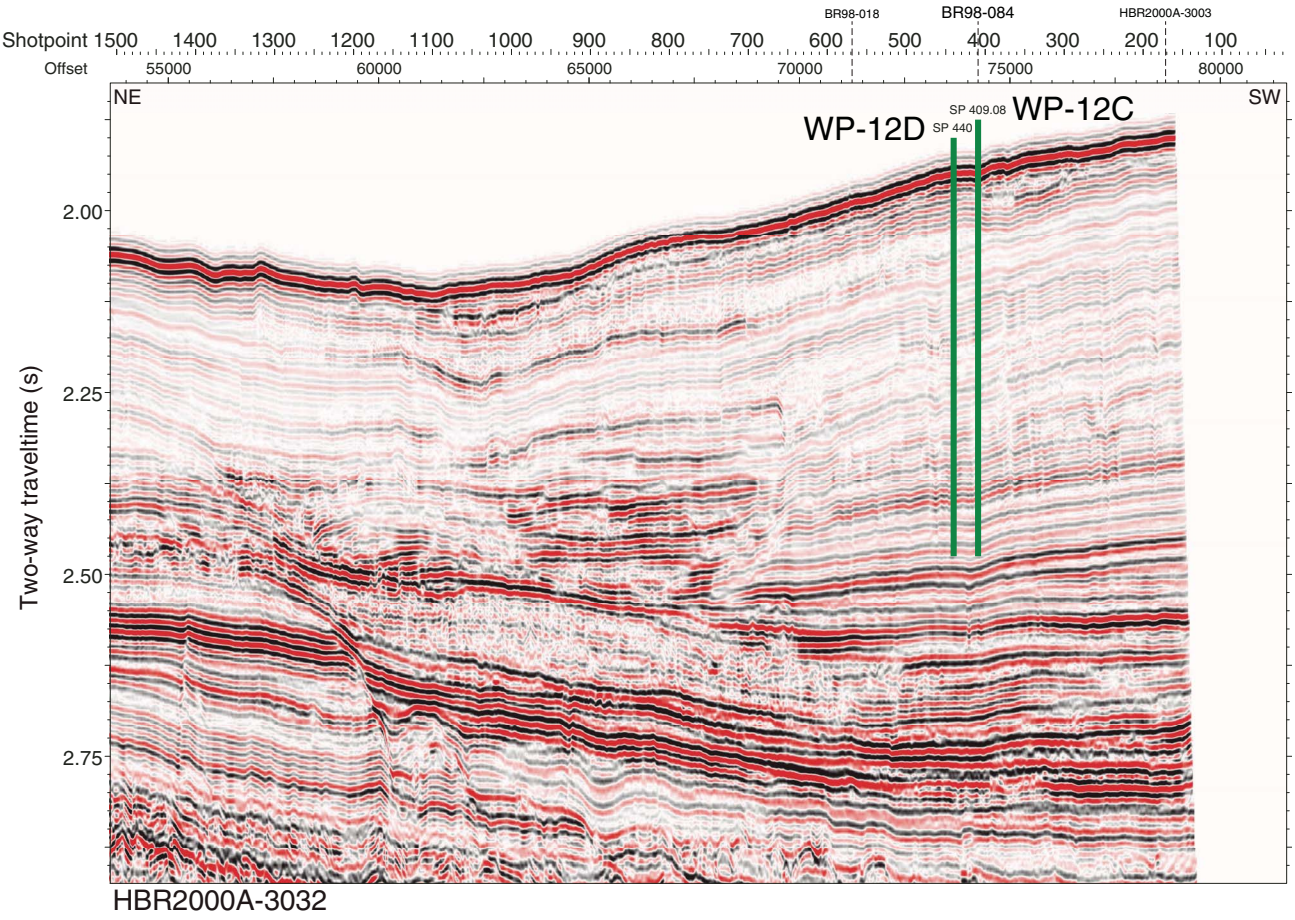

Figure AF3. Seismic reflection profile Line HBR2000A-3003 with location of proposed Site WP-12B (15°5.43′S, 120°27.88′E; shotpoint [SP] 178.57; water depth = 1430 m; target depth = 500 mbsf; requesting permission to drill as deep as 800 mbsf). Locations of crossing seismic profile lines shown with dashed lines at top.

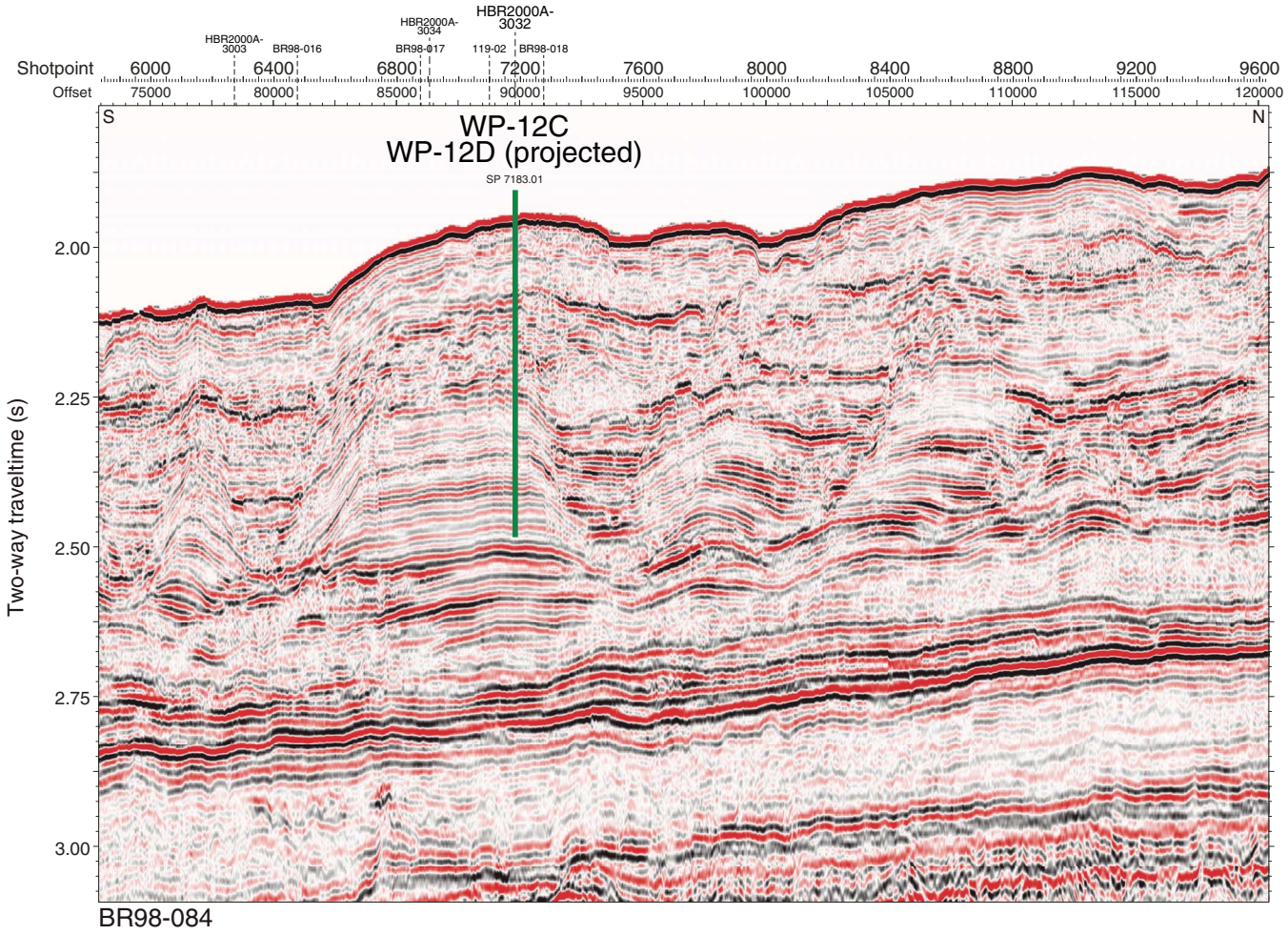

Figure AF4. Seismic reflection profile Line BR98-17 with location of alternate proposed Site WP-12A (15°5.646′S, 120°25.74′E; shotpoint [SP] 9564; water depth = 1480 m; target depth = 500 mbsf; approved depth = 800 mbsf). Locations of crossing seismic profile lines shown with dashed lines at top. Red dashed line = inferred late Miocene hiatus; yellow dashed line = inferred mid-Miocene hiatus.

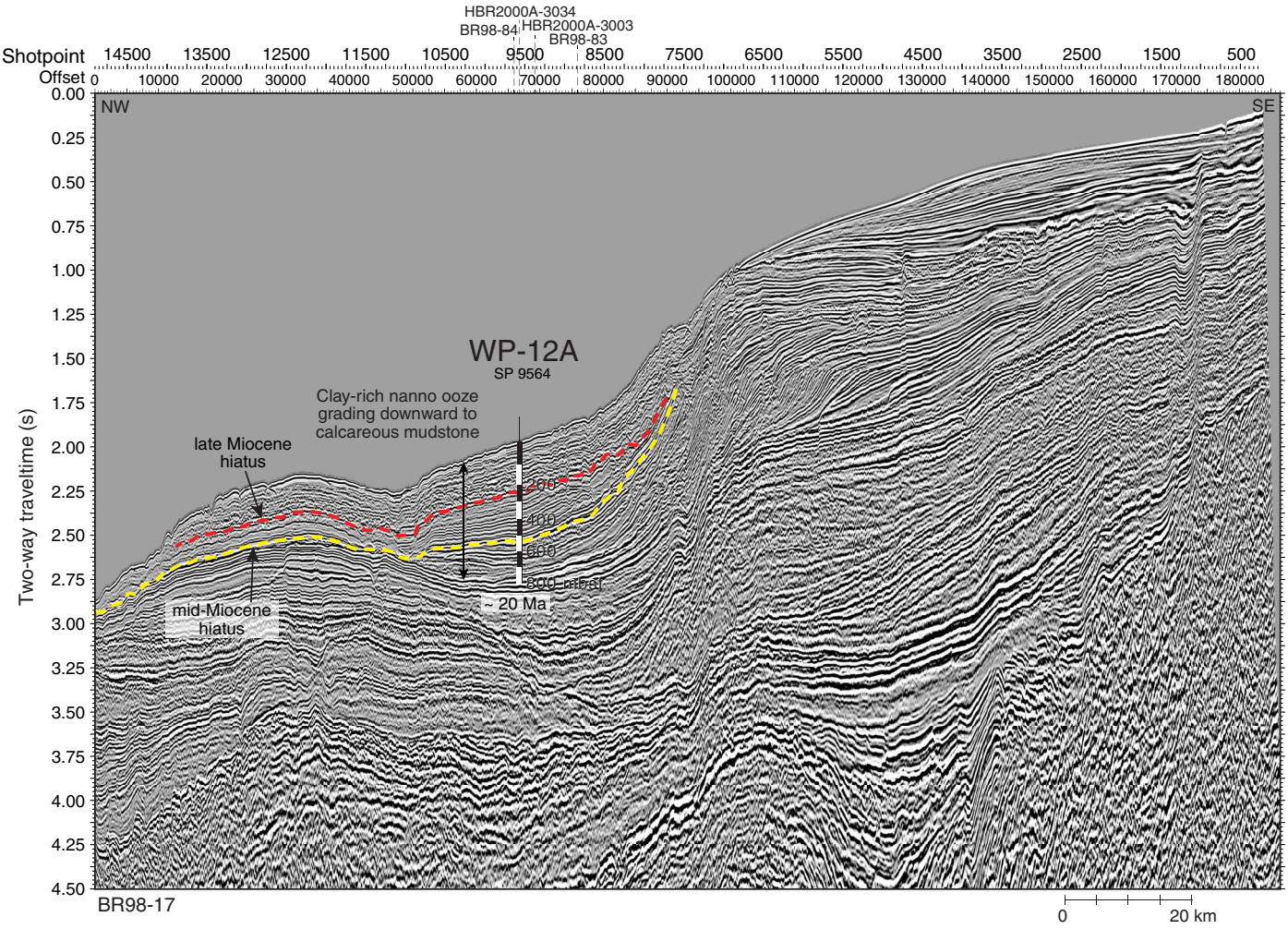

Figure AF5. Seismic reflection profile Line HBR2000A-3034 with location of alternate proposed Site WP-12A (15°5.646′S, 120°25.74′E; water depth = 1480 m; target depth = 500 mbsf; approved depth = 800 mbsf). Location of crossing seismic profile line shown with dashed line at top. Red dashed line = inferred late Miocene hiatus; yellow dashed line = inferred mid-Miocene hiatus.

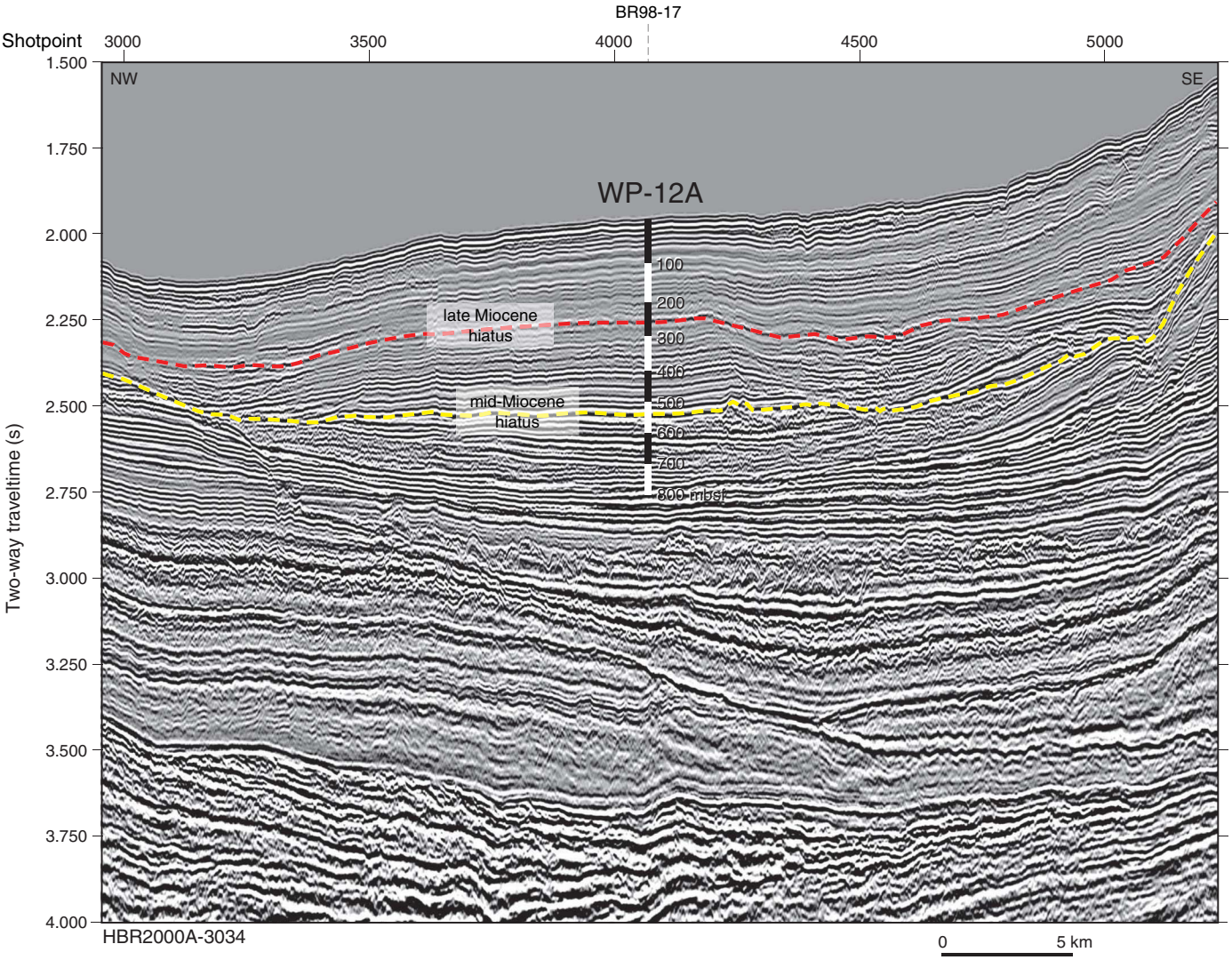

Figure AF6. Contoured bathymetric map showing the location of proposed Site WP-11B (red circle) on seismic reflection Profile BR98-168 (strike line; see Figure **AF7**), 1300 m northeast of the intersection with seismic reflection Profile BR98-117 (dip line; see Figure **AF8**). The thick red segments of the seismic reflection profiles are shown in Figures **AF7** and **AF8**. Bathymetry is based on an EM122 multibeam survey completed on *Sonne* Cruise SO-185. Contour interval = 100 m. The location of piston Core MD01-2378 is shown with a white circle.

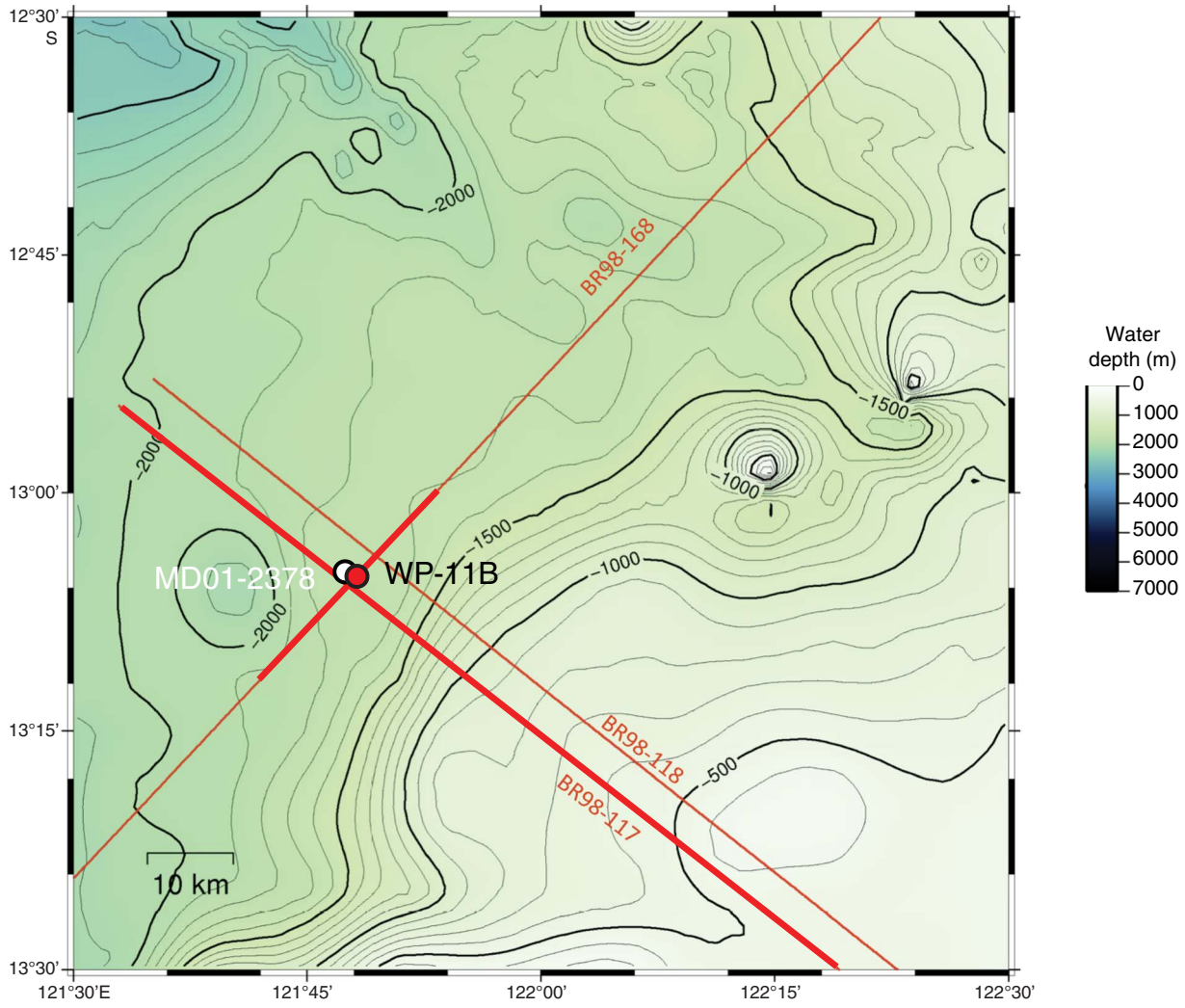

Figure AF7. Seismic reflection profile Line BR98-168 with location of proposed Site WP-11B (13°5.24′S, 121°48.24′E; shotpoint [SP] 14431; water depth = 1790 m; target depth = 350 mbsf; approved depth = 700 mbsf). Red dashed line = inferred late Miocene hiatus; yellow dashed line = inferred mid-Miocene hiatus.

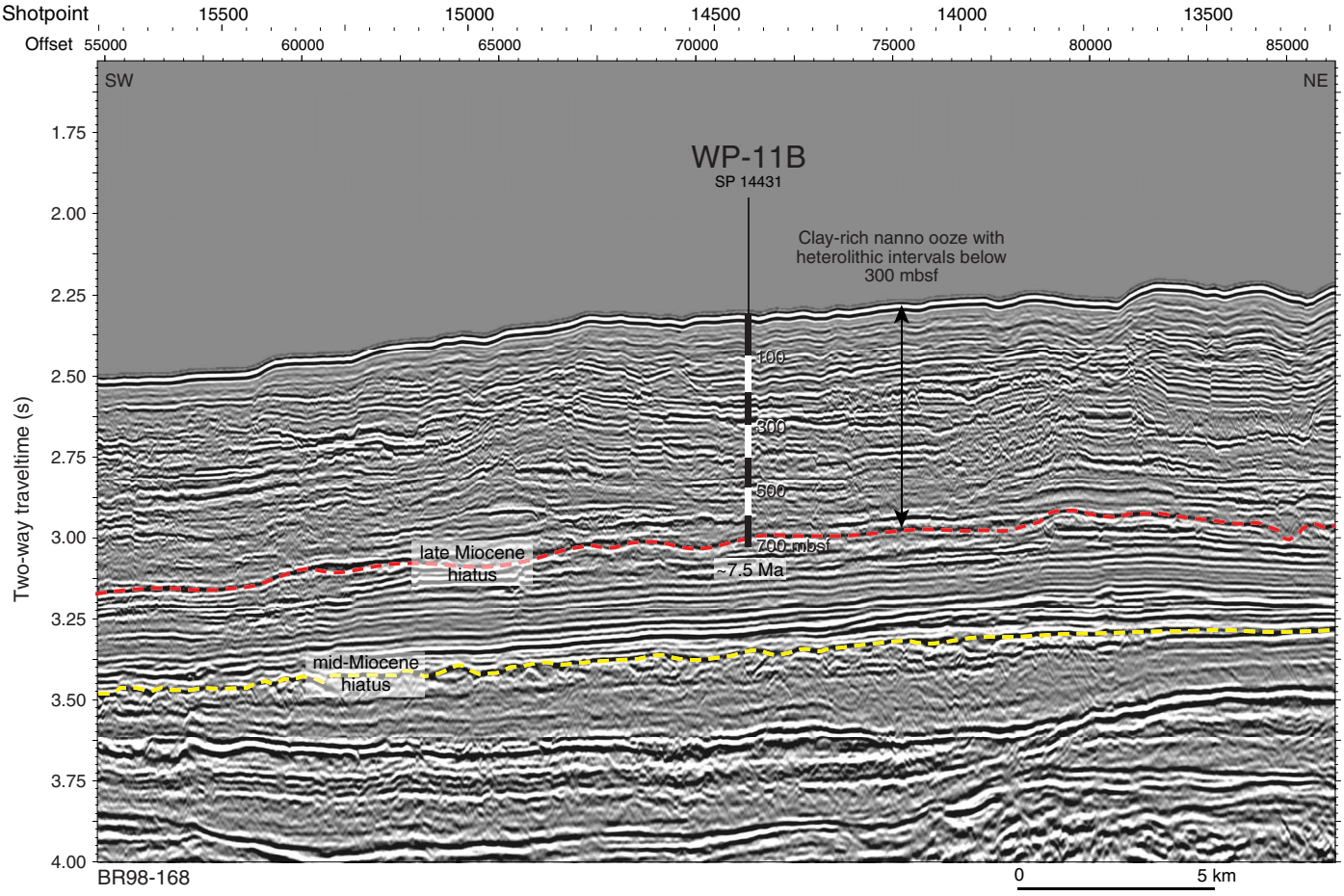

Figure AF8. Seismic reflection profile Line BR98-117 with location of proposed Site WP-11B (13°5.24′S, 121°48.24′E; projected at shotpoint [SP] 2723; water depth = 1790 m; target depth = 350 mbsf; approved depth = 700 mbsf) projected approximately 1300 m southwest onto the line. Red dashed line = inferred late Miocene hiatus; yellow dashed line = inferred mid-Miocene hiatus.

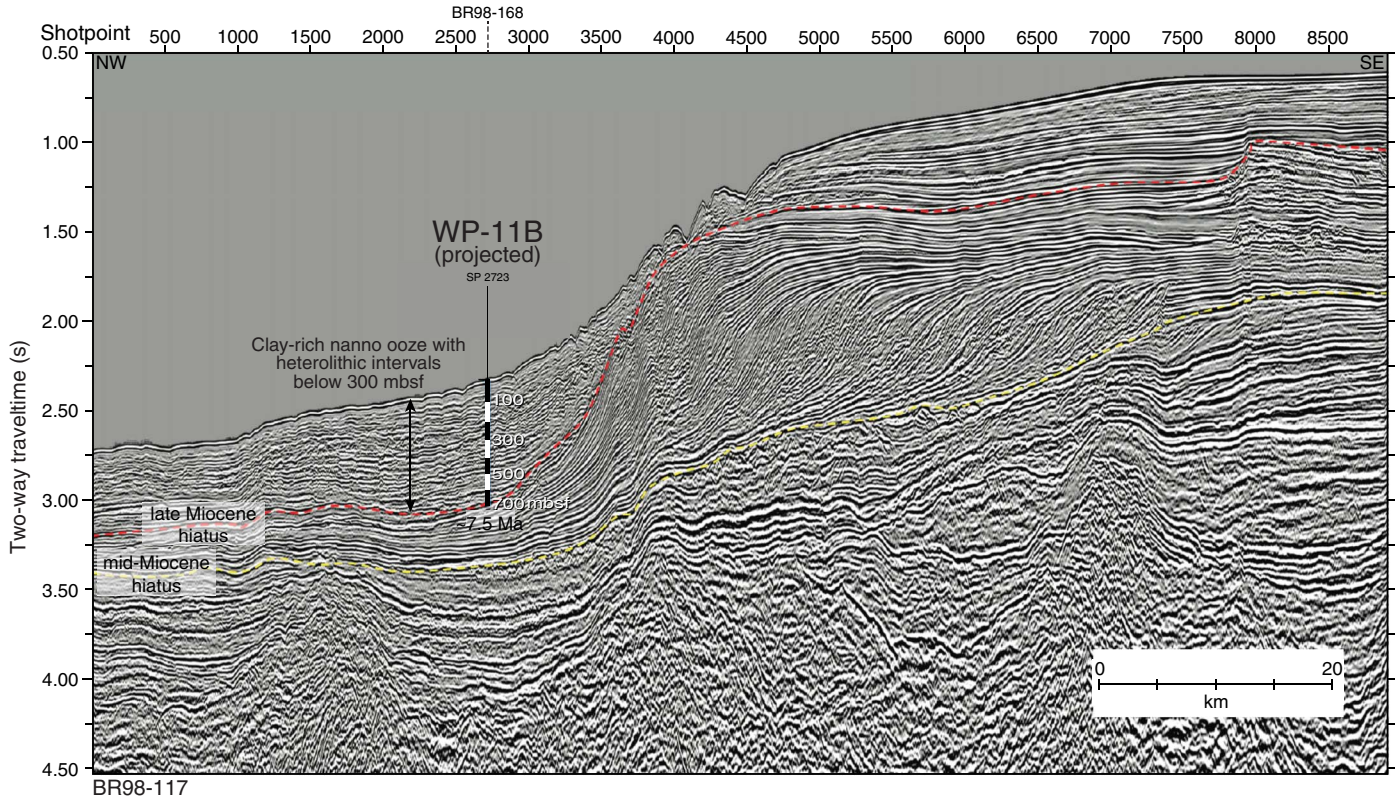

Figure AF9. Contoured bathymetric map showing the location of proposed Site WP-09A (red circle) on seismic reflection Profiles GeoB13-075 (strike line; see Figure **AF10**) and GeoB13-068 (dip line; see Figure **AF11**). Bathymetry is based on EM122 multibeam survey during *Sonne* cruise SO-228, with 2-D high-resolution multichannel seismic track lines (black) collected during the same cruise. The yellow dashed segments of the seismic reflection profiles are shown in Figures **AF10** and **AF11**. Numbers along the track lines are shotpoints. The location of piston Core MD98-2181 is shown with a white circle.

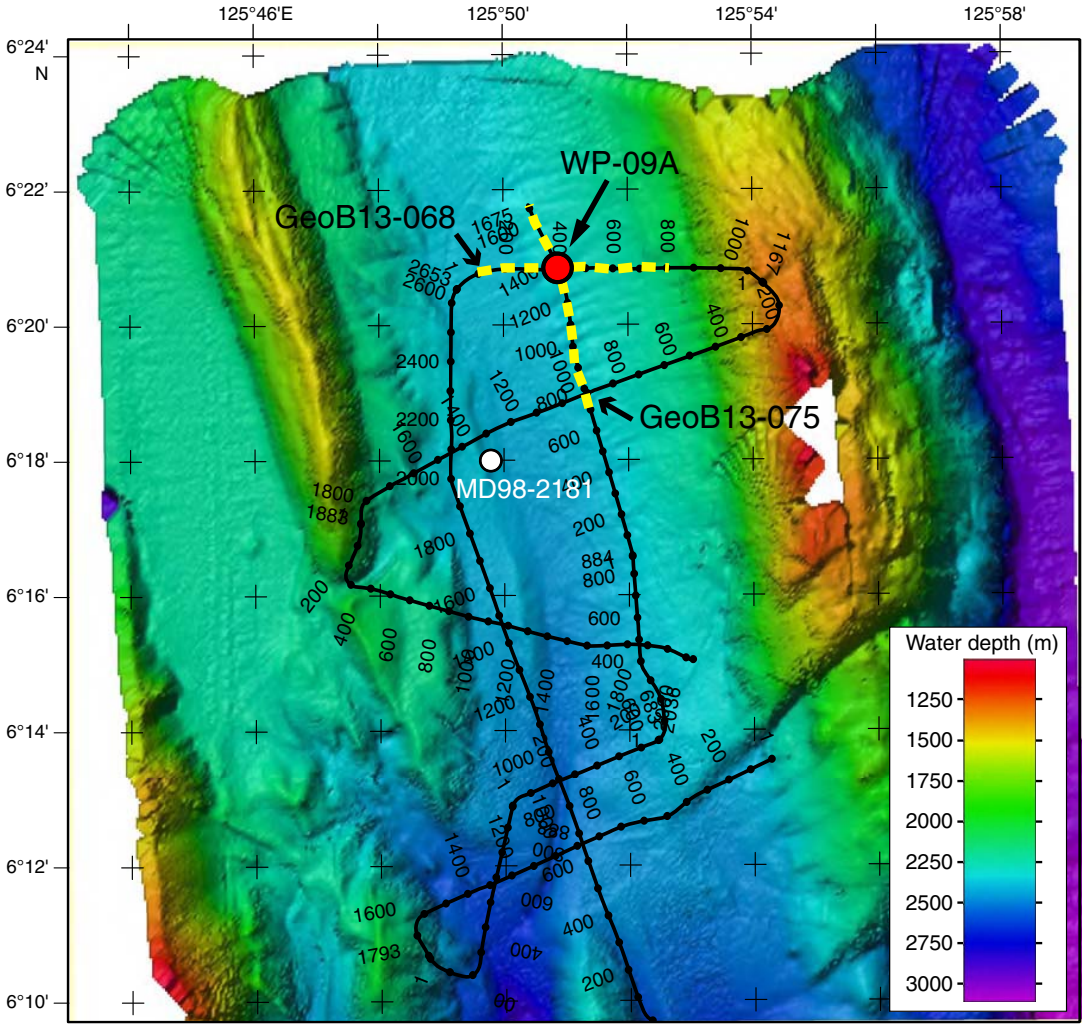

Figure AF10. Seismic reflection profile Line GeoB13-075 with location of proposed Site WP-09A (6°20.81′N, 125°50.89′E; shotpoint [SP] 1360; water depth = 2080 m; target depth = 350 mbsf; approved depth = 500 mbsf). Locations of crossing seismic profile lines shown with dashed lines at top. Red dashed lines trace reflectors.

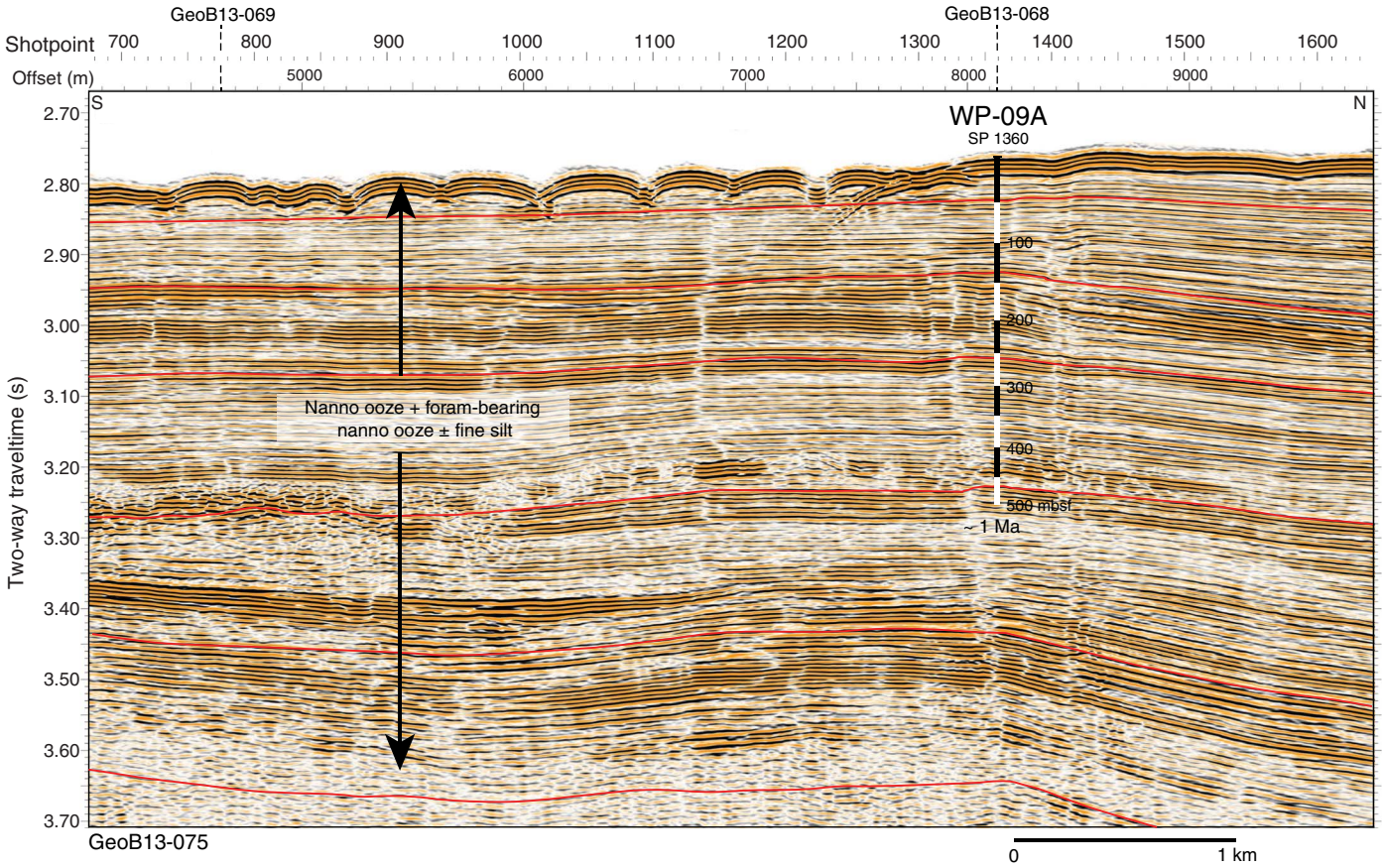

Figure AF11. Seismic reflection profile Line GeoB13-068 with location of proposed Site WP-09A (6°20.81′N, 125°50.89′E; shotpoint [SP] 398; water depth = 2080 m; target depth = 350 mbsf; approved depth = 500 mbsf). Location of crossing seismic profile line shown with dashed line at top. Red dashed lines trace horizons.

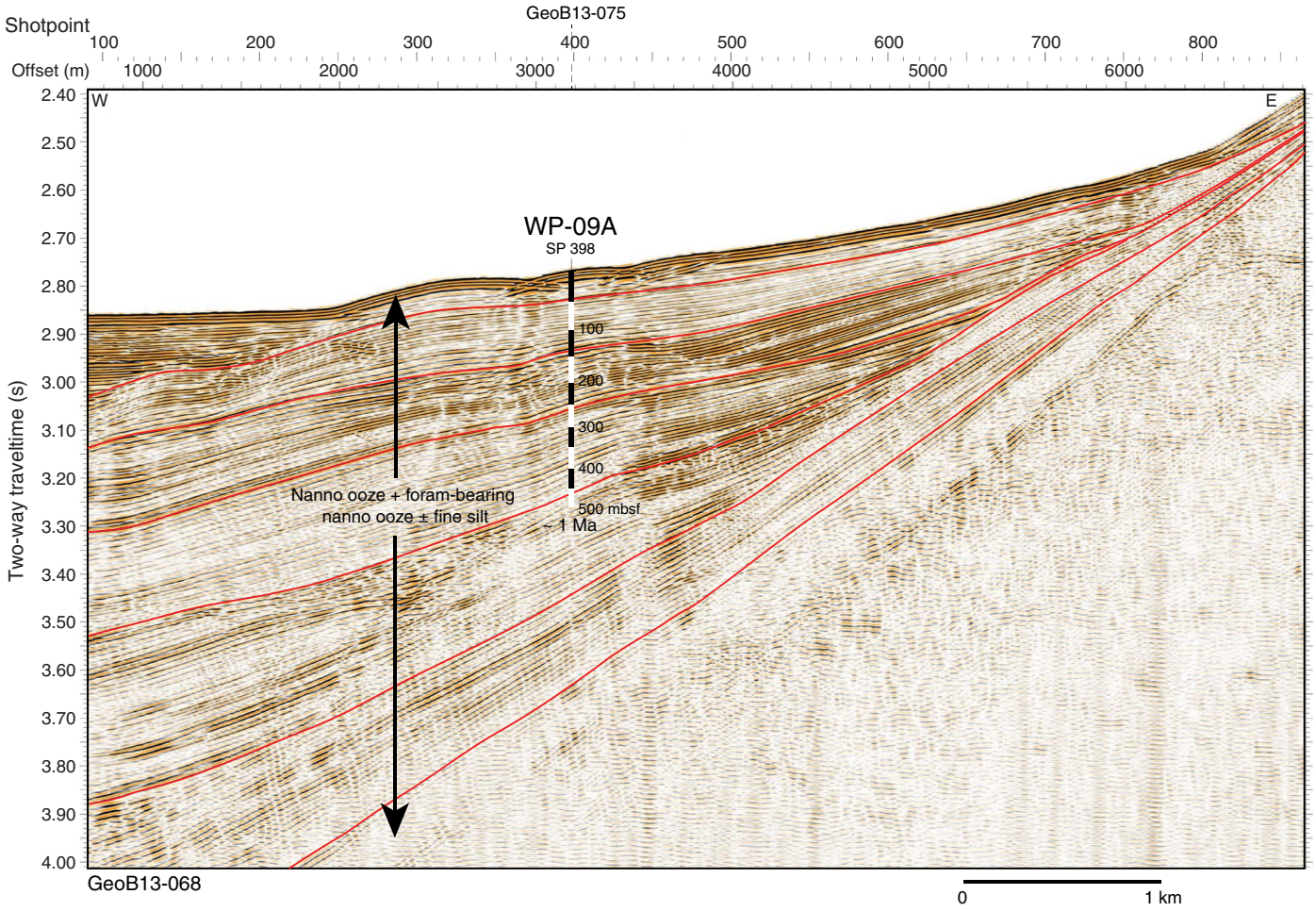

Figure AF12. Contoured bathymetric map showing the location of alternate proposed Site WP-13A (yellow circle) on seismic reflection Profile RR1313 WP13-1 (see Figure **AF13**) and projected 2.9 km south onto seismic reflection Profile RR1313 WP13-3 (see Figure **AF14**). Bathymetry based on EM122 multibeam survey collected during Cruise RR1313, with 2-D high-resolution multichannel seismic track lines (black) collected during the same cruise. Numbers along lines are common depth points (CDPs). Contour interval = 20 m. Black circle shows location of piston Core 44 taken during Cruise RR1313. Deep Sea Drilling Project Site 292 location shown as blue circle.

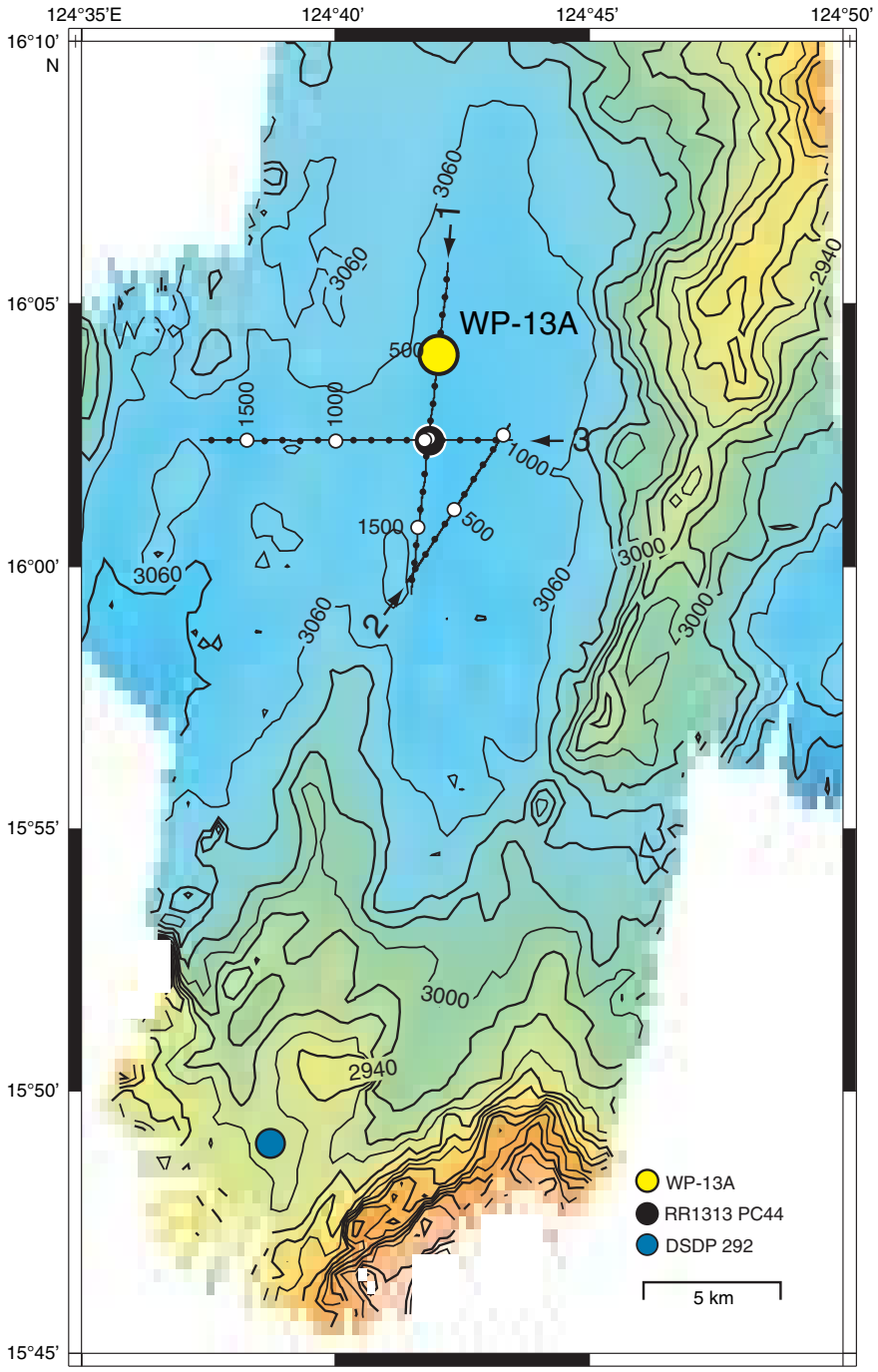

Figure AF13. Seismic reflection profile Lline RR1313 WP13-1 with location of alternate proposed Site WP-13A (16°3.98′N, 124°42.03′E; shotpoint [SP] 540; water depth = 3077 m; target depth = 280 mbsf; approved depth = 280 mbsf). Locations of crossing seismic profile lines shown with dashed lines at top.

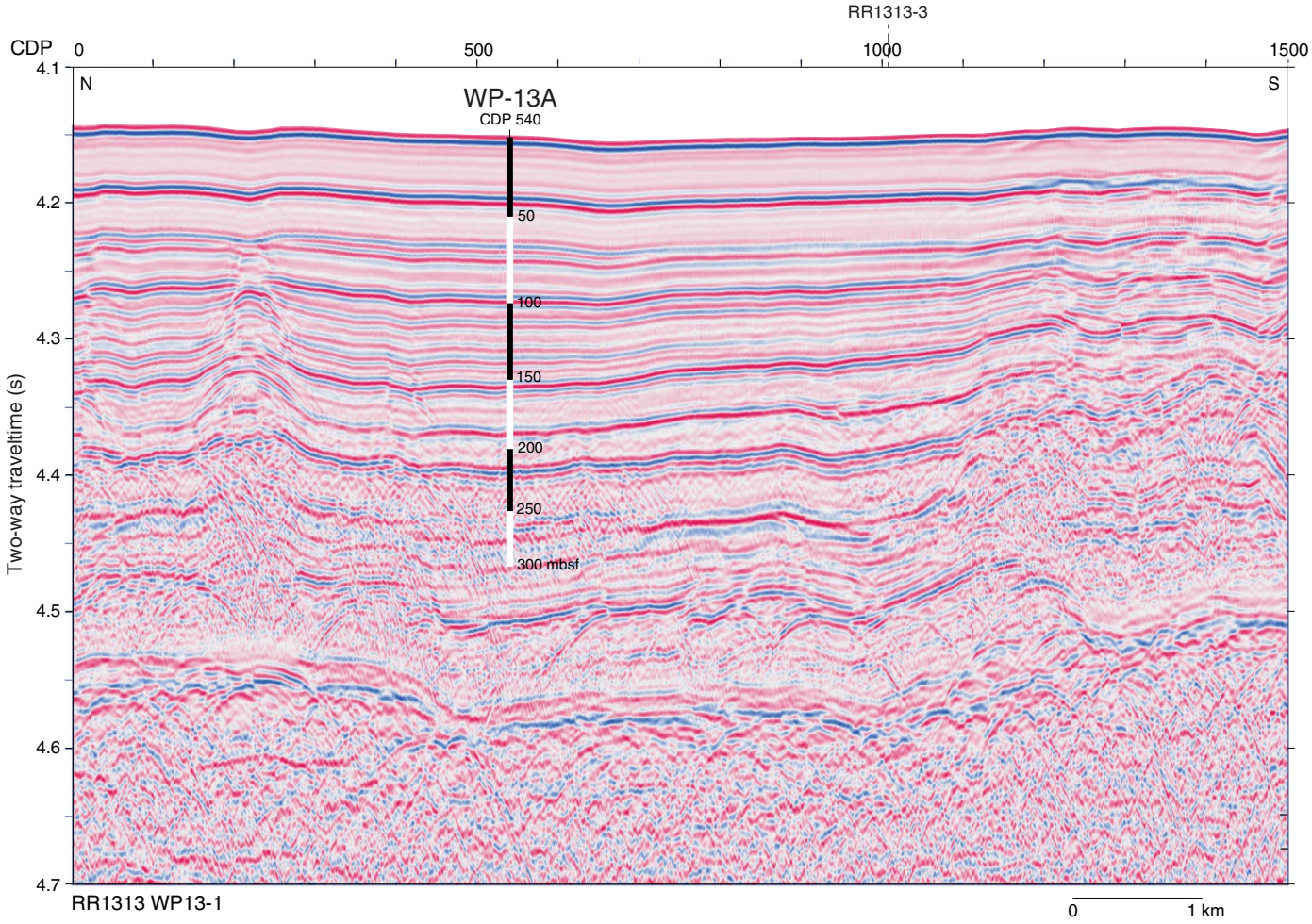

Figure AF14. Seismic reflection profile Line RR1313 WP13-3 with location of alternate proposed Site WP-13A (16°3.98′N, 124°42.03′E; projected at common depth point [CDP] 480; water depth = 3077 m; target depth = 280 mbsf; approved depth = 280 mbsf) projected 2.9 km south onto the line. Locations of crossing seismic profile lines shown with dashed lines at top.

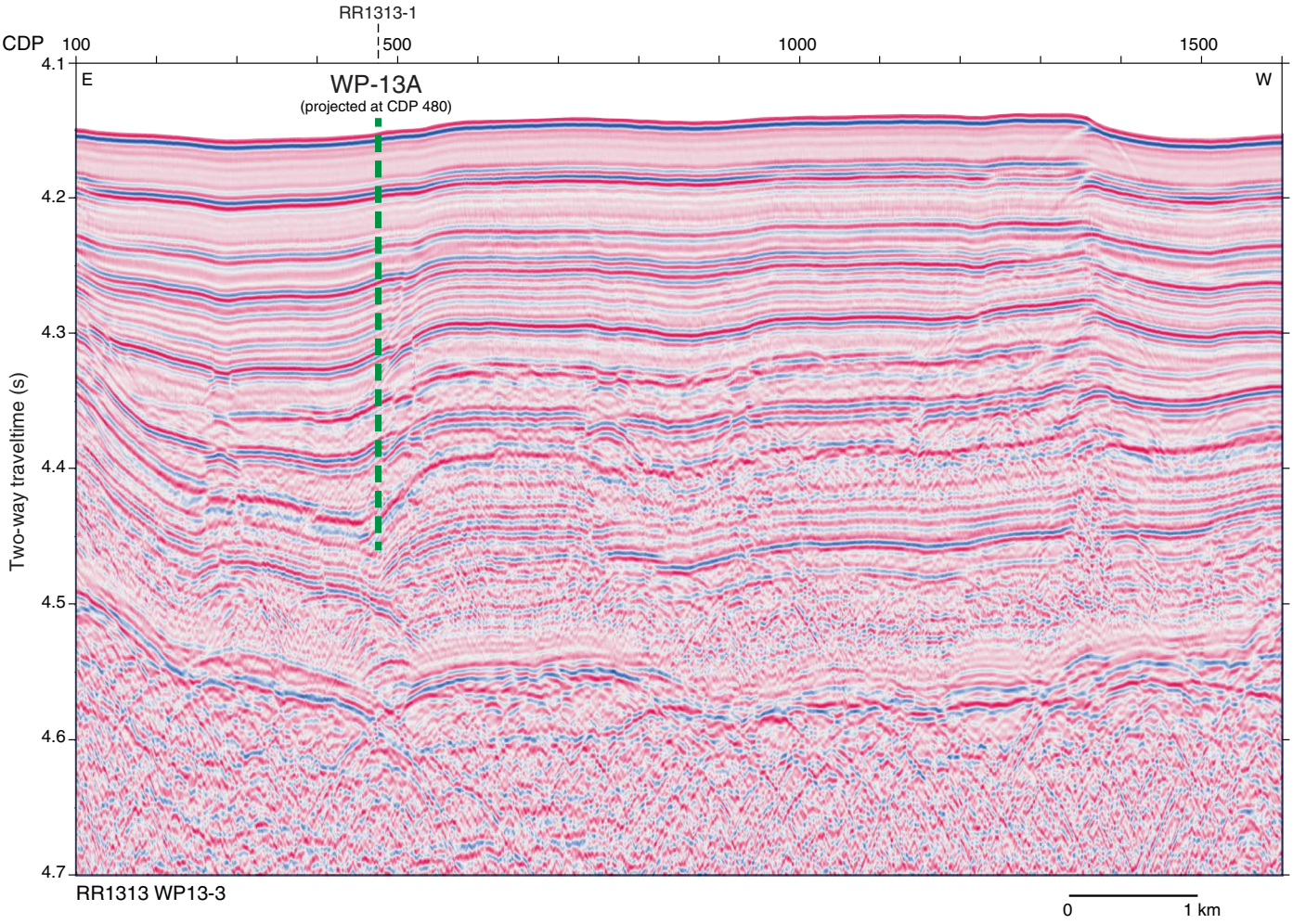

Figure AF15. Contoured bathymetric map showing the location of proposed Site WP-71A (red circle) and alternate proposed Site WP-72A (yellow circle) on seismic reflection Profile RR1313-WP7-2 (see Figure **AF16**) and projected onto seismic reflection Profile RR1313-WP7-5 (see Figure **AF17**). Bathymetry is based on EM122 multibeam survey collected during Cruise RR1313, with 2-D high-resolution multichannel seismic track lines (black) collected during the same cruise. Numbers along the lines are common depth points (CDPs). Contour interval = 50 m. Black circle shows location of piston Core 32 taken during Cruise RR1313.

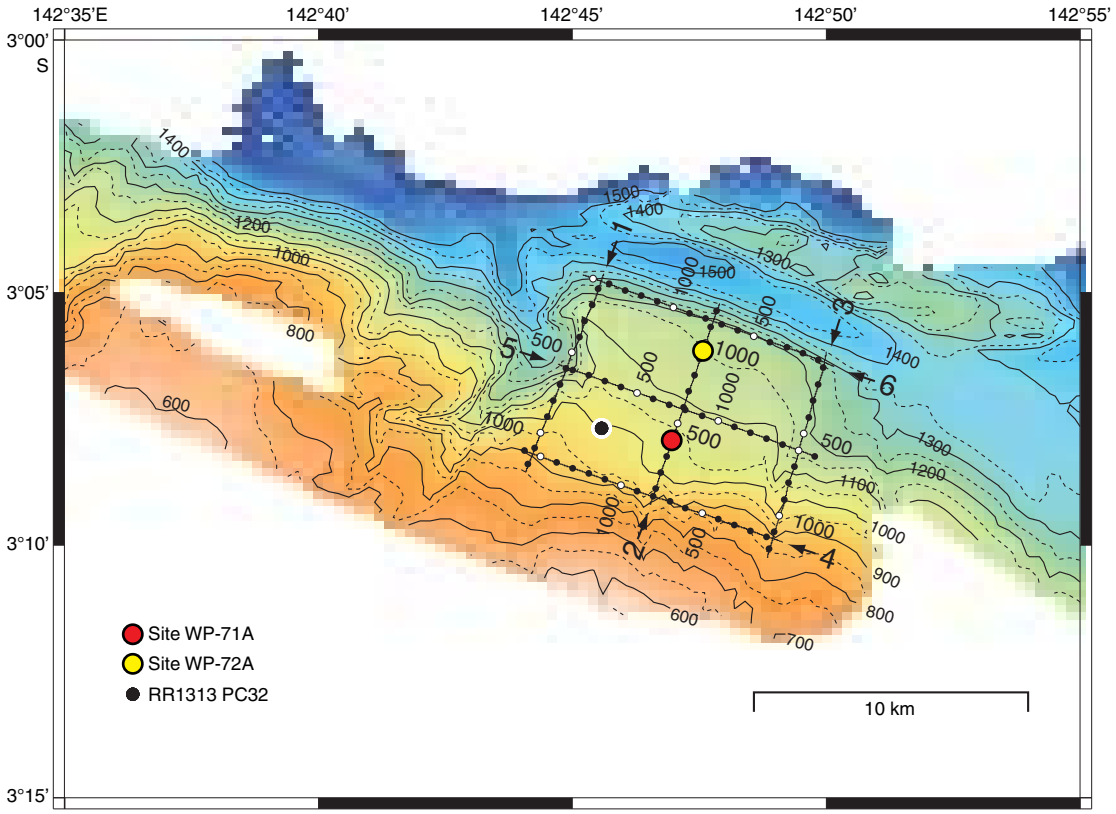

Figure AF16. Seismic reflection profile Line RR1313 WP7-2 with location of proposed Site WP-71A (3°7.92′S, 142°46.96′E; common depth point [CDP] 400; water depth = 1030 m; target depth = 225 mbsf; approved depth = 225 mbsf) and alternate proposed Site WP-72A (3°6.16′S, 142°47.57′E; CDP 950; water depth = 1147 m; target depth = 315 mbsf; approved depth = 325 mbsf). Location of crossing seismic profile line shown with dashed line at top.

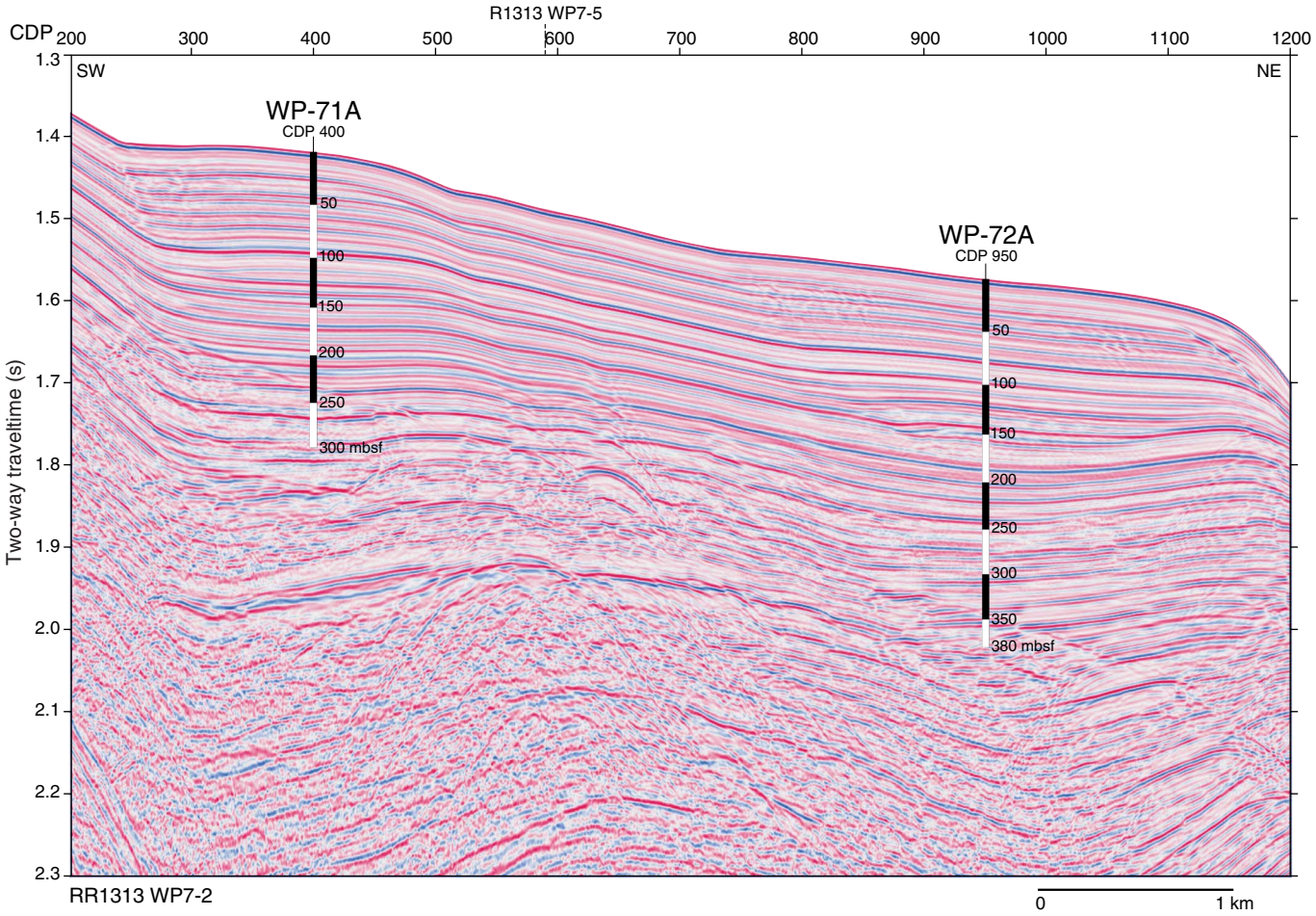

Figure AF17. Seismic reflection profile Line RR1313 WP7-5 with location of proposed Site WP-71A (3°7.92′S, 142°46.96′E; projected at common depth point [CDP] 782; water depth = 1030 m; target depth = 225 mbsf; approved depth = 225 mbsf) projected 1.2 km northeast onto the line and alternate proposed Site WP-72A (3°6.16′S, 142°47.57′E; projected at CDP 782; water depth = 1147 m; target depth = 315 mbsf; approved depth = 325 mbsf) projected 2.2 km southwest onto the line. Location of crossing seismic profile line shown with dashed line at top.

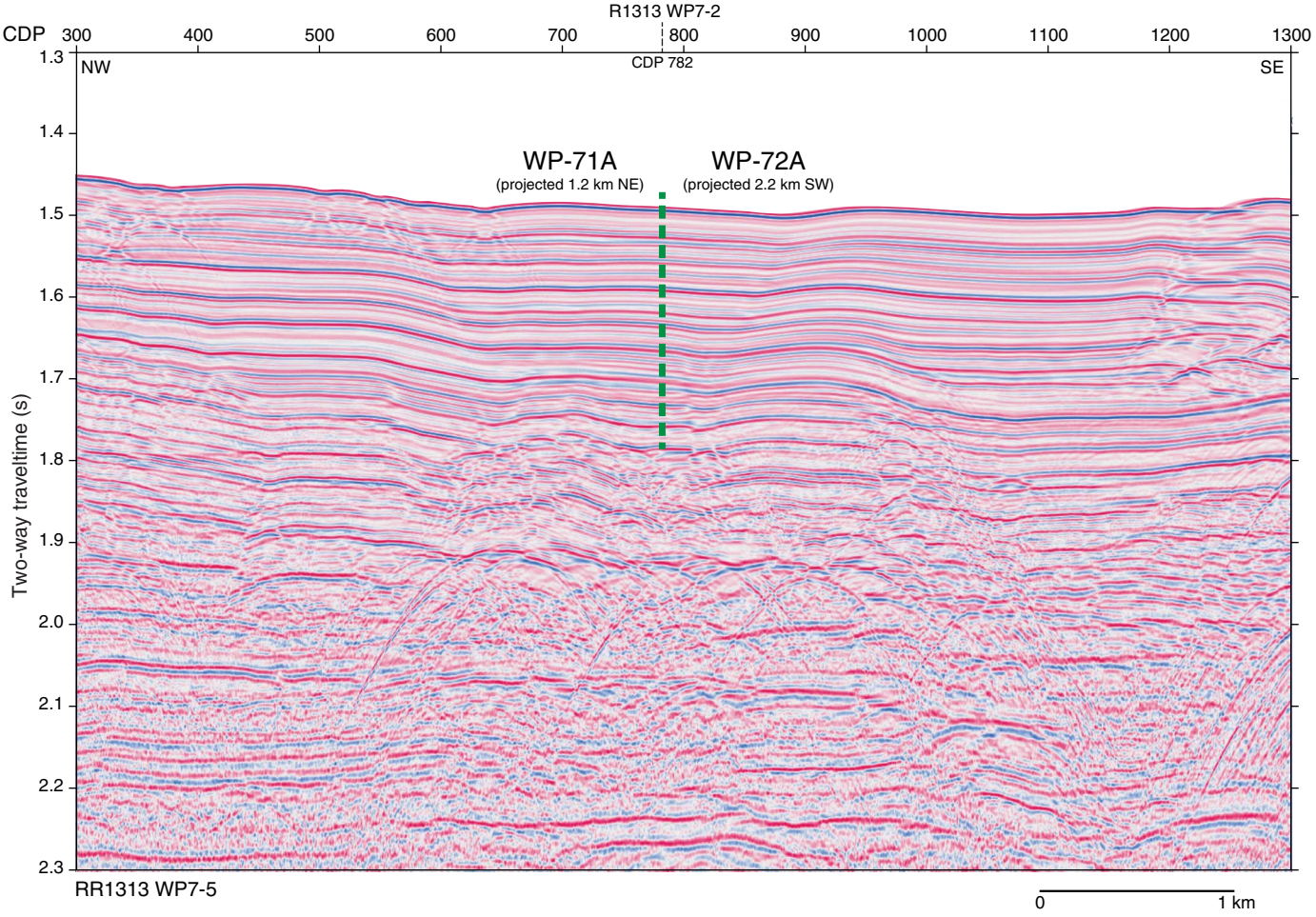

Figure AF18. Contoured bathymetric map showing location of proposed Site WP-05A (red circle) at the intersection of seismic reflection Profiles GeoB13-084 (see Figure **AF19**) and GeoB13-088 (see Figure **AF20**). Bathymetry is based on EM122 multibeam survey during *Sonne* Cruise SO-228, with 2-D high-resolution multichannel seismic track lines (black) collected during the same cruise. Numbers along the lines are shotpoints (SPs).

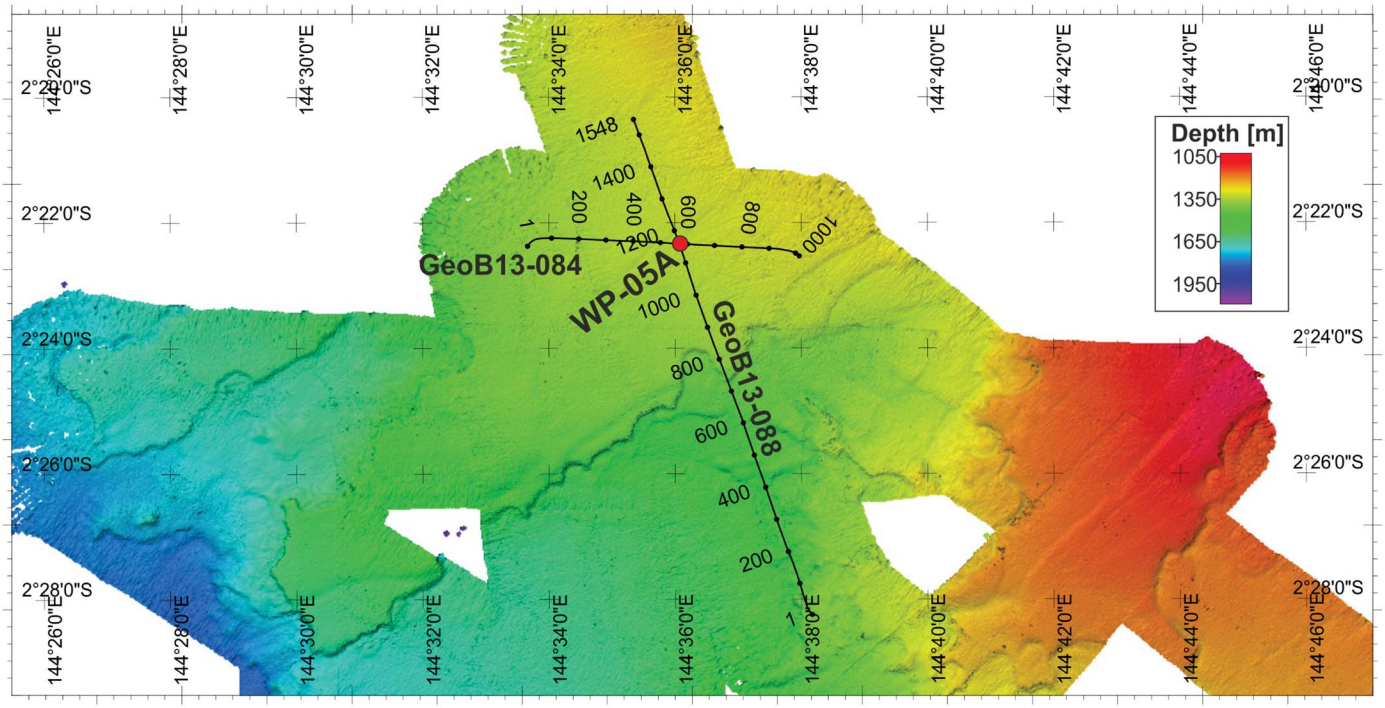

Figure AF19. Seismic reflection profile Line GeoB13-084 with location of proposed Site WP-05A (2°22.34′S, 144°36.07′E; shotpoint [SP] 570; water depth = 1337 m; target depth = 200 mbsf; approved depth = 224 mbsf). Location of crossing seismic profile line shown with dashed line at top.

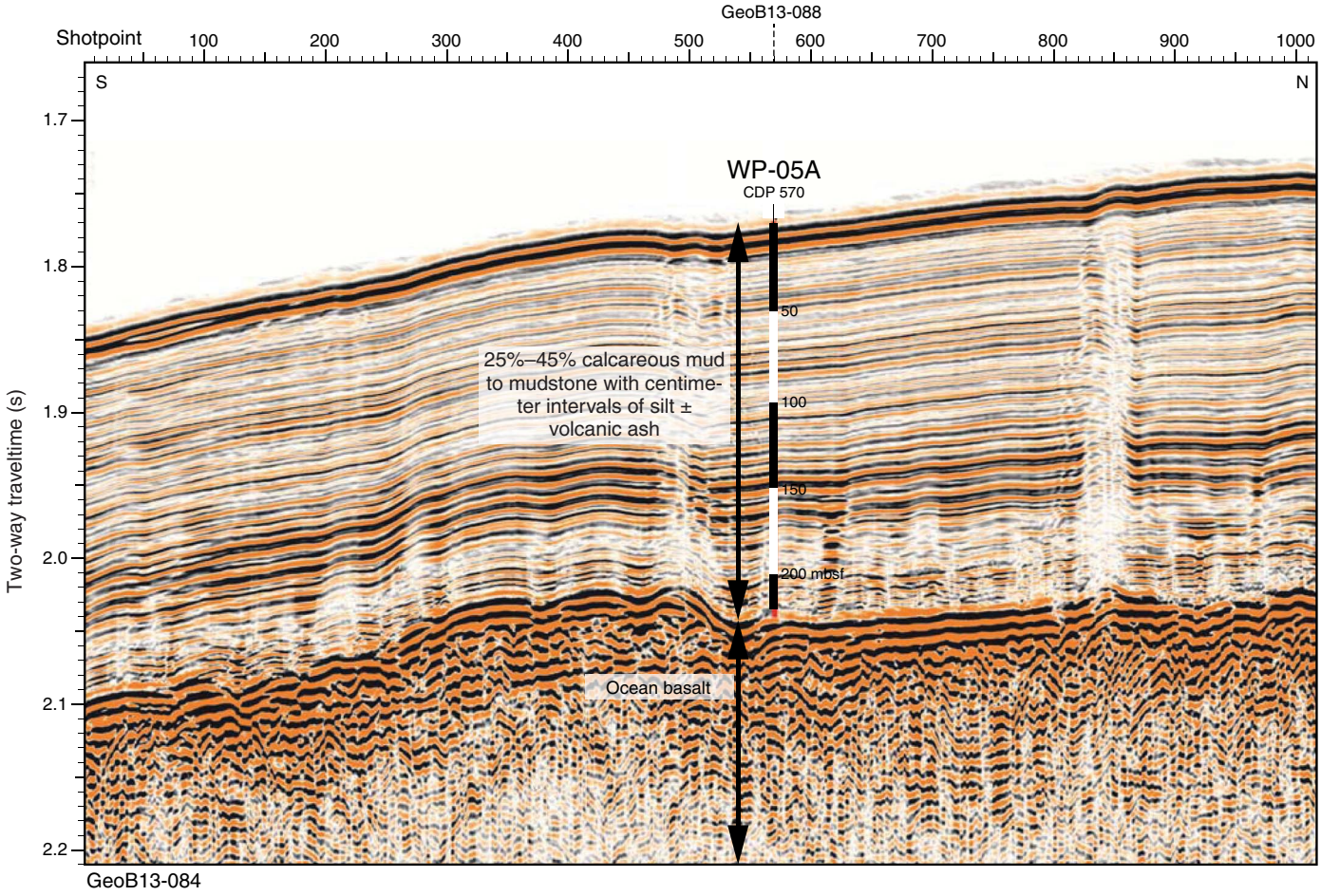

Figure AF20. Seismic reflection profile Line GeoB13-088 with location of proposed Site WP-05A (2°22.34′S, 144°36.07′E; shotpoint [SP] 1159; water depth = 1337 m; target depth = 200 mbsf; approved depth = 224 mbsf). Location of crossing seismic profile line shown with dashed line at top.

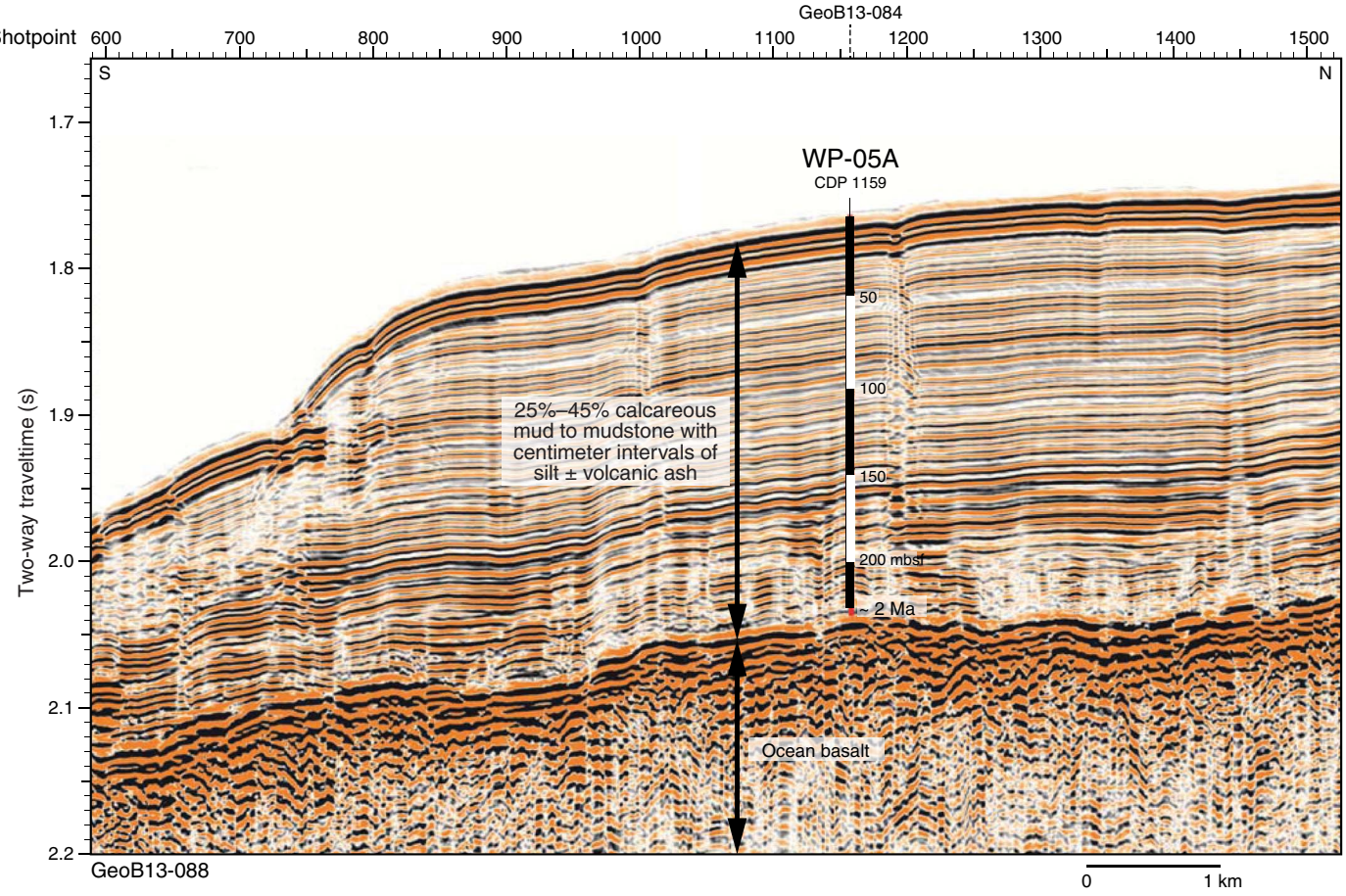

Figure AF21. Contoured bathymetric map showing the location of alternate proposed Site WP-06A (yellow circle) and alternate proposed Site WP-14A (green circle) on seismic reflection Profile RR1313 WP6-5 (see Figure **AF22**). Site WP-06A is located approximately 1.9 km northeast of the intersection with seismic reflection Profile RR1313 WP6-3a (see Figure **AF23**), whereas Site WP-14A is located approximately 1.4 km southwest of the crossing line. Bathymetry is based on EM122 multibeam survey collected during Cruise RR1313, with 2-D high-resolution multichannel seismic track lines (black) collected during the same cruise. The numbers along the lines are common depth points (CDPs). Contour interval = 50 m. Piston Core 26 taking during Cruise RR1313 is located very close to the position of Site WP-14A (green circle).

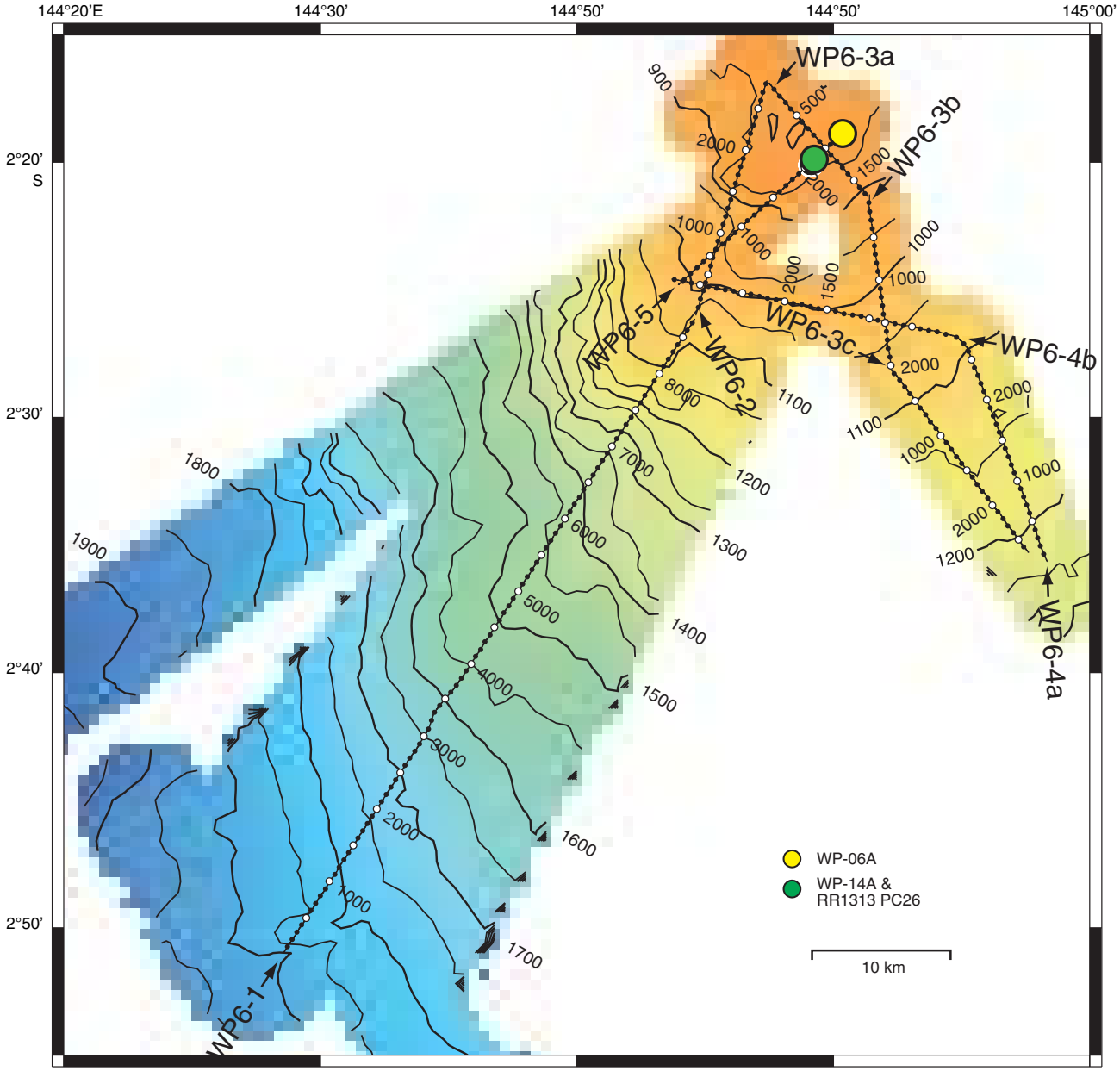

Figure AF22. Seismic reflection profile line RR1313 WP6-5 with locations of proposed alternate Site WP-06A (2°18.78′S, 144°50.47′E; common depth point [CDP] 2630; water depth = 880 m; target depth = 200 mbsf; approved depth = 215 mbsf) and alternate proposed Site WP-14A (2°19.98′S, 144°49.16′E; CDP 2100; water depth = 880 m; target depth = 175 mbsf; approved depth = 177 mbsf). Location of crossing seismic profile line shown with dashed line at top.

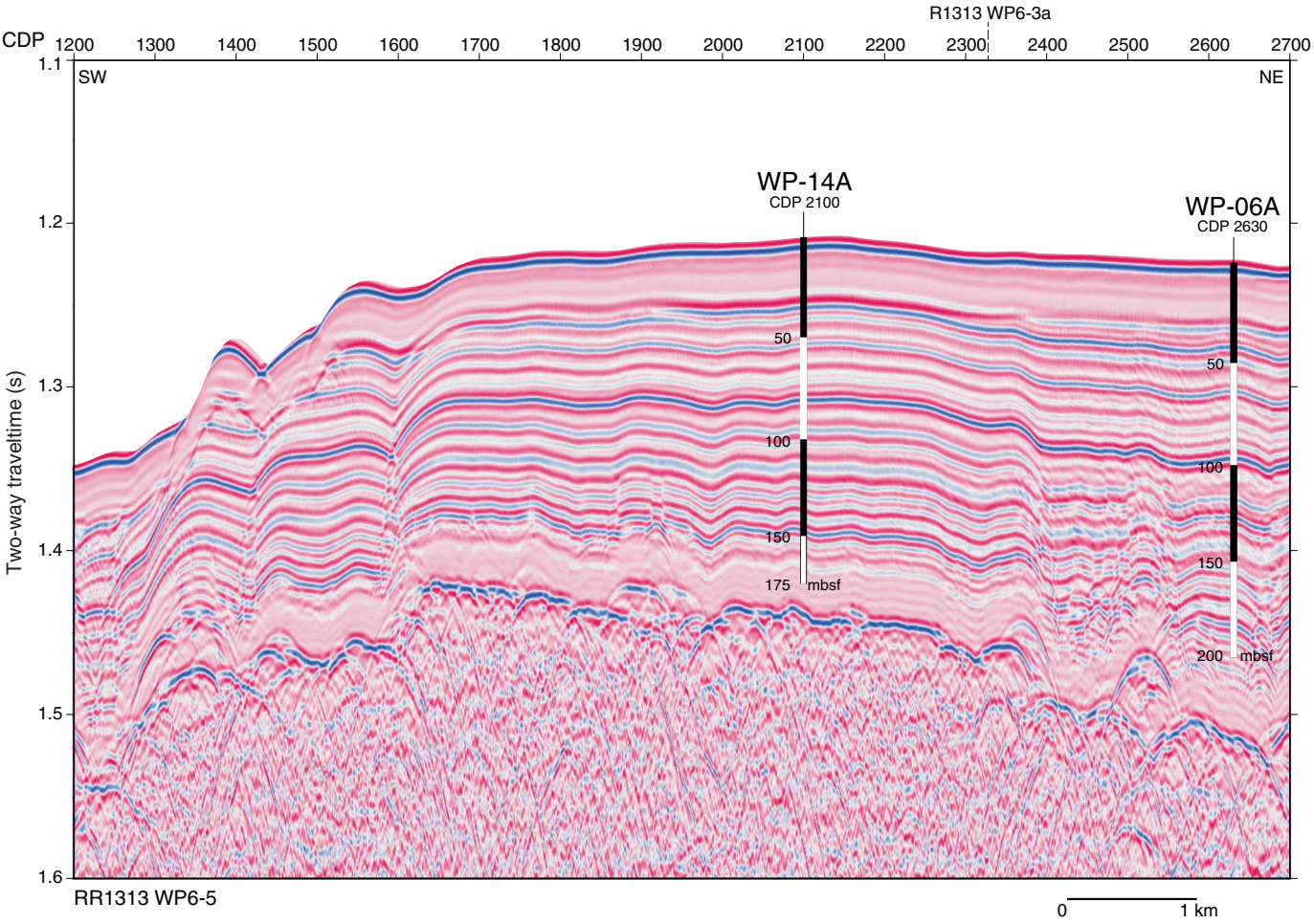

Figure AF23. Seismic reflection profile Line RR1313 WP6-3a with location of alternate proposed Site WP-06A (2°18.78′S, 144°50.47′E; projected at common depth point [CDP] 1013; water depth = 880 m; target depth = 200 mbsf; approved depth = 215 mbsf) projected 1.9 km southwest onto the line. Alternate proposed Site WP-14A (2°19.98′S, 144°49.16′E; projected at CDP 1013; water depth = 880 m; target depth = 175 mbsf; approved depth = 177 mbsf) is projected 1.4 km northeast onto the line. Location of crossing seismic profile line shown with dashed line at top.

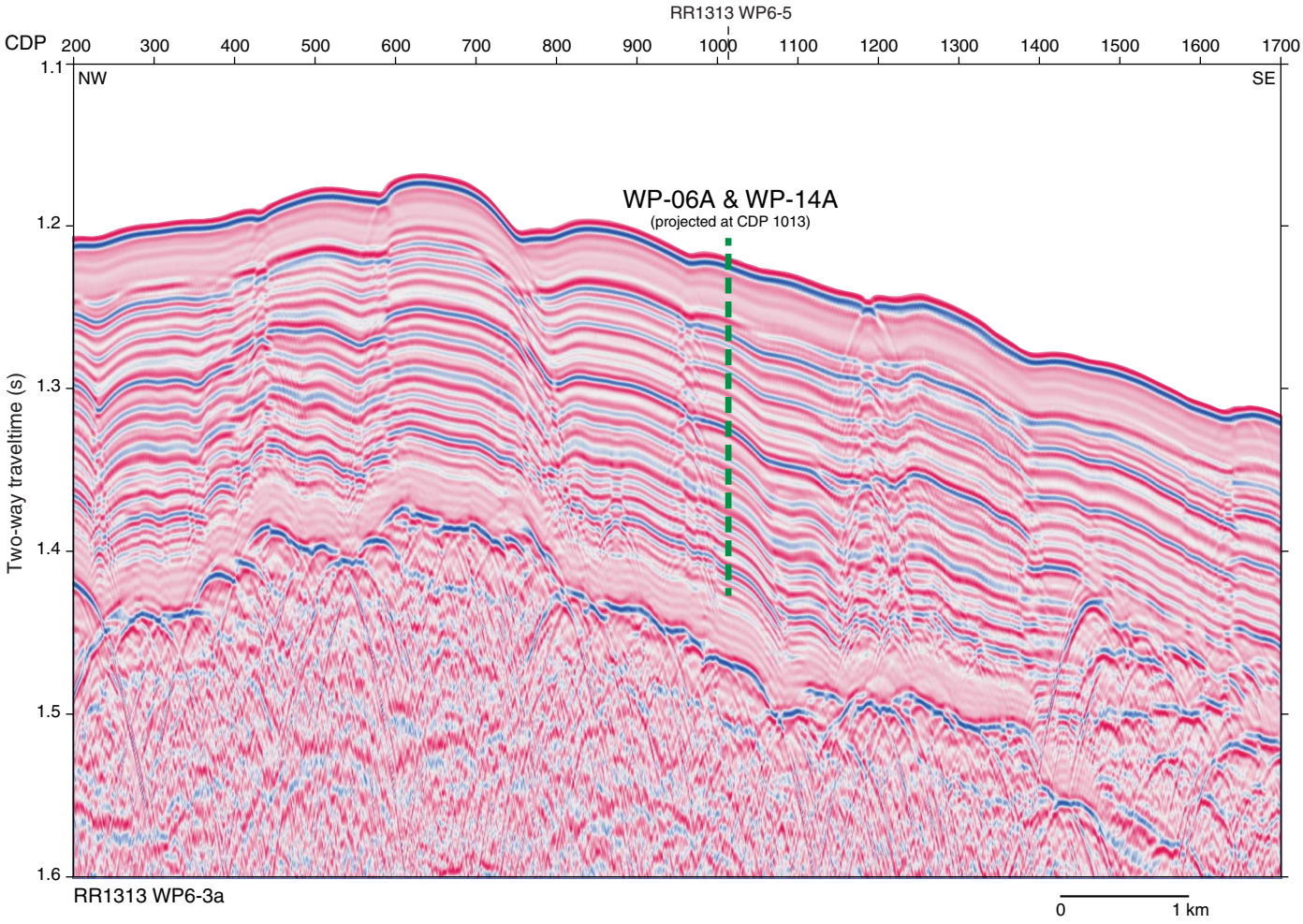

Figure AF24. Contoured bathymetric map showing the location of proposed Site WP-03A (red circle) on seismic reflection profile Line RR1313 WP3-1 (see Figure **AF25**), 4.4 km southwest of the intersection with seismic reflection profile Line RR1313 WP3-3 (see Figure **AF26**). Bathymetry is based on EM122 multibeam survey during Cruise RR1313, with 2-D high-resolution multichannel seismic track lines (black) collected during the same cruise. Numbers along lines are common depth points (CDPs). Contour interval = 30 m. The location of piston Cores RR1313 PC37 (black circle) and MD97-2140 (white circle) are shown, together with Deep Sea Drilling Project Site 62 (green circle).

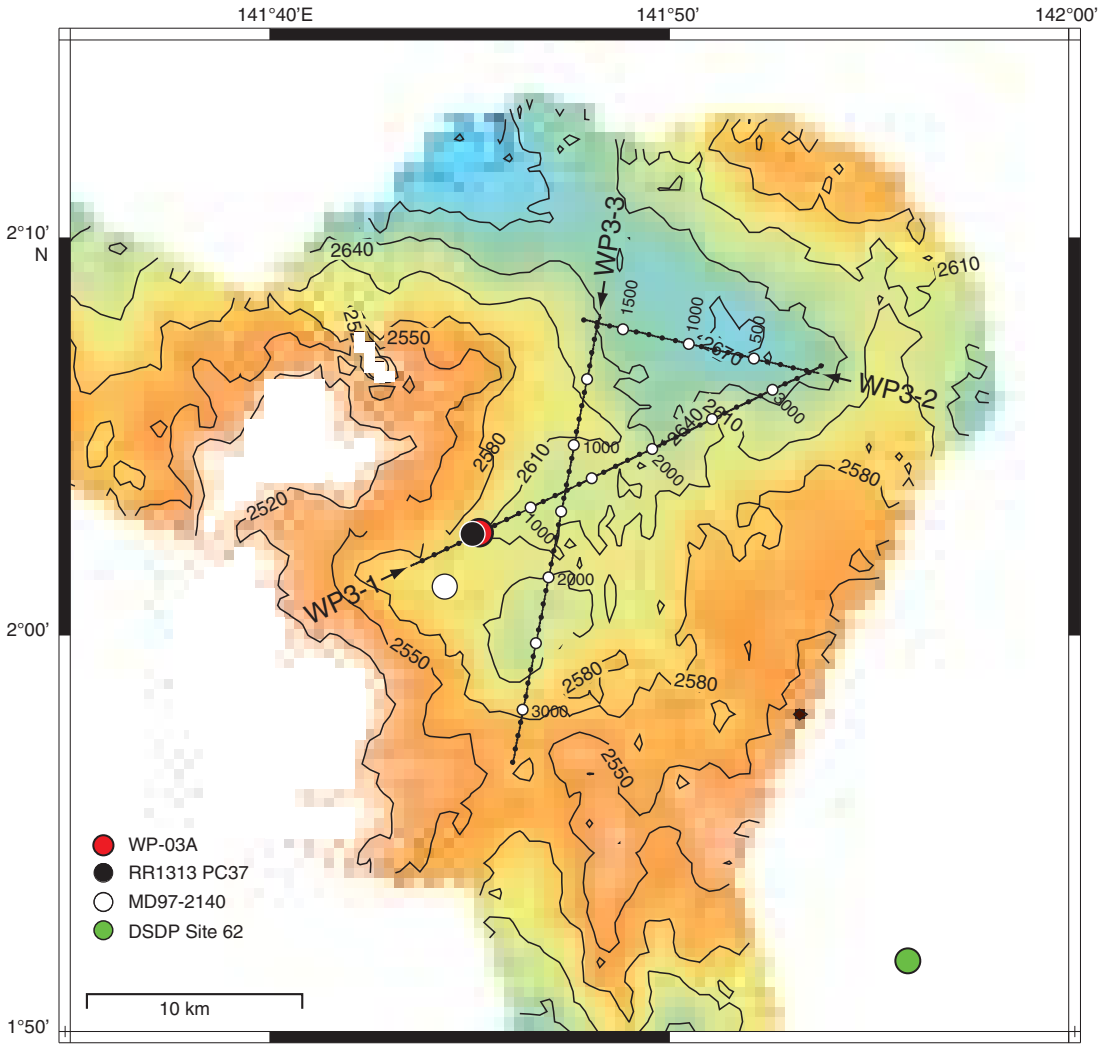

Figure AF25. Seismic reflection profile Line RR1313 WP3-1 with location of proposed Site WP-03A (2°2.59′N, 141°45.29′E; common depth point [CDP] 580; water depth = 2600 m; target depth = 300 mbsf; approved depth = 500 mbsf). Location of crossing seismic profile line shown with dashed line at top.

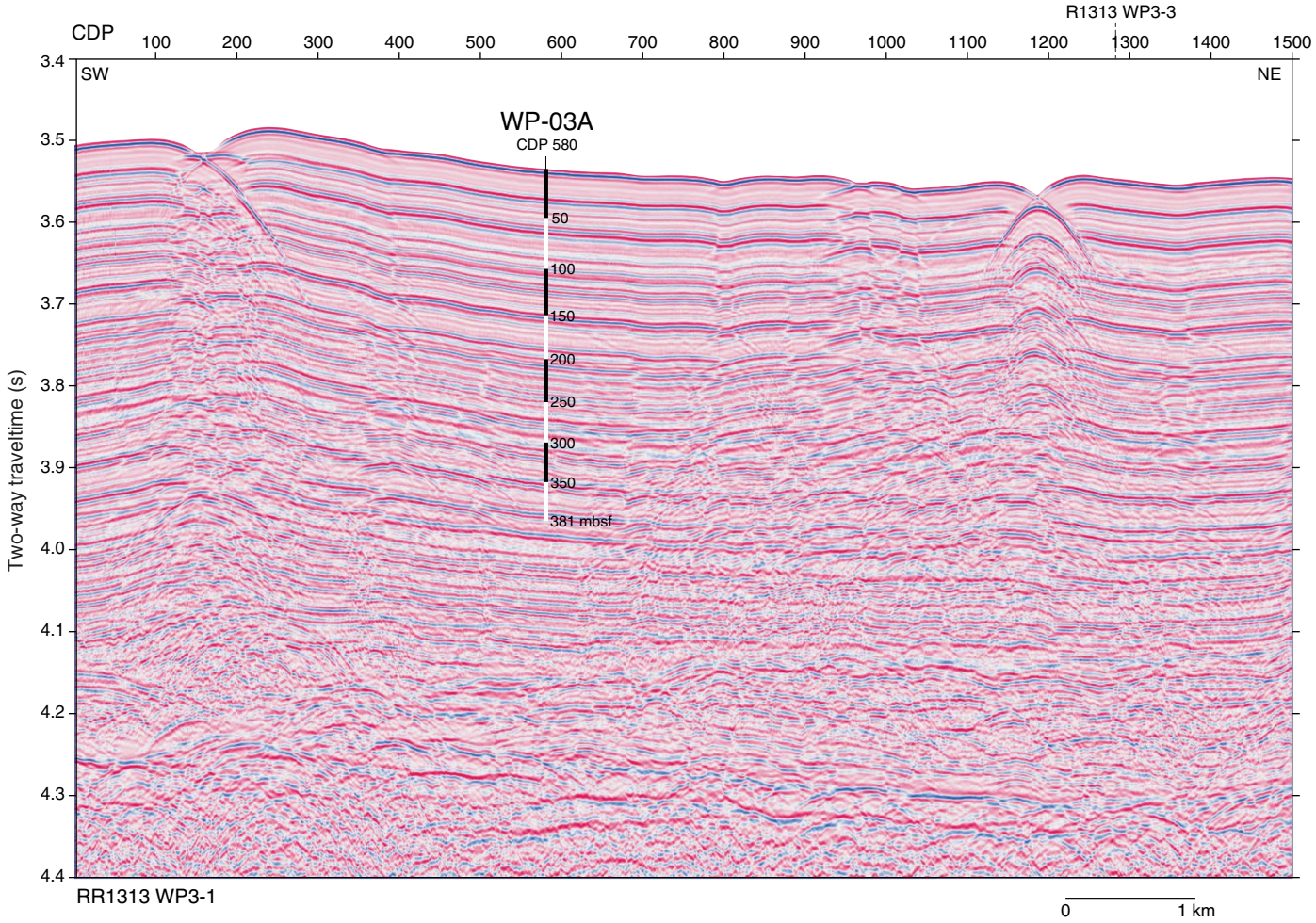

Figure AF26. Seismic reflection profile Line RR1313 WP3-3 with location of proposed Site WP-03A (2°2.59′N, 141°45.29′E; projected at common depth point [CDP] 1346; water depth = 2600 m; target depth = 300 mbsf; approved depth = 500 mbsf) projected approximately 4.4 km northeast onto the line. Location of crossing seismic profile line shown with dashed line at top.

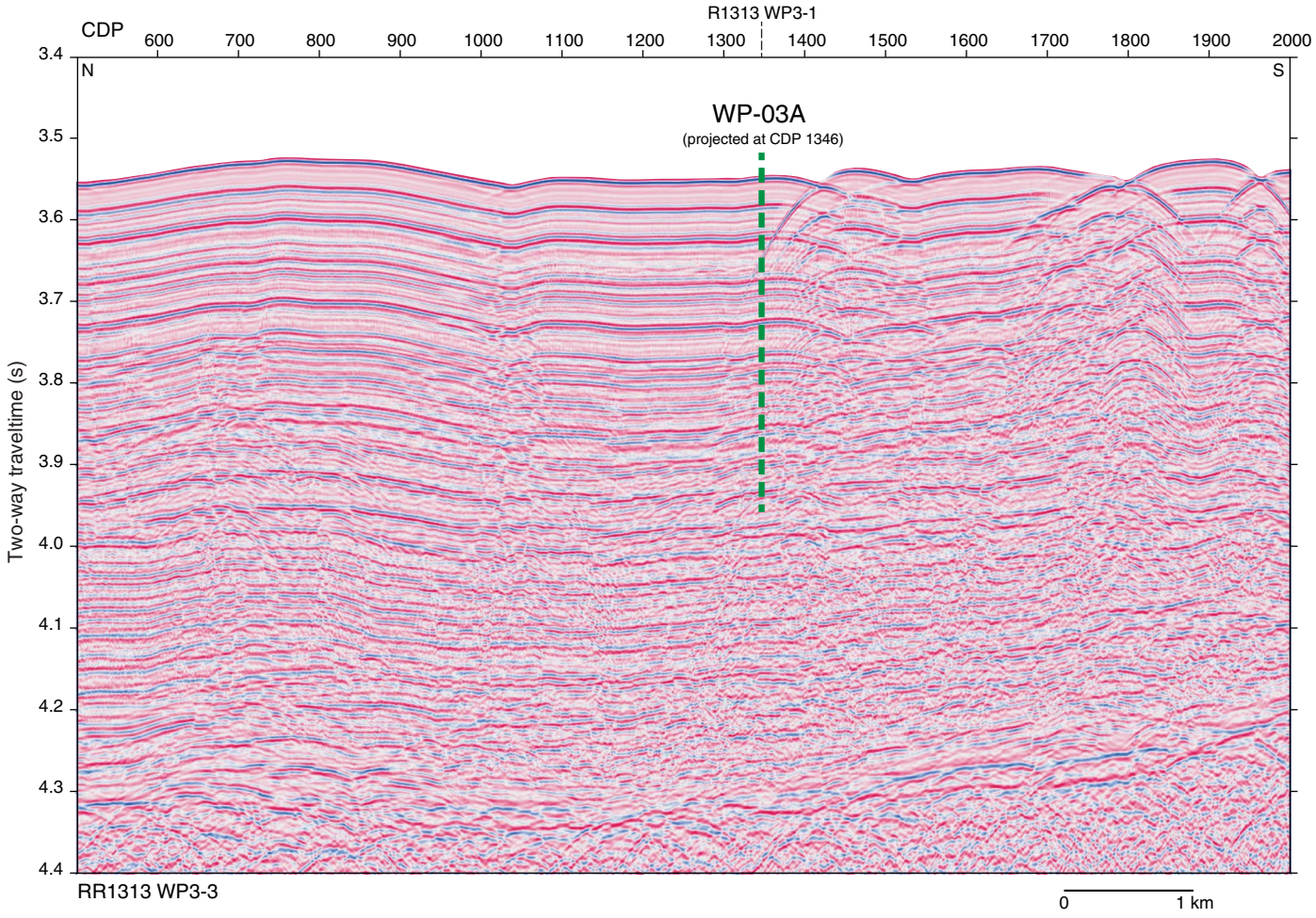

Figure AF27. Contoured bathymetric map showing the location of alternate proposed Site WP-04A (yellow circle) on seismic reflection profile Lines RR1313 WP4-2 (see Figure **AF28**) and RR1313 WP4-3 (see Figure **AF29**). Bathymetry is based on EM122 multibeam survey during Cruise RR1313, with 2-D high-resolution multichannel seismic track lines (black) collected during the same cruise. Numbers along the lines are common depth points (CDPs). Contour interval = 20 m.

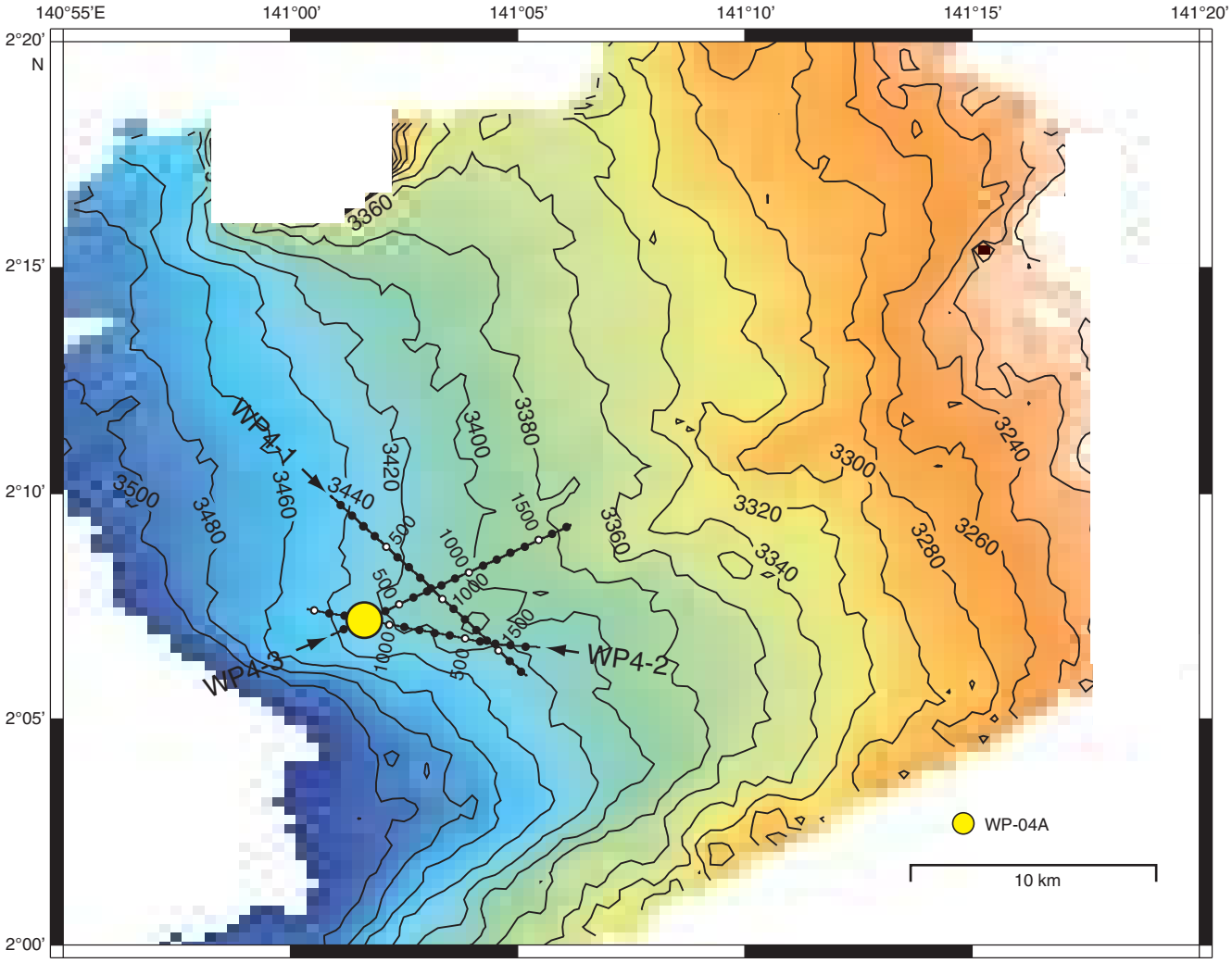

Figure AF28. Seismic reflection profile Line RR1313 WP4-2 with location of alternate proposed Site WP-04A (2°7.20′N, 141°01.66′E; common depth point [CDP] 1163; water depth = 3427 m; target depth = 150 mbsf; approved depth = 200 mbsf). Location of crossing seismic profile line shown with dashed line at top.

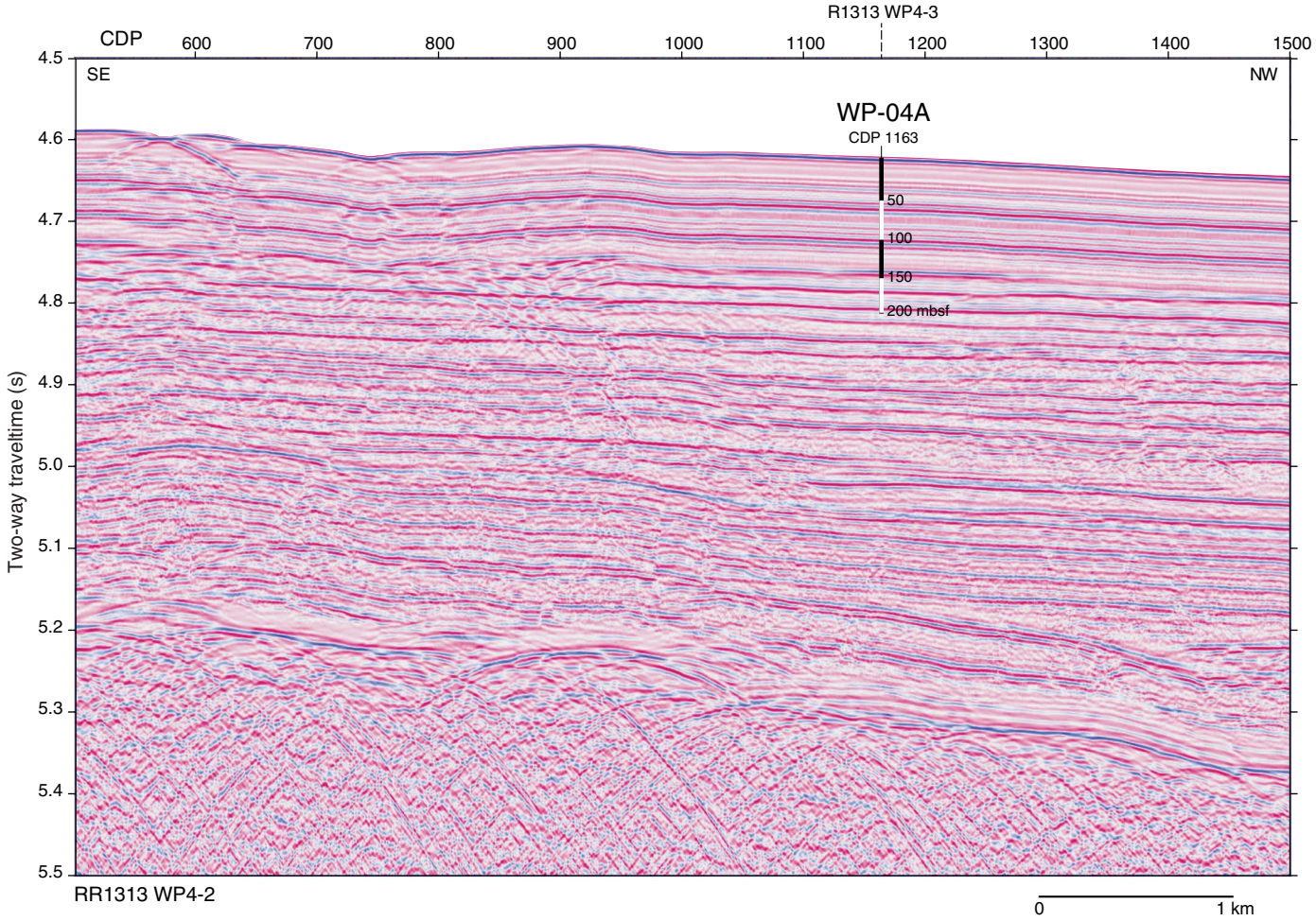

Figure AF29. Seismic reflection profile Line RR1313 WP4-3 with location of alternate proposed Site WP-04A (2°7.20′N, 141°01.66′E; common depth point [CDP] 253; water depth = 3427 m; target depth = 150 mbsf; approved depth = 200 mbsf). Location of crossing seismic profile line shown with dashed line at top.

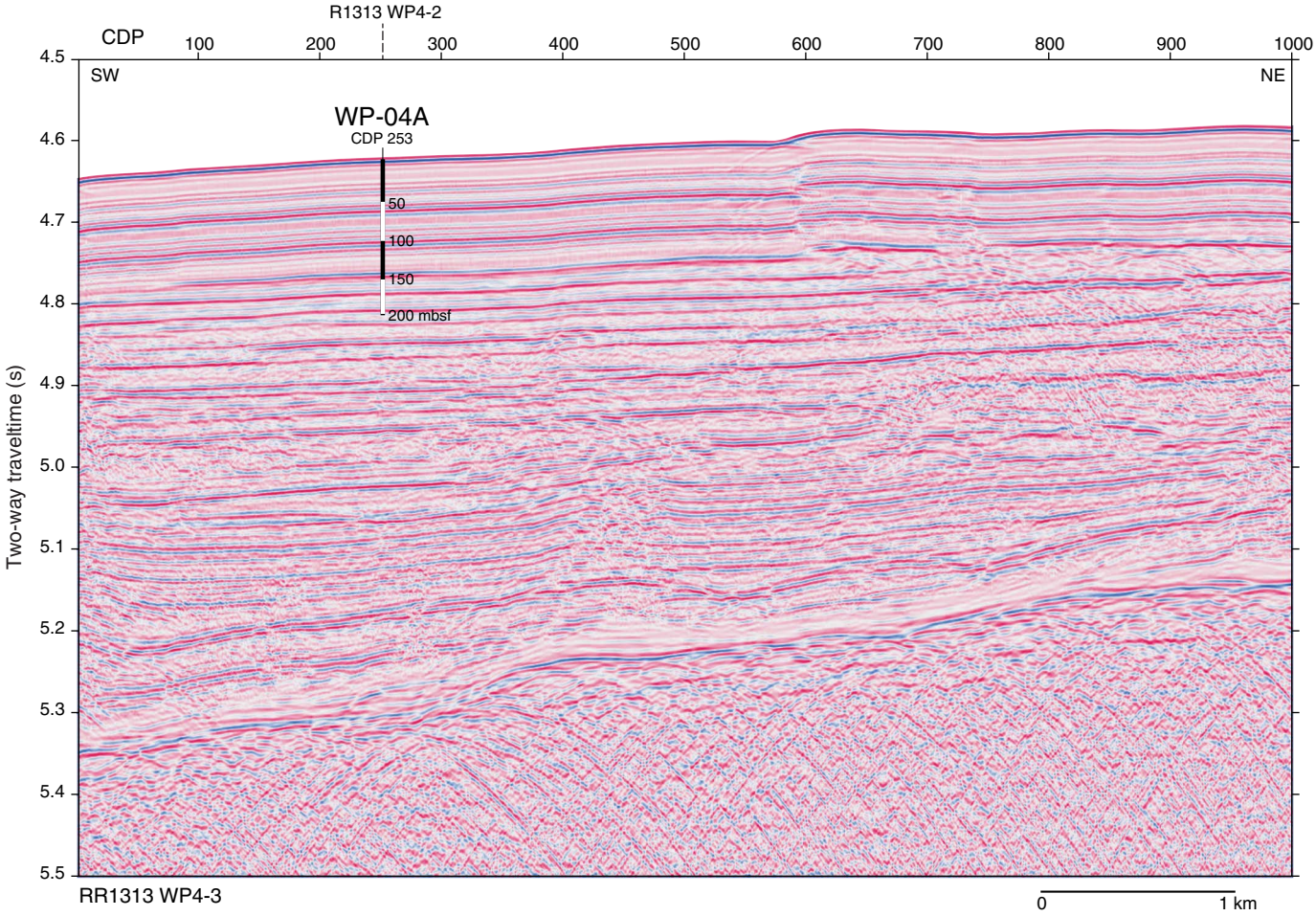

Figure AF30. Contoured bathymetric map showing the location of proposed Site WP-02A (red circle) and alternate proposed Site WP-21A (yellow circle) on seismic reflection Profile RR1313 WP2-1 (see Figure **AF31**). Site WP-02A is located approximately 3.6 km east of the intersection with seismic reflection Profile RR1313 WP2-6 (see Figure **AF32**), whereas Site WP-21A is located at this intersection. Bathymetry is based on EM122 multibeam survey during Cruise RR1313, with 2-D high-resolution multichannel seismic track lines (black) collected during the same cruise. Numbers along the lines are common depth points (CDPs). Contour interval = 20 m. Piston Core RR1313 PC39 (black circle) is located very close to Site WP-21A.

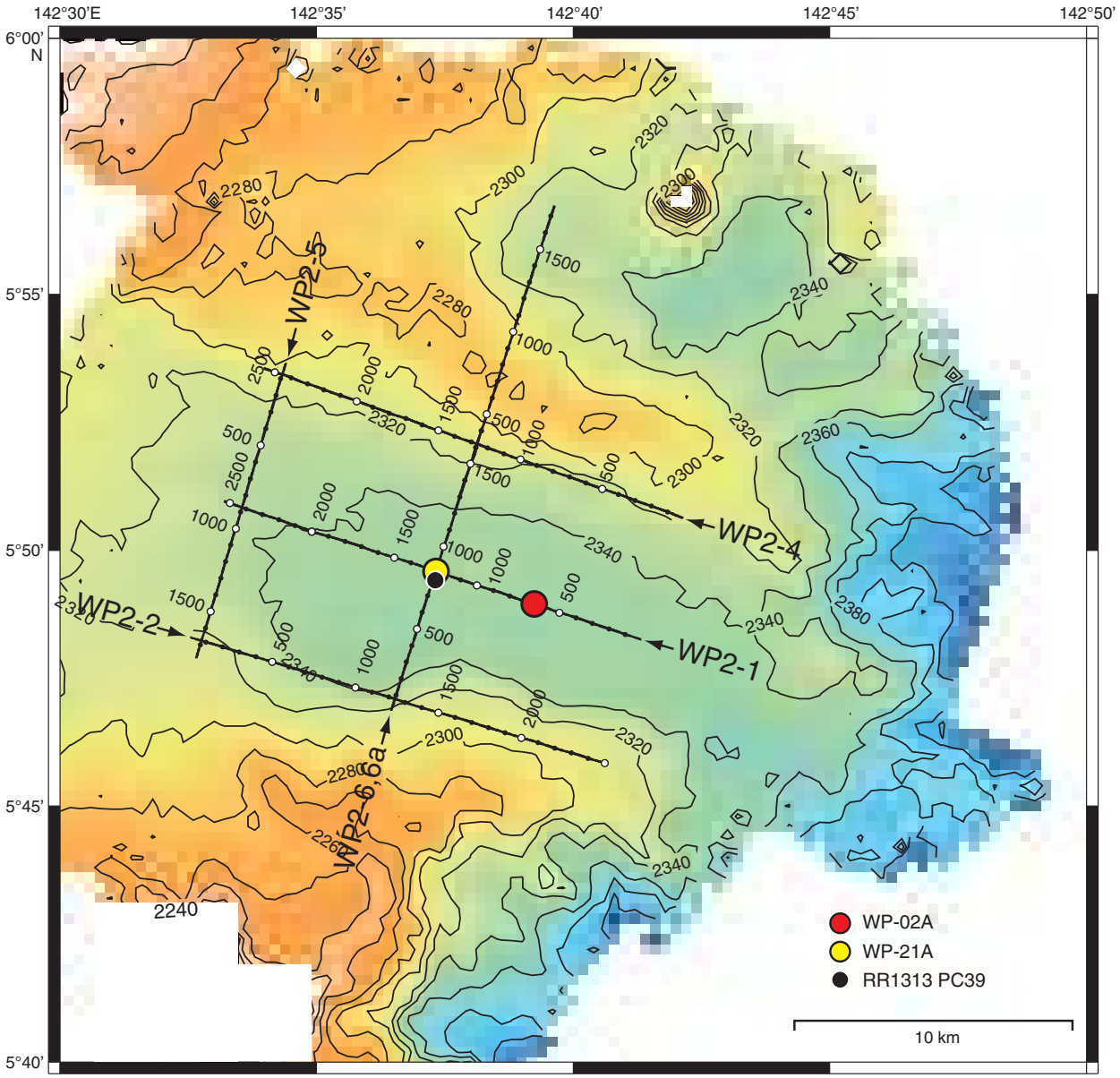

Figure AF31. Seismic reflection profile Line RR1313 WP2-1 with location of proposed Site WP-02A (5°48.95′N, 142°39.26′E; common depth point [CDP] 650; water depth = 2355 m; target depth = 250 mbsf; approved depth = 430 mbsf) and alternate proposed Site WP-21A (5°49.59′N, 142°37.33′E; CDP 1249; water depth = 2355 m; target depth = 100 mbsf; approved depth = 150 mbsf). Location of crossing seismic profile line shown with dashed line at top.

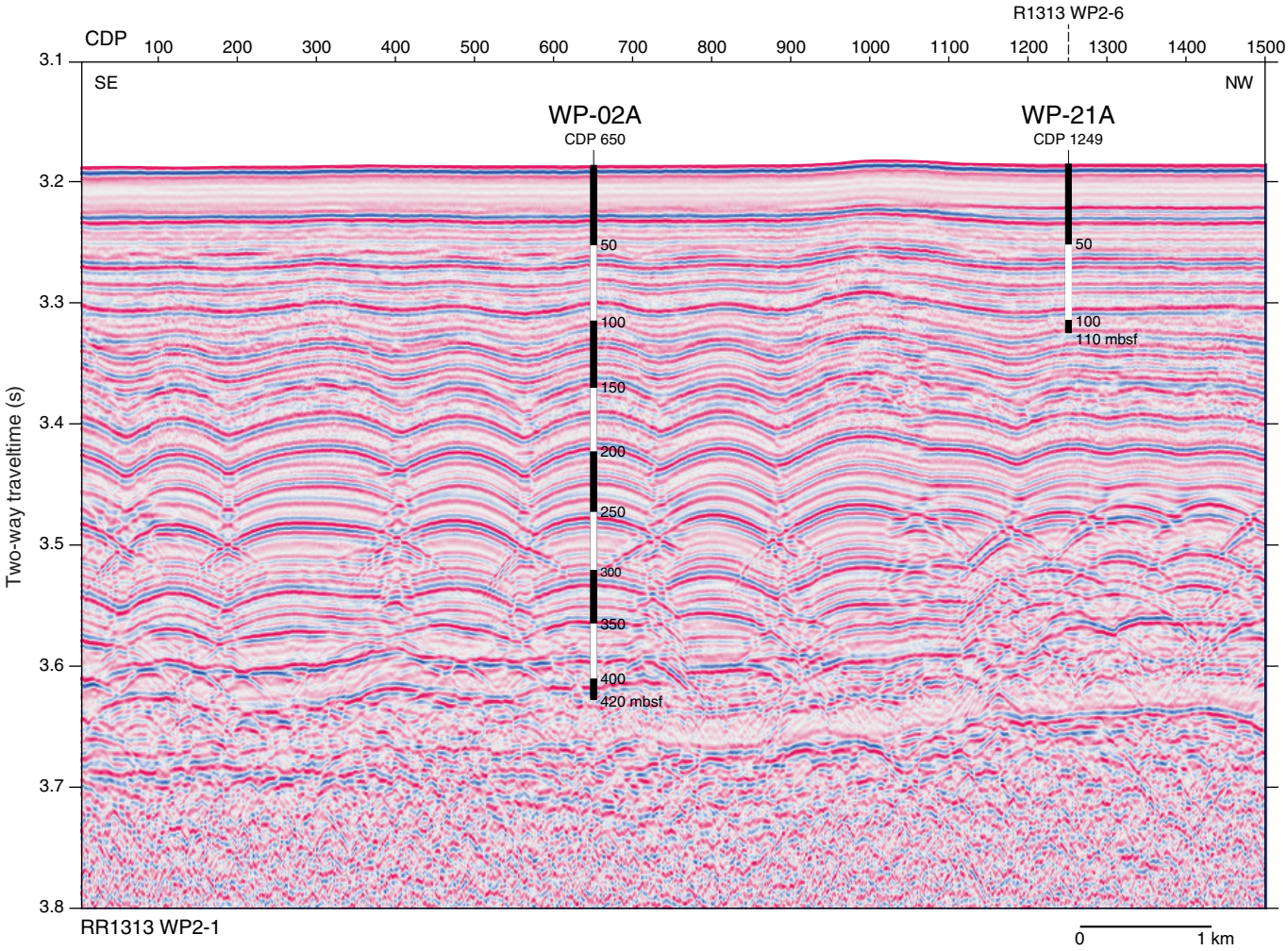

Figure AF32. Seismic reflection profile Line RR1313 WP2-6 with location of alternate proposed Site WP-21A (5°49.59′N, 142°37.33′E; common depth point [CDP] 844; water depth = 2355 m; target depth = 100 mbsf; approved depth = 150 mbsf) and proposed Site WP-02A (5°48.95′N, 142°39.26′E; CDP 844; water depth = 2355 m; target depth = 250 mbsf; approved depth = 430 mbsf) projected 3.6 km west onto the line. Location of crossing seismic profile line shown with dashed line at top.

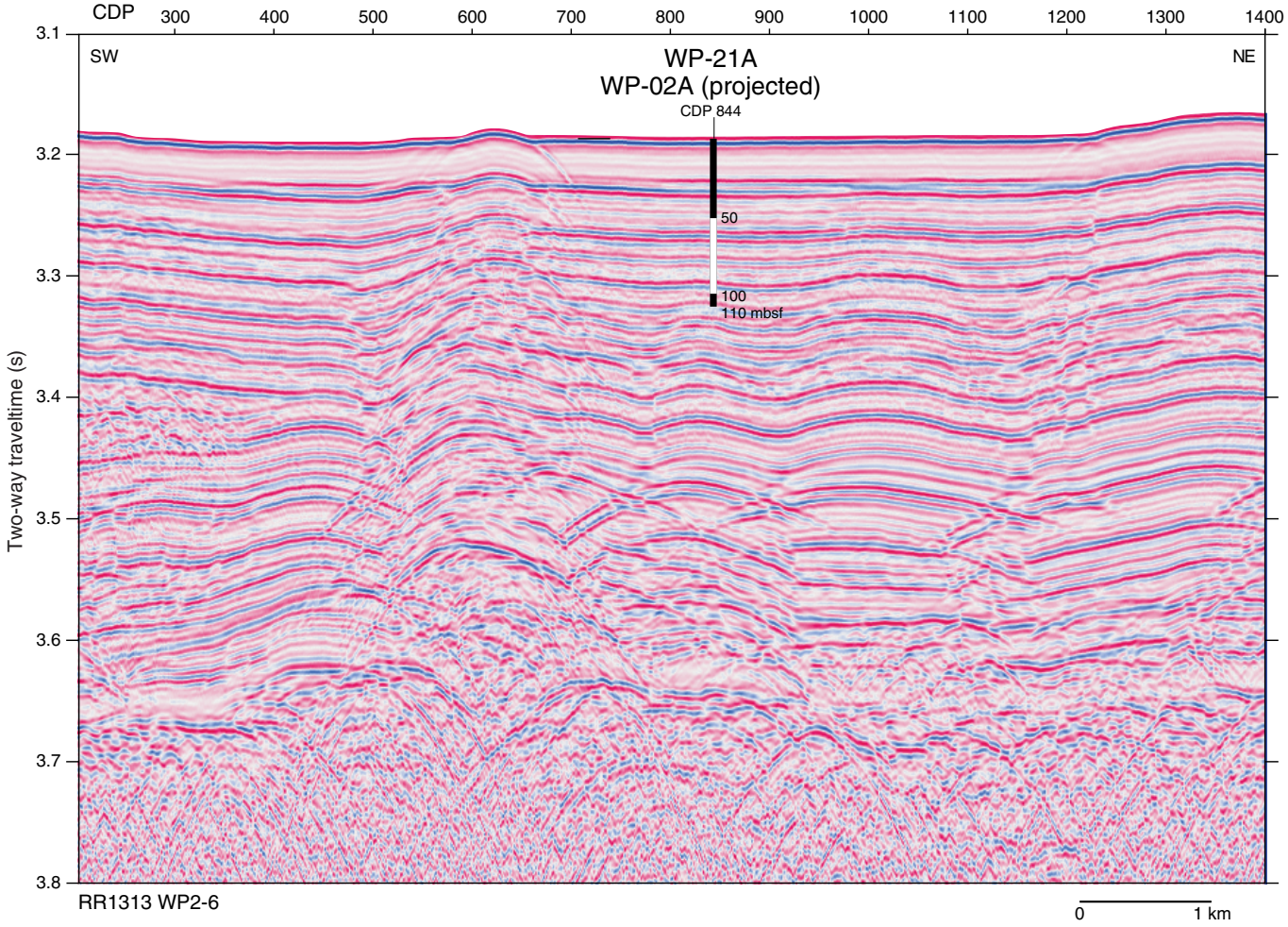

Figure AF33. Bathymetric map showing the location of alternate proposed Site WP-15A (yellow circle), which is a redrill of Ocean Drilling Program Site 806.

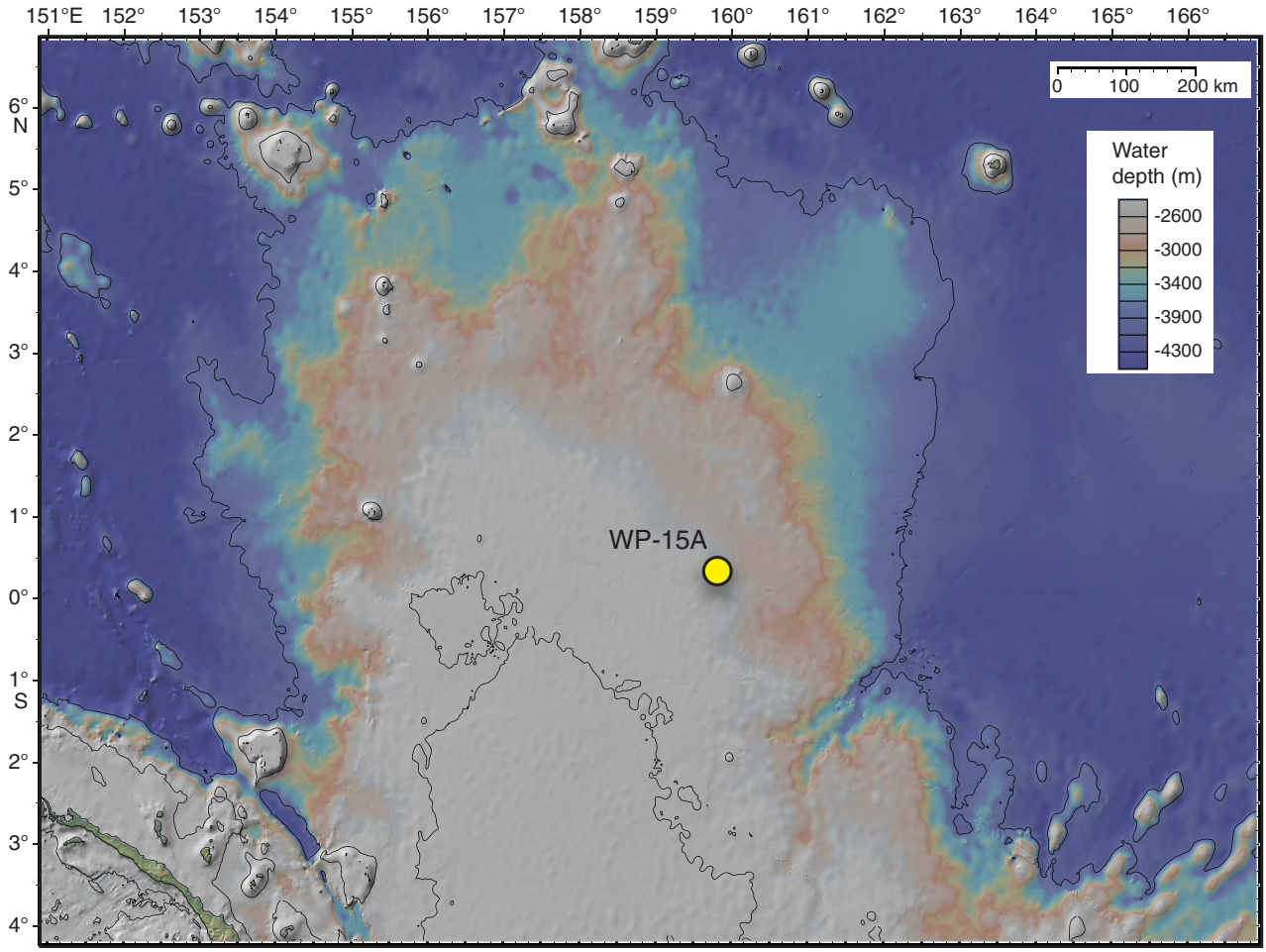

Figure AF34. Seismic line track map showing the location of proposed Site WP-15A (yellow circle) on seismic reflection Profile Ar33.0387 (see Figure **AF35**).

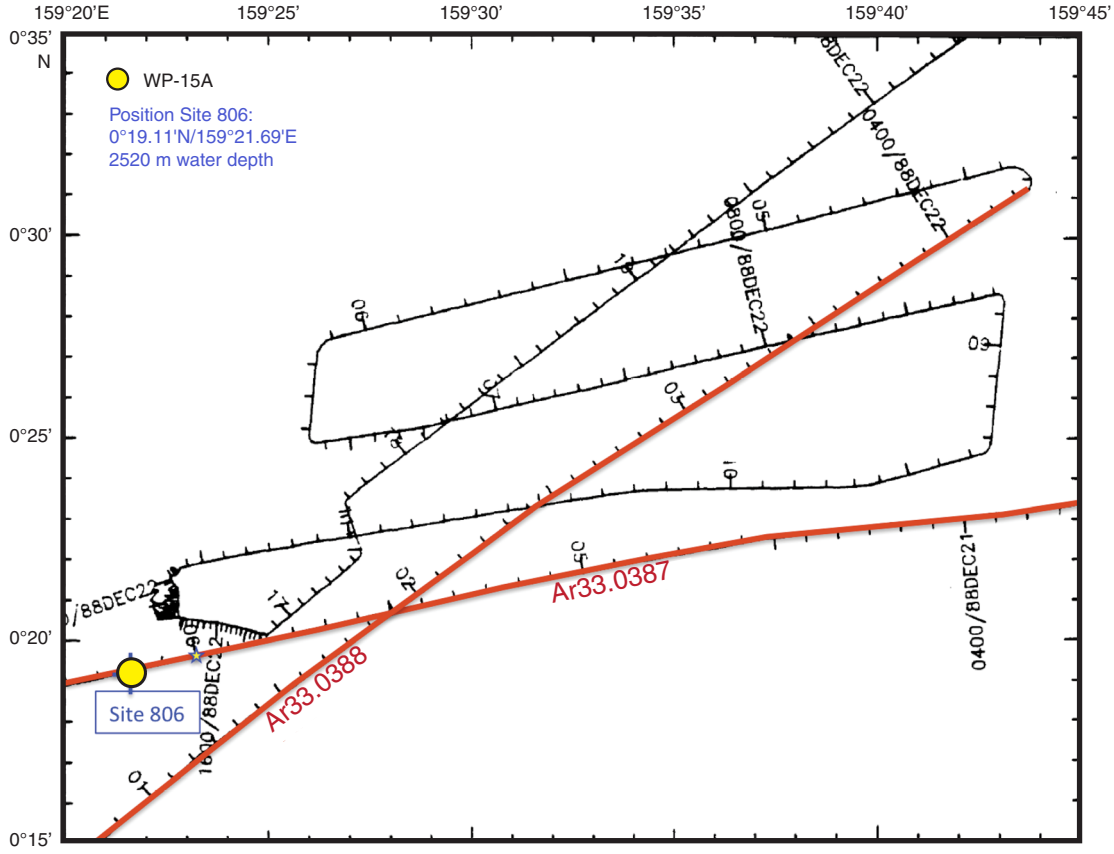

Figure AF35. Seismic reflection profile Line Ar33.0387 with location of alternate proposed Site WP-15A (0°19.11′N, 159°21.69′E; shotpoint [SP] 3250; water depth = 2520 m; target depth = 500 mbsf; requesting permission to drill as deep as 750 mbsf).